ENDURANCE22

Cruise Scientific Report

30th of April, 2022

Edited by Lasse Rabenstein (Chief Scientist)

on behalf of the

Falklands Maritime Heritage Trust

Table of Contents

1. About this report

The scientific cruise report of the Endurance 22 expedition summarises the performed research activities, its objectives, the recorded data and preliminary results. It was compiled shortly after the end of the Endurance 22 expedition and is a non-peer-reviewed scientific document. The content of each chapter is the responsibility of the respective authors. The report does not cover the marine archaeology survey work performed during the expedition, which will be published in a separate dedicated report.

2. Introduction and Scientific Aims

Written by Lasse Rabenstein & John Shears

Figure 1: *The 15 field scientists of the Endurance 22 expedition. From left to right standing: Jakob Belter, Lasse Rabenstein, Dmitrii Murashkin, Jukka Tuhkuri, Mira Suhrhoff, Carla Ramjukadh, Marc de Voss, Christian Katlein, James-John Matthee; From left to right sitting/kneeing: Stefanie Arndt, Beat Rinderknecht, Anriëtte Bekker, Alexandra Stocker, Thomas Busche, Ben Steyn*

The Endurance22 expedition was an international non-governmental expedition to the Weddell Sea, Antarctica, organised by the Falklands Maritime Heritage Trust. The expedition took place over a 43 day period between 5 February 2022 – 20 March 2022, and used the South African polar research and logistics vessel S.A. Agulhas II.

The aims of the expedition were to:

1.) Locate, identify and survey the wreck of Sir Ernest Shackleton's expedition ship the Endurance

2.) Undertake an education and outreach programme and the making of a film documentary
3.) Carry out a programme of scientific research.

The expedition was equipped with state-of-the-art Saab Sabretooth Autonomous Underwater Vehicles (AUVs), which were capable of deployment to water depths of 3,000m deep and fitted with a range of sensors in order to locate, image, photograph and scan the Endurance wreck.

The expedition science team brought together sea ice scientists, oceanographers, meteorologists and marine engineers to research the Antarctic sea ice, furthering our understanding of environmental changes in the surrounding Weddell Sea and Southern Ocean, whilst also providing operational data that assisted in finding the wreck of the Endurance and to improve the understanding of ship-ice interaction. Furthermore, the data gathered from this scientific research will help to improve future sea ice navigation systems. This report summarizes the scientific research carried out , shows first preliminary results and lists the created data sets and how to access them.

Development of new sea-ice information systems
Endurance22 served as a case study for today's operational capabilities to navigate and work effectively in sea-ice, and to define benchmarks for the next generation of ice information systems. Today, the creation of sea-ice charts is still a very cumbersome and time-consuming job. In Antarctica especially, there is little sea ice information to support shipping operations, as there is no dedicated national ice service responsible (although the Norwegian and Unites States Ice Services provide weekly ice charts). However, with today's advent of earth observation, producing terabytes of satellite data every day, there is the potential to create ice charts automatically in near-real-time and for tactical navigation. The ultimate sea ice information service would image the different types of ice continuously and automatically. Scientists involved in the Endurance 22 expedition are developing an artificial intelligence system to do the work of an ice analyst automatically and in a fraction of the time. However, the results of such created ice charts are not yet good enough for operational use, and to improve them more validation data are needed. During Endurance22 several camera systems measured and recorded the ice situation along the cruise track, an electromagnetic system continuously measured the ice thickness and manual ice observations from the bridge of Agulhas II complemented this dataset.

Environmental studies
Changes in the Weddell Sea sea-ice regime potentially impacts the global climate and ocean current system. At the same time the physical processes of the Weddell Sea sea-ice regime are still not completely understood. Every in-situ dataset of physical sea-ice measurements in this remote region is of value and helps to improve regional ice and snow climatologies. During Endurance 22 physical sea-ice and snow properties were observed and measured continuously from the ship and additionally during 17 stations on the ice.

MetOcean Science
Members of the science team on-board provided weather forecasts and operated meteorological measuring instruments. These measurements were supplemented with visual observations (such as weather, clouds, and sea-ice) done manually. Additionally, several weather balloons were released into the atmosphere (the highest reaching 22.6km – well into

the tropopause) and drifting weather buoys deployed into the Weddell Sea, one of the most under-researched parts of the world. This research will contribute to the global WMO GTS system collecting and sharing worldwide weather data.

Ship ice interaction

Members of the science team undertook a programme of monitoring of the vessel performance throughout the Expedition. One objective was to improve the understanding of how sea ice interacts with the S.A. Agulhas II. Another was to understand the ship's performance in ice to develop future routing systems. The scientists constantly measured the pressure of the ice on the hull of S.A. Agulhas II, and physical quantities of the ice around the ship, to understand better how the trafficability of an ice breaker is determined by different sea ice conditions.

Marine Biology and Sedimentology

The high-resolution digital photographs and video footage recorded by the Endurance 22 subsea team showed numerous deep-sea marine lifeforms living on the wreck. The subsea team also surveyed a large area of the seabed, over 300 km2, using side scan sonar while searching for the wreck. During the expedition no in-depth analysis was undertaken of the deep sea marine biology or the sedimentology of the seafloor. However, the Falklands Maritime Heritage Trust as the owner of the subsea data will in due course release the digital photographs, video, side scan sonar and other imagery collected for scientific research purposes.

3. Contributing Parties

Written by the respective contributors

3.1. Drift + Noise Polar Services

Description: Drift+Noise Polar Services (=DNPS) is a German based company and spin-off from the Alfred Wegener Institute for Polar and Marine Research. The company is fully committed to support shipping and other activities in the Polar Regions with best possible ice information. DNPS is involved in several international research projects with the goal to develop new ice information products. DNPS utilises satellite remote sensing data and operational weather models for consulting work on-board ships and from on-shore as well as to integrate it into Apps.

Participants: Dr. Lasse Rabenstein (Chief Scientist), Alexandra Stocker (Scientist), Beat Rinderknecht (Technician), Mira Suhrhoff (Student), Dr. Panagiotis Kountouris (Scientist, back office support)

Objectives:

- Support the subsea team and the nautical crew in their ice navigational and dive position related decisions.
- Enable a sea-ice information desk at the bridge which can be consulted 24/7 for the time the Agulhas II operated in ice
- Coordinate the science work and the involved parties
- Creation of a data set for trafficability analysis within the Fast-Cast 2 project
- Test the IcySea App and define future needs for improvement.

Contact: Stavendamm 17, 28195 Bremen, Germany, info@driftnoise.com

3.2. Shears Polar Ltd.

Description: Shears Polar Ltd is a polar consultancy company founded by Dr John Shears in January 2017, and is located near Huntingdon, UK. The company provides expedition leadership, consultancy and project management services for projects in the polar regions.
Participants: Dr John Shears
Objectives:

- Leading the Endurance22 expedition onboard the S.A. Agulhas II, including mob and demob in Cape Town, South Africa
- Managing the programming and scheduling for all expedition logistics and subsea and scientific activities, including overall responsibility for the effective co-ordination and delivery of the expedition project plan
- Co-ordinating closely with the Master S.A. Agulhas II, and the Ice Pilot, regarding ship routing to and from the search area, changes to the voyage schedule and any onboard management issues
- Supporting the subsea team to enable effective AUV diving operations in the search area
- Ensuring the Health and Safety of the Expedition team, including working with the Expedition doctor to manage and implement COVID-19 safety requirements

Contact: Dr John Shears, Shears Polar Ltd, 5, Mill Lane, Bluntisham, Huntingdon, Cambridgeshire, UK. E-mail: john_shears@btinternet.com

3.3. Alfred Wegener Institute

Description: The Alfred Wegener Institute, Helmholtz Centre for Polar and Marine Research (AWI) is located in Bremerhaven (headquarters), Germany and has about 1000 employees. The AWI is one of the largest polar research institutes in the world and conducts research (Biosciences, Geosciences, Climate Sciences) in the Arctic, the Antarctic, and the high and mid latitude oceans. As part of the Climate Sciences department the Sea Ice Physics section focusses on Arctic and Antarctic sea ice, which are vital components of our climate system. Specific focus lays on understanding changes in sea ice cover and the underlying physical processes and interactions with the atmosphere and ocean.
Participants: Dr. Stefanie Arndt (Sea Ice Scientist), Dr. H. Jakob Belter (Sea Ice Scientist), Esther Horvath (Communication and Media, Photographer), Dr. Christian Katlein (Project Polarstern II, Sea Ice Scientist), Dr. Helge Goessling (SIDFEx backoffice support, Sea Ice Scientist),), Dr. Valentin Ludwig (SIDFEx backoffice support, Sea Ice Scientist)
Objective: The AWI group on Endurance 22 had three major objectives:

- One of the main scientific goals is to collect representative ice and snow thickness distributions to investigate the overall state of sea ice in the target area and to complement earlier studies in the western Weddell Sea. Additionally, ice thickness measurements and mapping of ice floe thickness is planned for logistical support for the subsea team's ice camp scenario. Snow depth measurements on individual ice floes are also supported by up to three snow depth buoys that are to be deployed to investigate snow depth variations after the end of the expedition. The final scientific objective is to gather information on the vertical snow and ice properties and the degree of snow metamorphism to evaluate the intensity of snow melt during the preceding summer (2021/2022). This investigation includes ice core analysis and snow pits and complement existing data sets in the Weddell Sea. It will also

support the improvement and validation of radar and passive microwave remote sensing retrieval algorithms (Stefanie Arndt, H. Jakob Belter).
- Observation of and support for the subsea team. As part of the Underwater Robotics team, Christian Katlein joined the expedition to gain insight into the Saab Sabertooth underwater vehicle.
- Esther Horvath joined as photographer to accompany the search for Endurance and also the science.

Contact: H. Jakob Belter, jakob.belter@awi.de

3.4. German Aerospace Center DLR

Description: The **German Aerospace Center** (German: *Deutsches Zentrum für Luft- und Raumfahrt,* abbreviated **DLR)**, is a national research center of the Federal Republic of Germany, covering a multitude of research topics reaching from aerospace, communication, navigation, robotics, energy, to transportation and security. With the headquarter in Cologne, DLR maintains research facilities at 30 locations across Germany and several federal states. DLR has about 10.000 employees, and a national budget of €3.816 billion (in 2020). The German Aerospace Center (DLR) operates the two German space borne radar missions TerraSAR-X, and TanDEM-X, including several receiving stations for the data downlink. The two Synthetic Aperture Radar (SAR) satellite twins TerraSAR-X (TSX), and TanDEM-X (TDX) serve both missions. The main receiving station in Neustrelitz, Germany, as well as the German Antarctic Receiving Station (GARS) in O'Higgins are offering near-real time downlink and processing capability for the TerraSAR-X mission. DLR has supported (and continues supporting) polar expeditions by providing satellite imagery of the expedition environment with data of the TerraSAR-X mission, most recently the Multidisciplinary drifting Observatory for the Study of Arctic Climate (MOSAiC), and in 2019 the first Endurance expedition. Facilities of the ground segment of the TerraSAR-X mission are housed on the research campus of DLR in Oberpfaffenhofen (DLR-OP) near Munich, Bavaria. DLR-OP has – besides communication and robotics research topics - a strong focus on earth observation and remote sensing. The mother institutes (Microwaves and Radar Institute, Remote Sensing Technology Institute) of the 2 DLR employees participating in the Endurance22 expedition are based in DLR-OP as well, and are both involved in ground segment operations of the TerraSAR-X mission.

Participants: Thomas Busche (Scientist - Microwaves and Radar Institute) , Dmitrii Murashkin (Scientist, Remote Sensing Technology Institute)

Objectives:
- Ordering of TerraSAR-X near-real time data by an DLR operator under consideration of actual sea ice drift and weather forecast information during the whole passage through the ice, and during all operation at the Endurance wreck location. A short communication path and exchange between the DLR operator and other experts on board secures optimal image acquisition for scientific and navigational support.
- Preparing of all received TerraSAR-X, as well as other remote sensing and supplemental data in GIS based maps and information products for the expedition lead, the ship command, and other teams on the ship for navigation support, ice camp support, and media activities.

- Assisting the sea ice team in interpretation of sea ice conditions and features, as well as to support the identification of target locations the Automated Underwater Vehicle (AUV) operations with the help of the Sea Ice Information System on the bridge
- Assisting in collecting situ data with the other research groups during field work activities on sea ice floes
- Maintain a thermal infrared camera mounted on the vessel, and collect imagery during all the time in the sea ice.

Contact:

Thomas Busche, German Aerospace Center (DLR), Microwaves and Radar Institute, Muenchener Str. 20, 82234 Wessling, Germany, Email: Thomas.Busche@dlr.de, Telephone: 0049 (0)8153-28-2193, Web: https://www.dlr.de/hr/en

Dmitrii Murashkin, German Aerospace Center (DLR), Remote Sensing Technology Institute, Maritime Safety and Security Lab Bremen, Am Fallturm 9, 28359 Bremen, Germany. Email: Dmitrii.Murashkin@dlr.de, Phone: 0049 (0)421 24420 1045, Web: https://www.dlr.de/eoc/en/desktopdefault.aspx/tabid-5426/10518_read-23261

3.5. South African Weather Service

Description: The South African Weather Service (SAWS) is a national meteorological service (NMS) and member of the World Meteorological Organization (WMO). The SAWS provides a range of weather and ocean information for public good and commercial purposes. The Marine Research Unit is a sub-group within the SAWS focusing on marine environmental intelligence. Its mandate includes the development of high-resolution coastal ocean forecasting systems, observation of the oceans within METAREA VII, and operational support for marine activities. To this end, the SAWS Marine Unit utilises a mix of numerical models, satellite data and in-situ measurements from various types of buoys and stations.

Participants: Marc de Vos (MetOcean Scientist), Carla-Louise Ramjukadh (MetOcean Scientist)

Objectives:

- Assistance to navigation team for ship routing in respect of weather and ocean conditions via direct communication with vessel masters.
- Daily briefing of expedition team for operational planning.
- Provision of required met-ocean information to sub-sea teams during search operations.
- Surface synoptic and upper air meteorological data collection/ transmission for assimilation into numerical weather prediction models.

Contact: capetown.marine@weathersa.co.za

3.6. Aalto University

Description: Aalto University, located in Espoo, greater Helsinki in Finland, has 12.000 students, 400 professors and about 4000 other faculty and staff. Aalto University has six school and is conducting research and teaching in engineering, business as well as in arts and design. Arctic marine technology is a research focus area at Aalto School of Engineering. This focus is unique in Finland and there are only a few others with a similar focus on an international level. The research combines solid and fluid mechanics fundamentals in studying the physical phenomena behind key arctic engineering problems. Current research topics include ice loads on ships and structures, ship performance, ice mechanics, and risk and safety.

Participants: Professor Jukka Tuhkuri (Engineering Scientist)

Objective: To measure ice loads on the hull of SA Agulhas II, to monitor sea ice conditions visually and by cameras, to measure small scale sea ice properties, and to combine all these measurements to increase our understanding of the mechanics and statistics of sea ice loads on ships. In addition, to provide information about the measured ice loads during the voyage to the captain of SA Agulhas II.

Contact: Otakaari 4, FI-02150 Espoo, Finland. jukka.tuhkuri@aalto.fi

3.7. Stellenbosch University

Description: Stellenbosch University is located in the town of Stellenbosch in the Western Cape of South Africa. It is home to an academic community of 29 000 students (including 4 000 foreign students from 100 countries) as well as 3 000 permanent staff members (including 1 000 academics) on five campuses. Stellenbosch University comprises ten faculties: AgriSciences, Economic and Management Sciences, Medicine and Health Sciences, Engineering, Military Sciences, Arts and Social Sciences, Science, Education, Law and Theology. The faculty of engineering offers degrees in Electrical & Electronic Engineering, Civil Engineering, Process Engineering, Industrial Engineering and Mechanical & Mechatronic Engineering. The faculty houses approximately 4 000 engineering students, of whom 25% are post-graduate.

Participants: Professor Anriëtte Bekker (Engineering Scientist), James-John Matthee (Student), Ben Steyn (Student)

Objective: To measure full-scale hull and propulsion responses on the SA Agulhas II during her operations in the harsh Southern Ocean and Weddell Sea ice. To use data from these measurements towards situational awareness of the crew and tactical route planning in ice.

Contact: Professor Anriëtte Bekker, annieb@sun.ac.za, +27 82 878 2698

3.8. Dr. Thomas König und Partner, Fernerkundung GbR (K&P)

Description: Dr. Thomas König und Partner, Fernerkundung GbR (K&P) is a company founded in January 2018. It is located in the greater Munich area, Germany. The goal of the foundation was to improve an inovative sea ice algorithm which had been developed by the founders since 2004 on the basis of NOAA-AVHRR satellite data and was now transferred to the data of the new SLSTR instrument on board the Sentinel-3 satellites.

Participants: Dr. Thomas König (EisKlass 2 back office support, founder), Dr. Christine König (EisKlass 2 back office support, founder)

Objective: With the help of this new algorithm it became possible to distinguish between multiple sea ice and snow types and stages of development. K&P, together with its partner DLR/Bremen was first supported by the German government for the Project Eisklass31, leaded by K&P. Beyond the transfer and improvement of the optical/thermal ice classification, another goal of EisKlass31 was to outline ways to achieve further improvement by combining it with synthetic aperture radar data. It could be shown, that better ice-information were generated

already by simple combinations of the different remote sening systems. For the follow-up project Eisklass-2 (Lead: DLR), further partners as Drift& Noise, O.A.Sys, Hamburg and The Inversion Lab, Hamburg could be won. This project aims to combine both independent ice classifications into a fully automated processing chain using artificial interlegence.
Contact: Dr. Christine König and Dr. Thomas König, Kunissastraße 11, 86911 Dießen am Ammersee, Germany, URL: http://remote-sensing-ice-office.de, https://kup-koenig.feste-ip.net/kupWebpage, Email: rs.iceoffice@googlemail.com

3.9. Reach the World

Description: Reach the World (RTW) is a global education non-profit organisation based in New York City. For more than 20 years, RTW has used virtual exchange to bring the world into classrooms, inspiring students to become curious, confident and compassionate global citizens. To date, more than 1,200 RTW travellers have shared their journeys online with over 30,000 young students, making the eye-opening benefits of travel and exploration accessible to the decision-makers of tomorrow.
Participants: Timothy Jacob (Onboard Education & Outreach Coordinator)
Objective: Throughout the 2021-22 academic year, Reach the World has brought 30,000+ students around the world to the Endurance22 Expedition through live video calls with expedition team members and student-friendly articles covering onboard science initiatives and the real-time search for the Endurance. This multidisciplinary virtual exchange offered all students the chance to walk in Sir Ernest Shackleton's footsteps and interact with modern-day explorers.
Contact: 222 Broadway, 18th Floor, New York, NY 10038; rtwinfo@reachtheworld.org

4. Cruise overview

4.1. Time Line and Cruise track

Written by Alexandra Stocker (DNPS), Lasse Rabenstein (DNPS), and John Shears (SP)

From Cape Town to the ice edge
The *S.A. Agulhas II* departed from Cape Town, South Africa on February 5, 2022 and sailed directly to the western Weddell Sea, Antarctica. As this was comparably late into the Antarctic summer season everything possible was done to reduce the transit time through the south Atlantic to a minimum. (see ***Figure 2***). The ship reached the ice edge in the western Weddell Sea on February 15 (see ***Figure 3***). Passage to the wreck site was quick and through a mixture of loose first-year and multi-year ice, and the ship entered the Endurance search box on February 16.

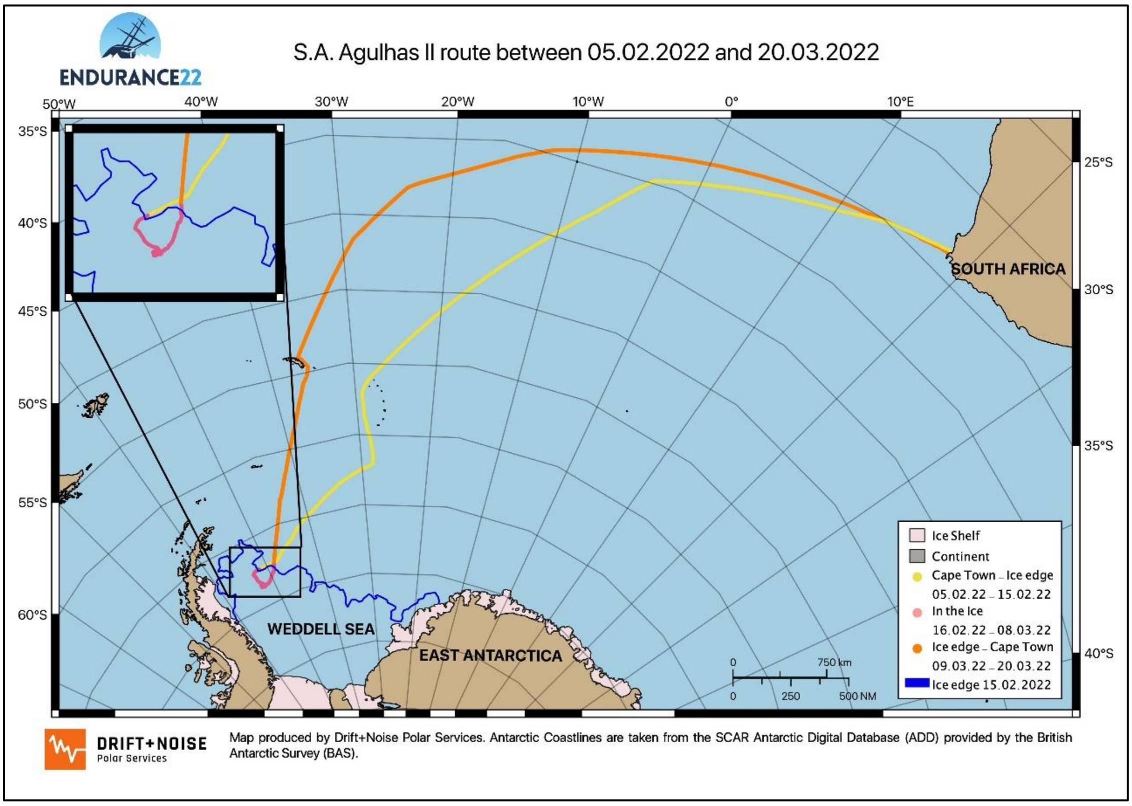

Figure 2: *Overview map of S.A. Agulhas II route between February 5, 2022, and March 20, 2022. Ice edge in the this map in the limit of 15% sea ice concentration.*

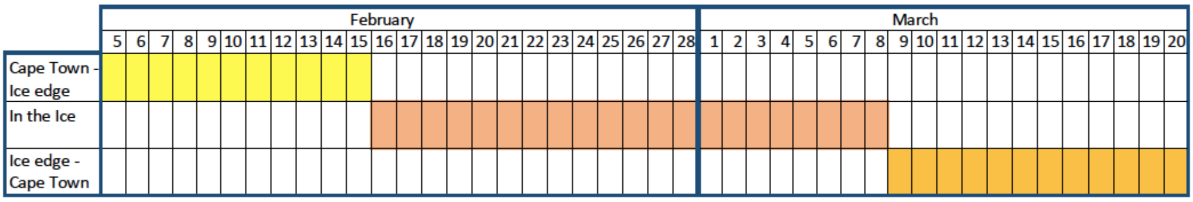

Figure 3: *Timeline of the S.A. Agulhas II between February 5, 2022, and March 20, 2022*

In the ice

The navigation and the expedition were not only dependent on sea ice concentration and ice regimes, but the ice drift was an important variable to consider. In **Figure 4**, we can see how the *S.A. Agulhas II* drifted with the ice pack. In this map, GPS positions were taken every ten minutes, as a result the spaced points connected by a black line shows the periods where the ship was sailing, and the colored tracks represent the periods where the ship was stationary (relative to the surrounding sea-ice). During the stationary modes, the ship was parked in a large ice floe to reduce the risk of sea ice interfering with the sub-sea operations. As a result, we can observe the distance and direction the ship drifted within the ice pack. Daily maps including the latest TerraSAR-X radar images (section 5.1.1) coupled with the updated ice drift forecasts (section 5.3) were used for decision making between the bridge and the sub-sea team to determine the following parking position. During the time that we were parked in an ice floe and the AUV from the sub-sea time was scanning the ocean floor, the science team had time to go on the ice to take various ice and snow samples (see section 7.1). Multiple AUV dives were undertaken on the Endurance search box between February 16 and March 8, with the historic discovery of the Endurance being made on March 5 2022.

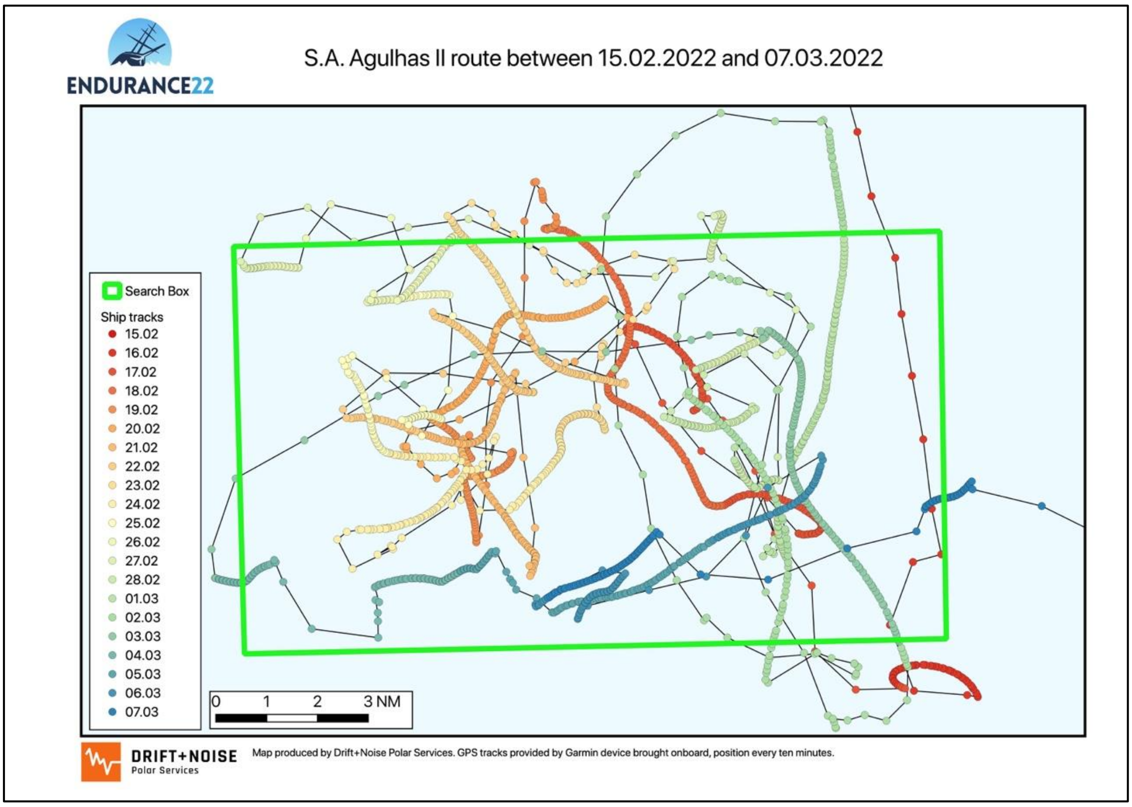

Figure 4: *S.A. Agulhas II ship track (Garmin GPS position every 10 minutes) within the search area between February 16 and March 7, 2022.*

From the ice-edge to Cape Town

S.A. Agulhas II left the ice on March 8 and then sailed to South Georgia. After a 12 hours stop at King Edward Point, South Georgia on March 11 to visit the old whaling station Grytviken and Shackletons grave, S.A. Agulhas II then returned to Cape Town, South Africa. The expedition arrived back in Cape Town on March 20

Timeline

1 – 4 Feb	Mobilisation of personnel and equipment on to S.A. Agulhas II in Cape Town.
5 Feb	S.A. Agulhas II departs Cape Town for Antarctica
5 - 15 Feb	Transit to Endurance wreck survey area in the Weddell Sea
16 Feb	Arrival at Endurance wreck survey area and AUV operations commence
5 Mar	Discovery of Endurance wreck
7 Mar	AUV operations completed
8 Mar	Departure from Endurance wreck survey area
11 Mar	Visit to Grytviken, South Georgia
11 – 20 Mar	Transit to Cape Town, South Africa
20 – 21 Mar	Demobilisation of personnel and equipment from S.A. Agulhas II in Cape Town

4.2. General Meteorological conditions

Written by Marc de Voss (SAWS) and Carla Ramjukadh (SAWS)

During transit to and within the search area, conditions were generally within expected climatological ranges, with a handful of high frequency weather events. **Figure 5** shows a timeseries summary of basic meteorological/oceanographic (met-ocean) variables for the cruise.

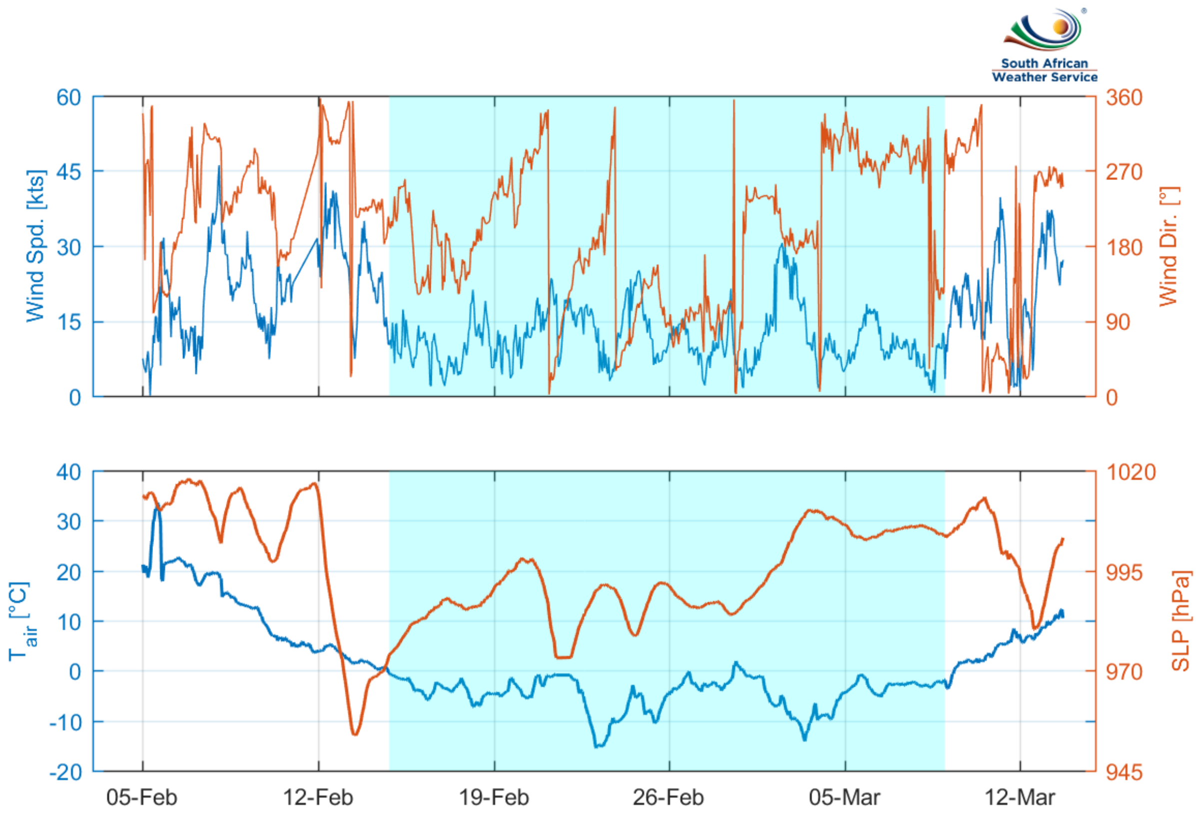

Figure 5*. Timeseries summary of basic met-ocean variables as measured during the cruise. The period during which the vessel was in sea ice is shaded in blue.*

During the outbound transit, one large midlatitude cyclone challenged the south-westerly routing of the vessel as it moved eastward across the intended route from Cape Town to the search area. This necessitated a significant westerly deviation in order to limit risk to equipment and passenger fatigue. Maximum significant wave heights of around 6 m and wind speeds of 40 knots were encountered as the vessel skirted around the north-western quadrant of the low-pressure system. It delayed arrival at the search by approximately 1 day. **Figure 6** shows the outbound cruise track overlaid on snapshot map of significant wave height. The signature of the midlatitude cyclone is seen in the area of large wave heights, and the westerly deviation taken to avoid it is evident.

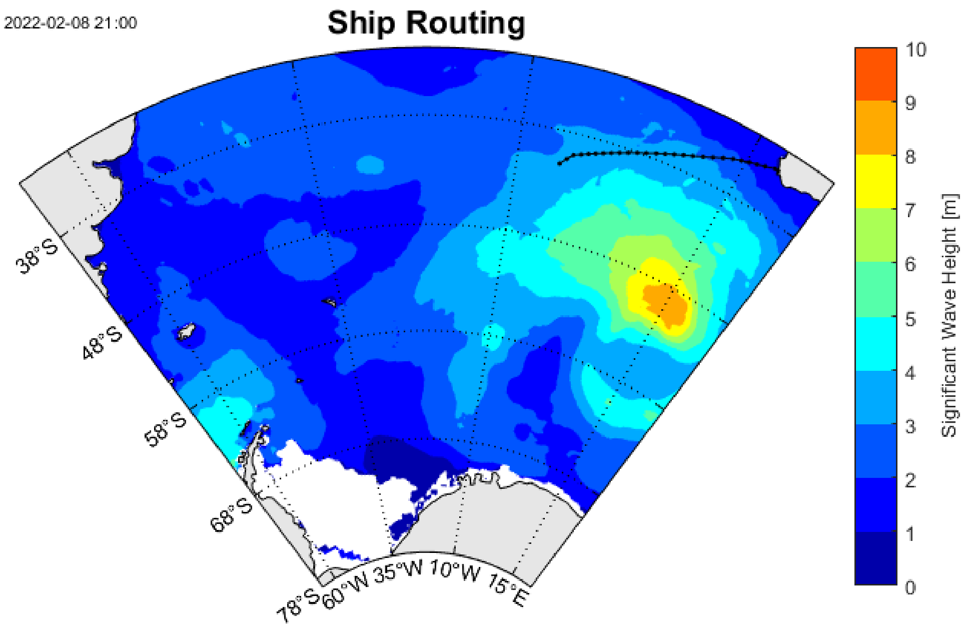

***Figure 6**. A snapshot map of significant wave height (in colour) showing the westerly deviation made during the outbound leg in order to avoid severe sea state associated with a strong midlatitude cyclone. The ship's track is shown in black*

During operations in the search area, two noteworthy cold events occurred, with temperatures at the lower limits of the climatological expectation. Temperature minima of -15.6 °C and -14.1 °C respectively were observed during these events. **Figure 7** shows observed temperatures overlaid on a 42-year daily climatology from ERA5.

During the outbound transit, two noteworthy midlatitude cyclones necessitated a more northerly initial routing prior to turning north-eastward to Cape Town. Maximum significant wave heights of around 4 m were encountered as the vessel passed around the western and north-western quadrants of these storms respectively. **Figure 8** shows the same as **Figure 6** but for the inbound cruise track.

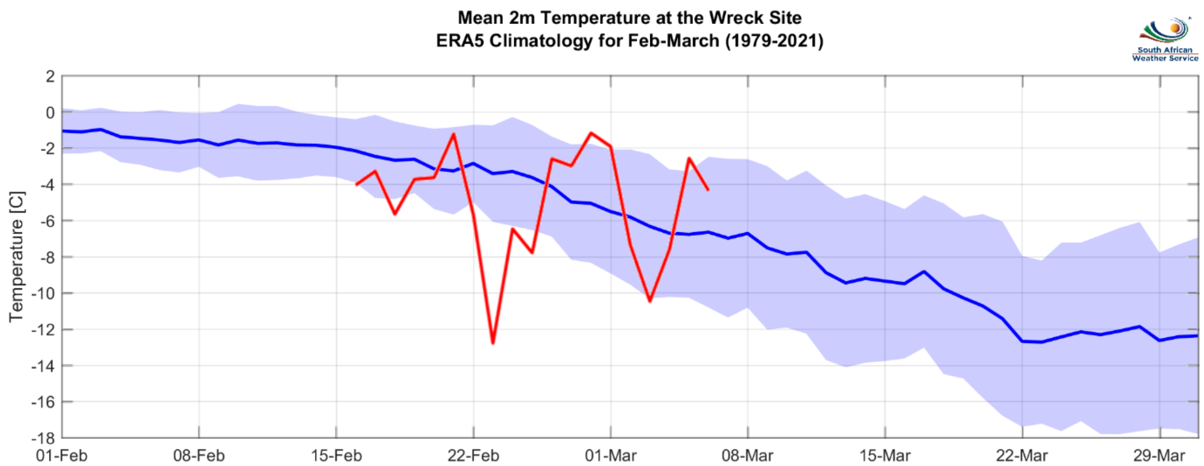

***Figure 7.** 42-year daily climatological mean for surface temperature (blue curve), variability about the mean (one standard deviation; blue shading) and measured temperature (red curve) in the vicinity of the wreck site. The two cold events are clearly evident.*

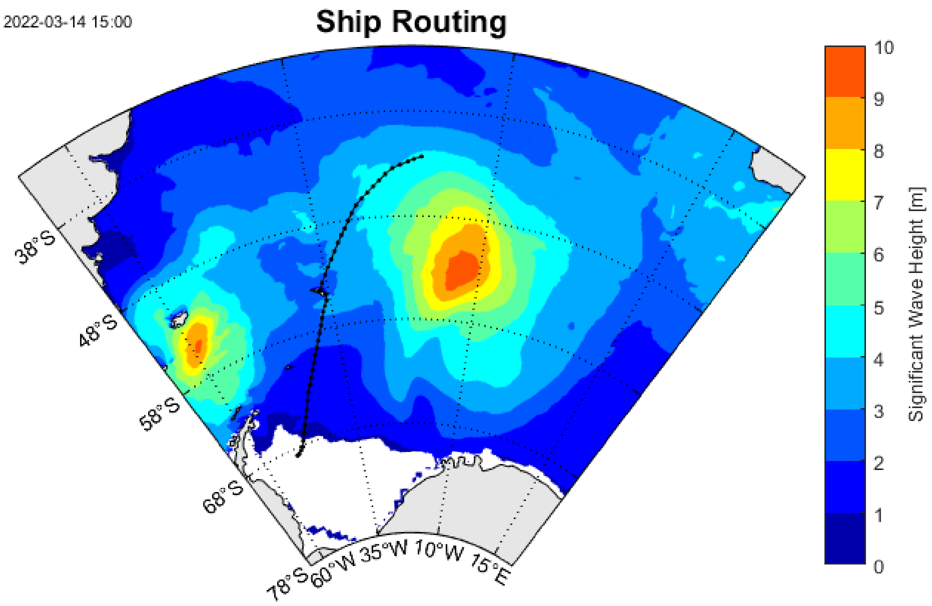

Figure 8. *A snapshot map of significant wave height (in colour) showing the northerly deviation made after departing from South Georgia in order to avoid severe sea state associated with a strong midlatitude cyclone. The ship's track is shown in black.*

4.3. General Sea-ice conditions

Written by Lasse Rabenstein (DNPS) & Alexandra Stocker (DNPS)

The western Weddell Sea encompass the largest areas of multi-year sea-ice in Antarctica. The reason is that sea-ice drifts for time spans of more than a year in the prevailing long-term ice drift pattern of the cyclonic Weddell Gyre (=WG). The WG transports sea-ice from the eastern Weddell Sea parallel to the Antarctic coastline westwards and eventually northwards along the Antarctic Peninsula before it is exported into the South Atlantic. Another reason for the existence of multi-year ice are air temperatures in the Weddell Sea which rarely exceeds the freezing point even in summer. This hampers melting of sea-ice from the top within the Weddell Sea. Average mean ice thickness of second-year ice in the western Weddell during summer can be more than 3 m in contrast to mean thicknesses of 0.8 to 1.5 m in the eastern Weddell Sea (Haas et al., 2008; Harms et al.,2001). The multi-year sea ice in the western Weddell Sea is interlaced with younger sea ice formed in polynyas at Queen Maud Land, the Filchner Ronne Ice Shelf and locally within the drifting sea-ice cover.

Compared to the expected average sea-ice conditions for February and March in the western Weddell Sea, namely large areas of thick multi-year ice, 2022 showed favourable conditions for the wreck search for the following reasons:

Ice retreat in the western Weddell Sea:
In 2022 the Weddell Sea sea-ice extent during the annual minimum in February was the 7th year in a row below the long-term average (see e.g. meereisportal.de). In 2022 this was specifically pronounced in the western Weddell Sea with an unusual southerly retreat of the ice edge. There was open water all the way from the Antarctic Strait down to Larsen C. The strong southerly retreat goes in hand with an unusually long southward drift of sea-ice between mid-December 2021 and mid-January 2022. During this period the AWI snow buoy 2021S114 drifted 40 nautical miles southward, against the long-term drift of the WD. In contrast to the

western Weddell Sea, sea-ice concentration was above average in the eastern Weddell Sea, which is counterintuitive to the usual westward drift of the WD and therefore a rare sea-ice situation. **Figure 9** illustrates the difference of sea-ice concentration between Feb 25 2022 and the mean of the Feb 25's of the five preceding years

.

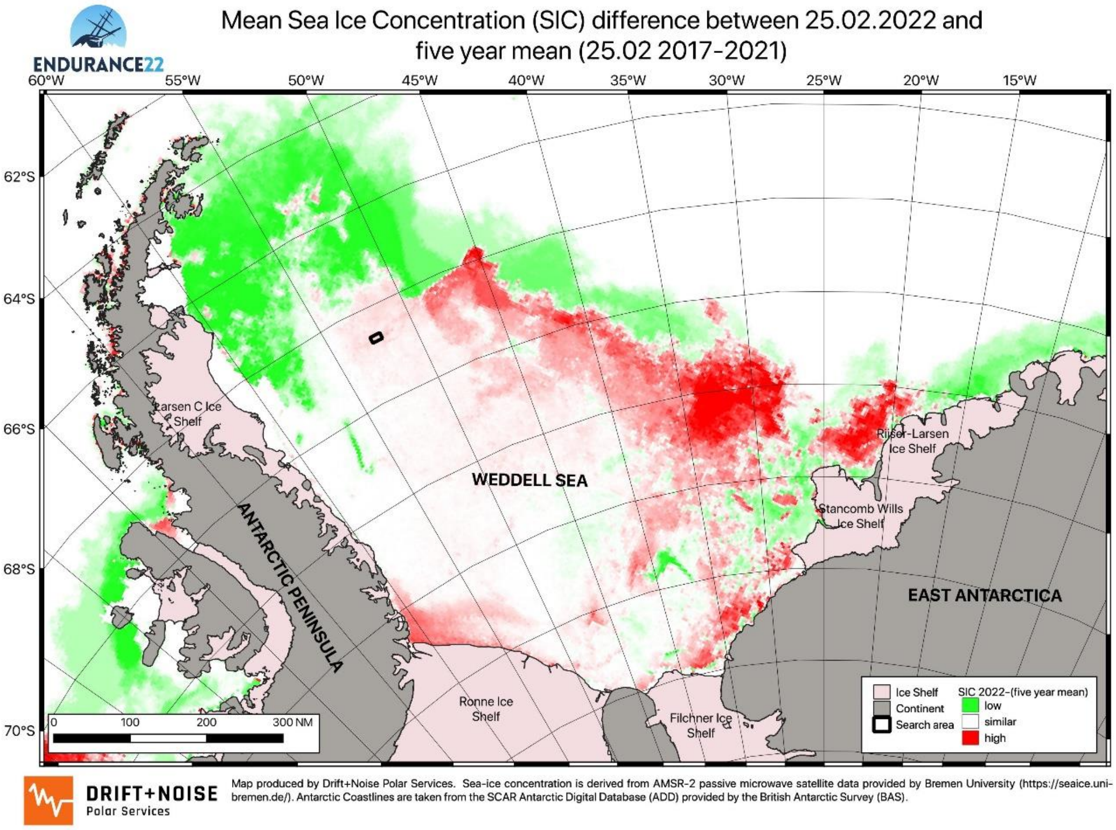

Figure 9: *Comparison of sea-ice concentration on the 25th of February, 2022, with the mean sea-ice concentration on that day of the years 2017-2021. Green colours show regions with less sea-ice in 2022 and red regions with more ice in 2022. This plot shows how exceptional the retreat of the sea-ice from the north westerly Weddell Sea was, compared to the 5 years average.*

Short distance to ice edge:

As a consequence of the western Weddell Sea sea-ice retreat in December and January, the distance from the ice edge of the marginal ice zone to the search area was only about 60 nm on February 15, from which less than 10 nm were in high ice concentrations >90% (see **Figure 10a**). On the way out 22 days later the sea-ice edge did drift slightly to the north and about 90 nm needed to be transited through sea-ice concentrations >90% until the end of the marginal ice zone was reached (see **Figure 10b**).

Ice regime encompasses significant amount of first-year ice

The ice regime in the search area was a mixture of first-year and multi-year ice, in contrast to a homogeneous thick second-year ice regime. This was visible on SAR satellite images where the thinner first-year ice mostly had a lower backscatter signature than the multi-year ice floes (see **Figure 11**). This fact is also expressed in a broad sea-ice thickness distribution function along the ship track (see 6.4) with a mode at 1.4 m.

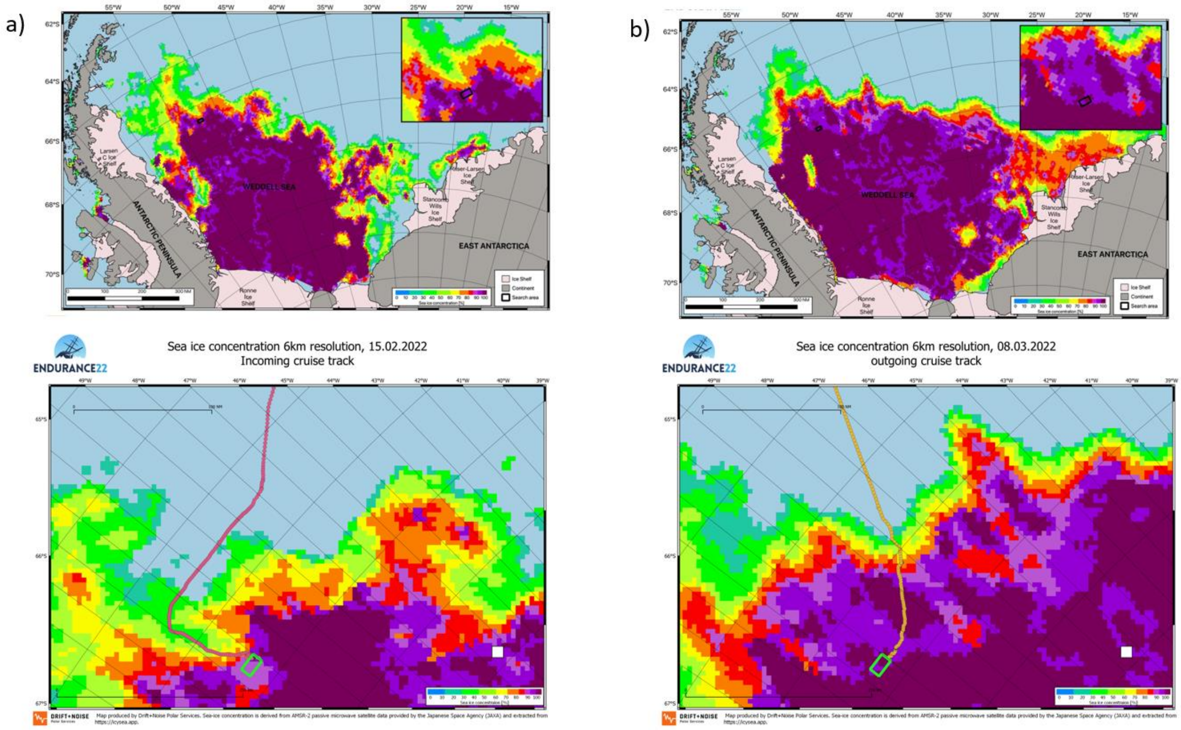

Figure 10: *Sea-ice concentration during the (a) incoming transit to the search box (green box) at February 15, 2022 and (b) during the outgoing transit at March 8, 2022. The incoming transit went through a large area of about 50% ice concentration and only 10 nautical miles traversing of >90% ice concentration was needed. The way out was along 70 nautical miles of >95% ice concentration, along open lead systems and 20 nm through a marginal ice zone of <90% ice concentration mainly consisting of brash ice.*

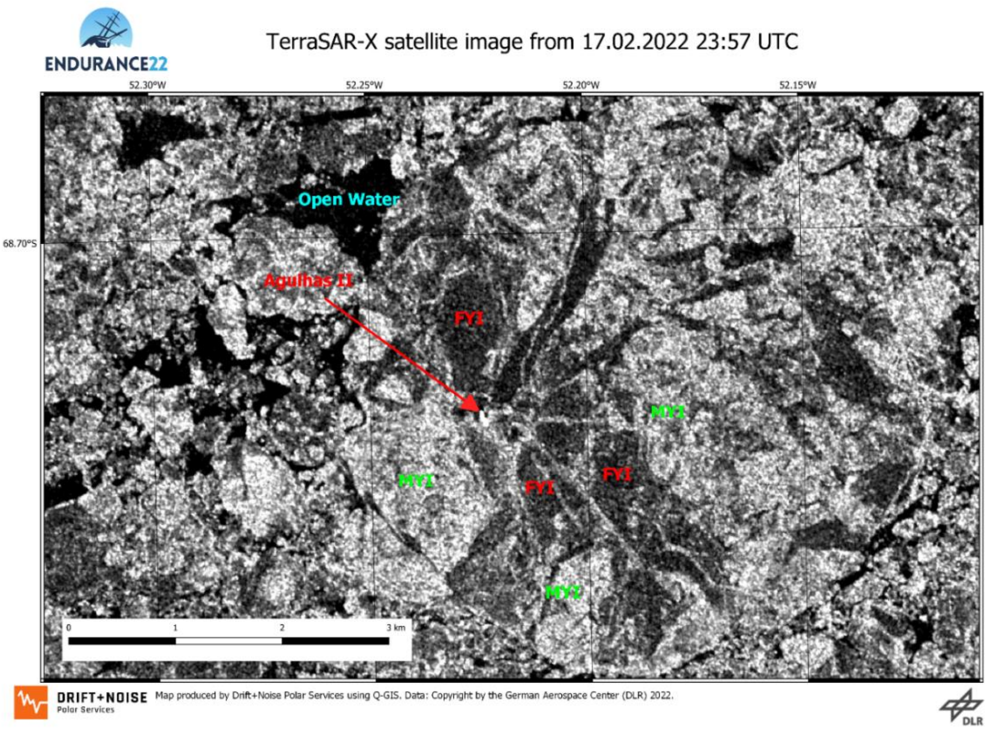

Figure 11: *A Terra SAR-X stripmap scene provided by DLR. The center of the image is dominated by a single ice floes which consists of differently old fragments. The darker patches were first-year ice (FYI) of less than a meter in thickness) and the brighter parts were second*

year ice of more than 1.5 m thickness. The very bright spot in the center of the floe is the Agulhas II.

Ice concentration was never a full 100%

It is interesting to note, that according to the POLARIS risk system and the U.S. National Ice Center Ice charts the entire region should not have been entered with a PC5 vessel (see **Figure 12** and **Figure 13**). However, manoeuvring with a PC5 ice strengthened ship in a mixed multi-first-year sea ice regime is possible when the ice concentration in an area is never exactly 100%. Even though the sea-ice concentration shows 80-100% for the “old ice” type for the search area in the ice charts in **Figure 12** and **Figure 13**, enough open leads (later refrozen open leads) were present to keep up the trafficability on an acceptable level, provided that detailed satellite remote sensing data were used to locate them. In fact, along the open leads vessel speeds of more than 6 or 8 knots were possible. The work done on the bridge by the science team to support the ice navigation, resulted in avoiding thick ice floes and navigate as often as possible in open leads.

Figure 14 and **Figure 15** show typical ice situations at February 8 and February 16 from space via a LandSat optical satellite image and from helicopter, respectively. Those ice conditions caused almost no navigational limitations to the Agulhas II as long as the larger floes could be avoided.

Later into the search at the beginning of March the ice regime changed slightly to more larger ice floes with fewer open leads. Most of the open leads were then refrozen to a thickness which already prevented fresh fallen snow from melting (**Figure 16**). At this stage the ice cover became rigid enough to react on wind driven pressure with long elongated crack systems ranging several nautical miles wide. Some of them could be identified and used as navigational pathways (**Figure 17**).

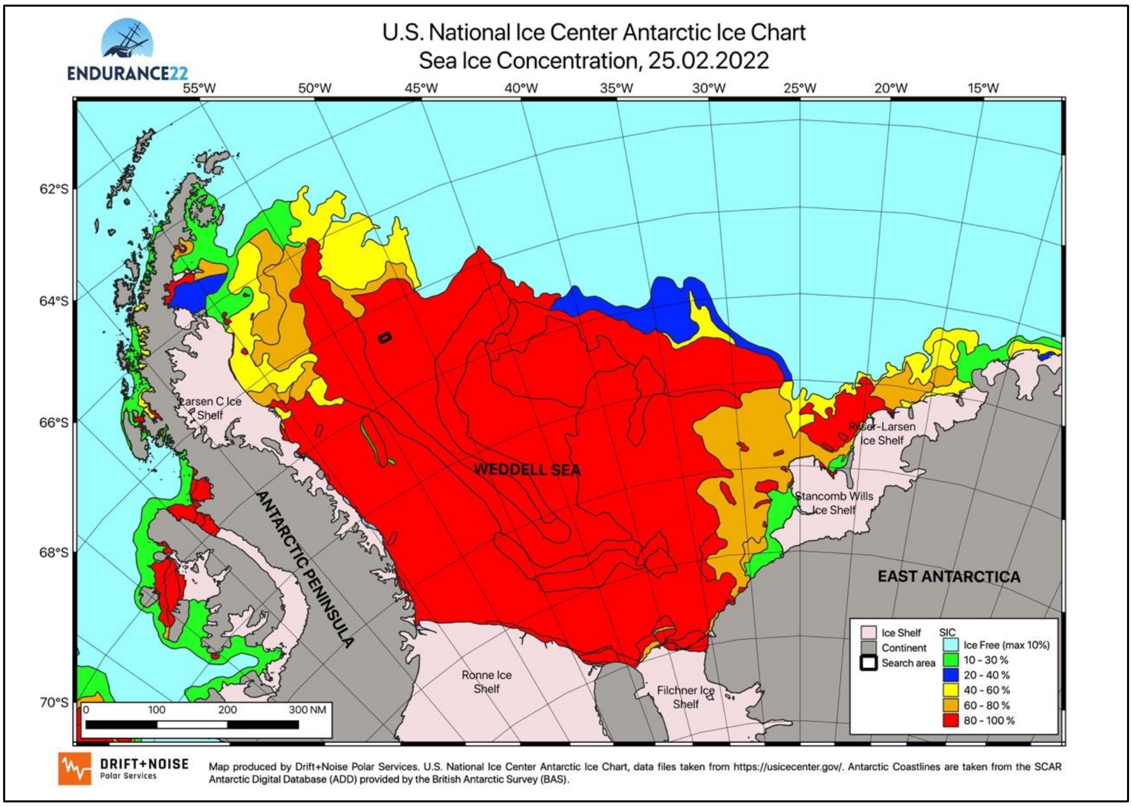

Figure 12: *Weekly sea-ice concentration chart from February 25, 2022, data provided by the U.S. National Ice Center. Red polygons refer to ice concentrations above 80%.*

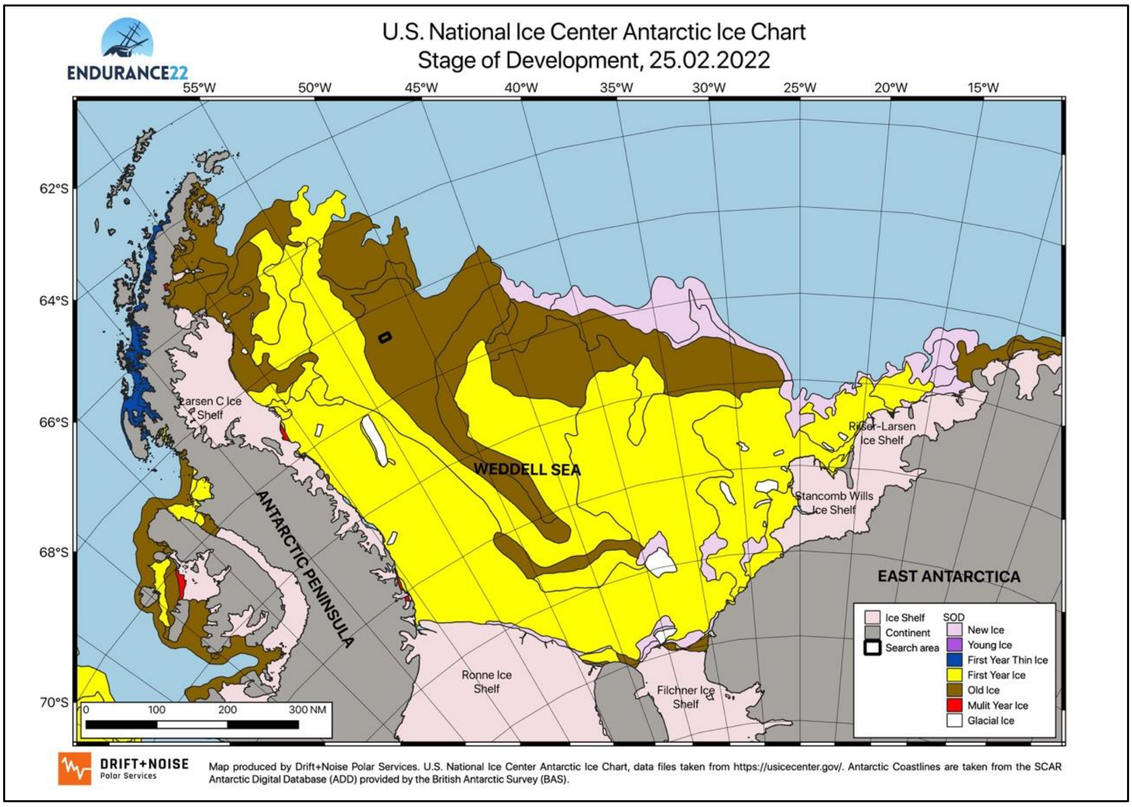

Figure 13*: Weekly stage-of-development ice chart from February 25, 2022, data provided by the U.S. National Ice Canter. Brown polygons refer to regions with a dominant multi-year ice regime and yellow regions to dominant first-year ice regimes.*

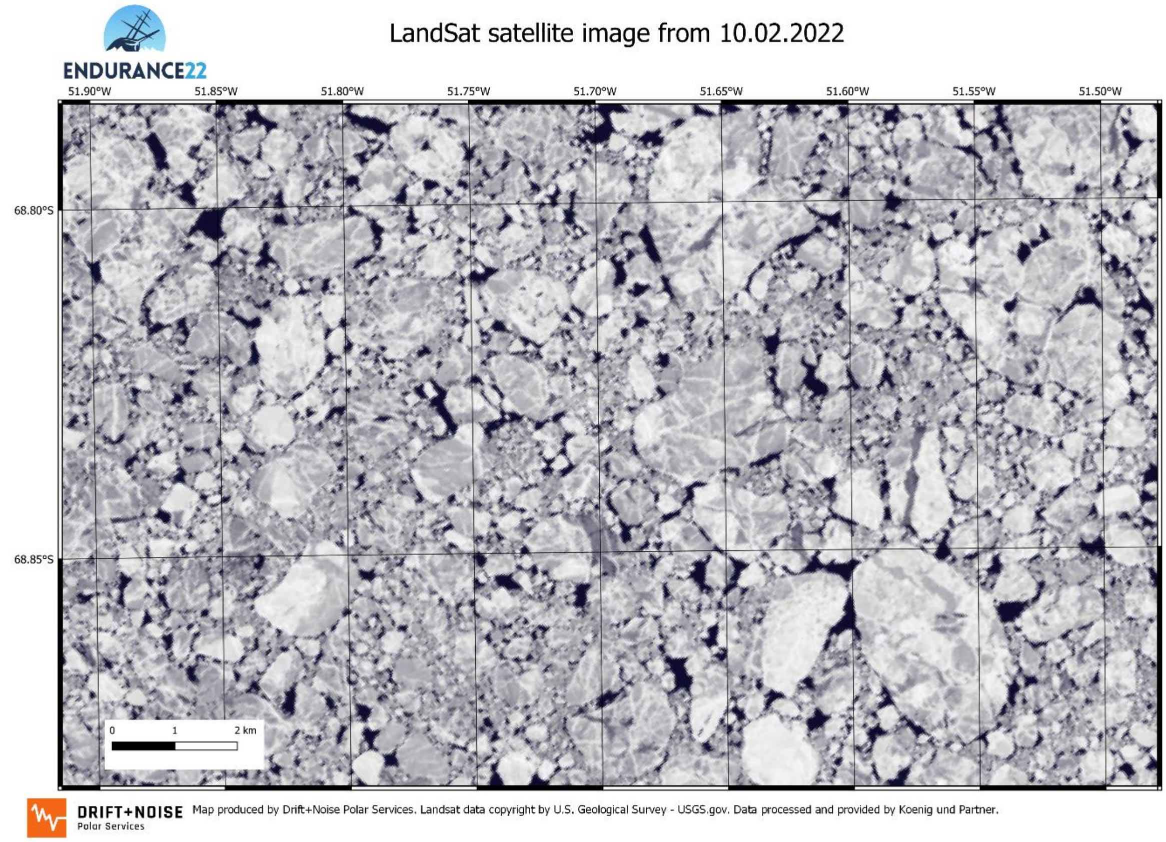

Figure 14: *Optical satellite image from the US Geological Service LandSat 8 mission recorded on February 8, provided and processed by Koenig und Partner. The displayed sea-ice situation was typical for the sea-ice situation at the beginning of the wreck search . Some larger ice floes surrounded by a conglomerate of smaller floe fragments and open leads in between.*

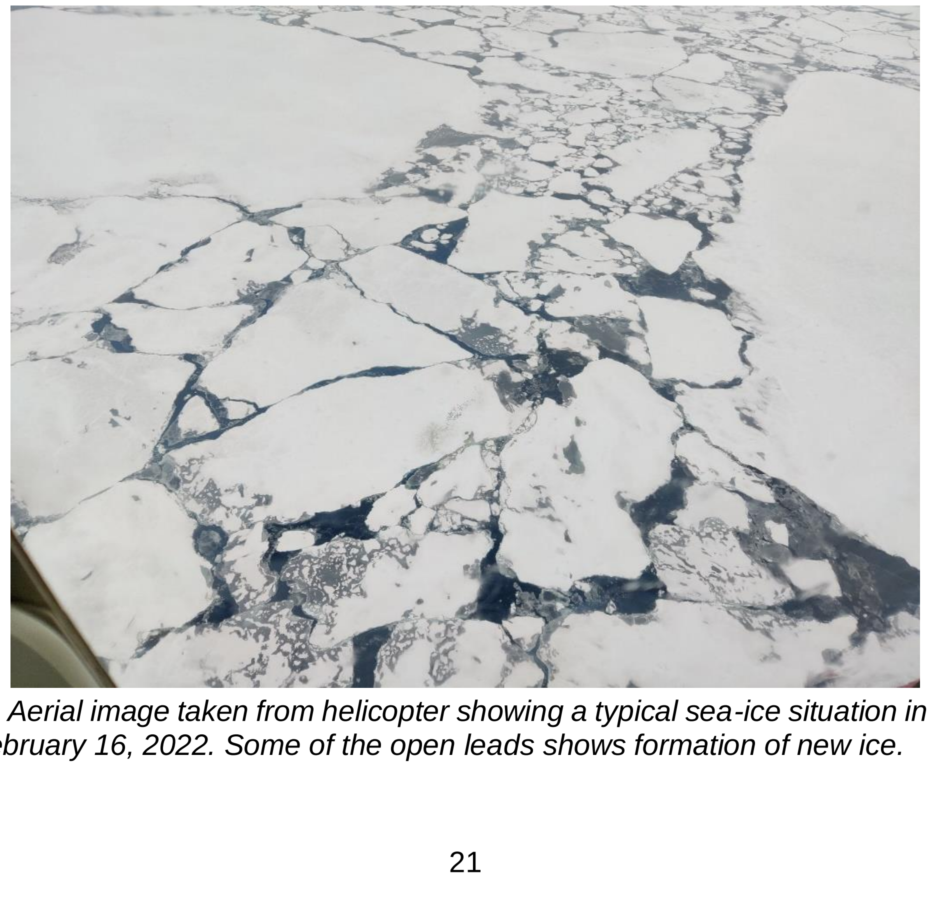

Figure 15: *Aerial image taken from helicopter showing a typical sea-ice situation in the search area on February 16, 2022. Some of the open leads shows formation of new ice.*

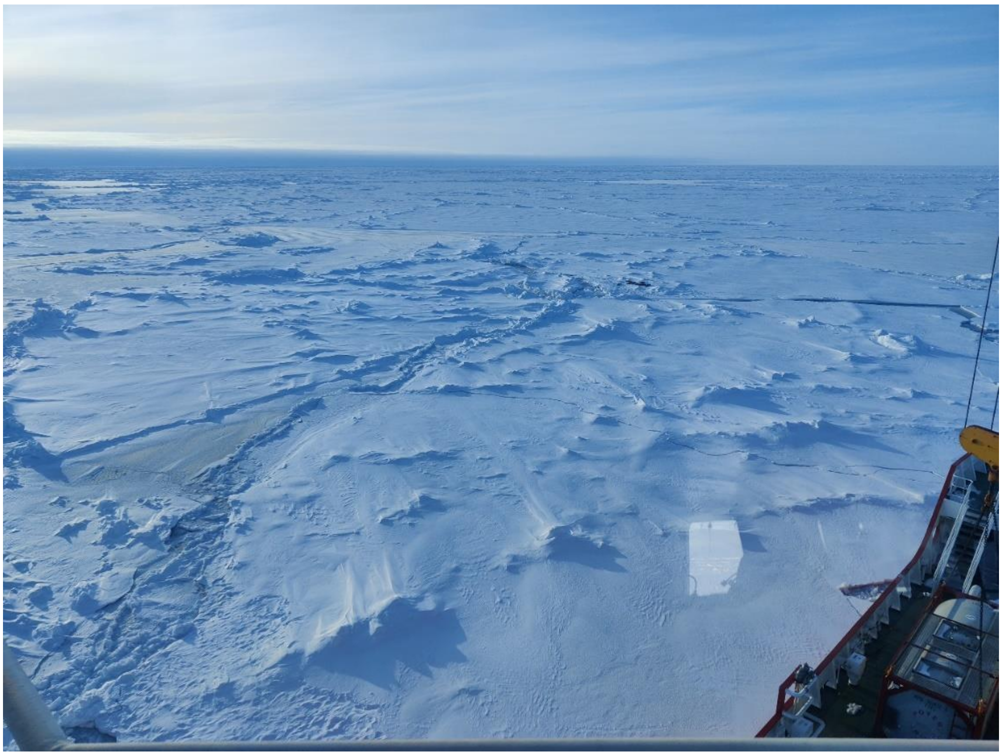

***Figure 16**: A typical sea-ice situation in the search area at the beginning of March 2022 photographed from the bridge of Agulhas II. Most of the sea-ice features are covered with freshly fallen and wind transported snow. The refrozen leads are still visible on this photograph.*

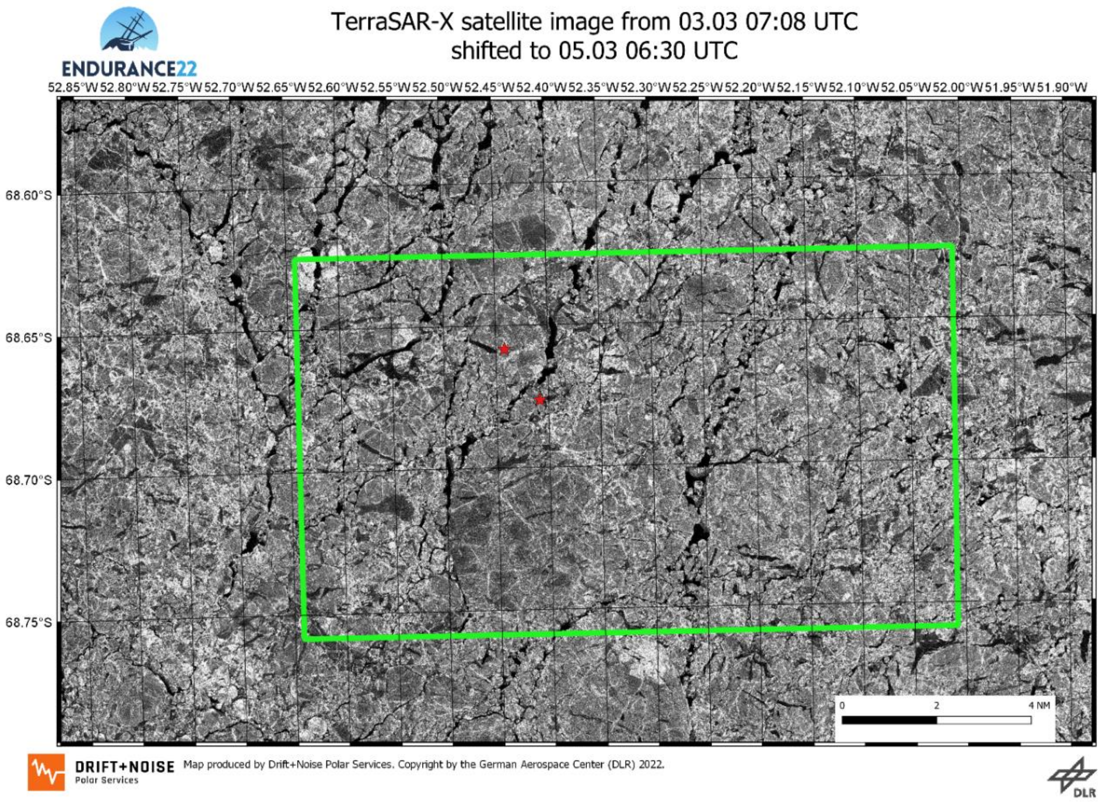

***Figure 17:** A Terra-SAR-X scene provided by DLR taken on March 2, 2022. In contrast to the sea-ice situation during mid-February, with a lot of smaller open water spots in between larger floes, in March fewer but longer cracks and open leads served as pathways for the Agulhas II. They can be identified as longer black elongations in the image.*

Comparison to the 2019 Weddell Sea expedition

In contrast to the Endurance22 expedition, the ice navigation was reportedly more difficult during the 2019 Weddell Sea expedition with the same ship. Interestingly in 2019 the Agulhas II approached the wreck site from the east whereas in 2022 the wreck site was approached from the north. The reason for the different approaches is visualized in **Figure 18**. Compared to 2019 in 2022 the regions north of the Wreck site were to a large degree even ice free (solid green colour in **Figure 18**) whereas the regions east-southeast of the wreck site showed less ice in 2019 than in 2022 (red colours in **Figure 18**). In consequence the Agulhas II had to travel a much farther way through closed ice in 2019 than in 2022. The bridge crew also reported that in 2019 the ice regime consisted mainly of second-year ice and had less first-year ice inclusions.

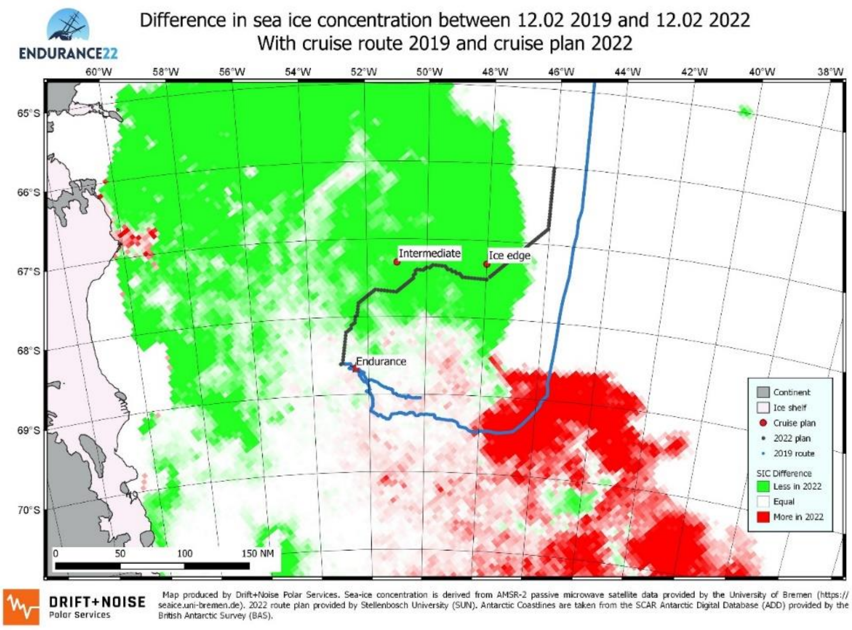

Figure 18: *Comparison of the sea-ice concentration on February 12, 2022 and 2019. Green areas had more sea-ice in 2019 and red areas had more sea-ice in 2022. Whitish colours refer to no substantial difference in sea-ice concentration between the two years. Naturally, the cruise track in 2019 avoids green colours and the 2022 cruise track avoids red colours. It is obvious that in 2022 the Agulhas II had to transit a much shorter distance through the dense ice cover and the Endurance wreck site.*

5. Operational Support of the Ice Navigation

5.1. Satellite Remote Sensing

5.1.1. SAR images

Written by Thomas Busche (DLR) & Dmitrii Murashkin (DLR)

Radar satellite imagery from 3 different missions were by far the most important remote sensing information source to assist the vessel command navigating through the dense pack ice during the Endurance22 expedition. The radar sensors utilize electromagnetic waves at a wavelength in the cm range, and in opposite to wavelength of optical sensors in nanometer range, are capable of penetrating dense cloud cover. In addition, radar waves can penetrate through dry snow cover and deliver visual information about the underlying sea ice, and to a certain amount allow the discrimination of different ice types.

The involved radar sensors and processing steps for the received radar imagery is described in the following.

Terra SAR-X

The TerraSAR-X mission started its operation in June 2007 with the launch of the TerraSAR-X (TSX) satellite from Baikonur. In June 2010 TSX got a twin in orbit, the TanDEM-X (TDX) satellite. Both satellites, build by AIRBUS Defence & Space (former: Astrium), feature a Synthetic Aperture Radar (SAR) instrument with a phased array radar antenna with 384 transmit and receive modules operating at X-band frequency (wavelength 3.1 cm, frequency 9.6 GHz). The two satellites are flying at an orbit height of 514km in a sun-synchronous polar orbit. A complete period (= one complete revolution around Earth) takes approximately 95 minutes. The revisit cycle of the satellite is 11 days. This means that for a given point on Earth the satellite is in the exact same range, and observes the point in the same imaging geometry every 11th day. For the latitude of the Endurance wreck location the satellite can on average capture 2 images a day in ascending or descending pass direction, with only one day in a 11 day cycle without any visibility. The satellite allows different imaging modes, but the spatial resolution is always a compromise to the swath width/area coverage. The satellite also provides polarisation options, and data can be ordered in single polarisation (=one channel) in VV, HH or HV polarisation, or in dual polarisation mode (=two image channels), with combinations of either HH-VV, HH-HV, or VV-VH (StripMap and Spotlight only). The dual polarisation would be normally preferred, as a second channel allows a better discrimination of sea ice feature and ice types, but compared to a single polarisation mode, the acquisition in dual pol mode reduces the spatial resolution, and the swath width by about 50%.

The ground segment of the TerraSAR-X mission is operated by the German Aerospace Center (DLR). The exclusive commercial exploitation rights for the TerraSAR-X mission are held by AIRBUS DS, while DLR serves the international science community. Access for scientific use of the satellite can be accessed through a proposal submission and evaluation procedure via DLR's TerraSAR-X science coordination (https://www.sss.terrasar-x.dlr.de/). A research proposal was submitted by the attending DLR personal to the Science Coordination in the fore field of the expedition for the Endurance22 research team. Acquisition time for the wreck location is between 6 - 7 o' clock in the morning, and around midday.

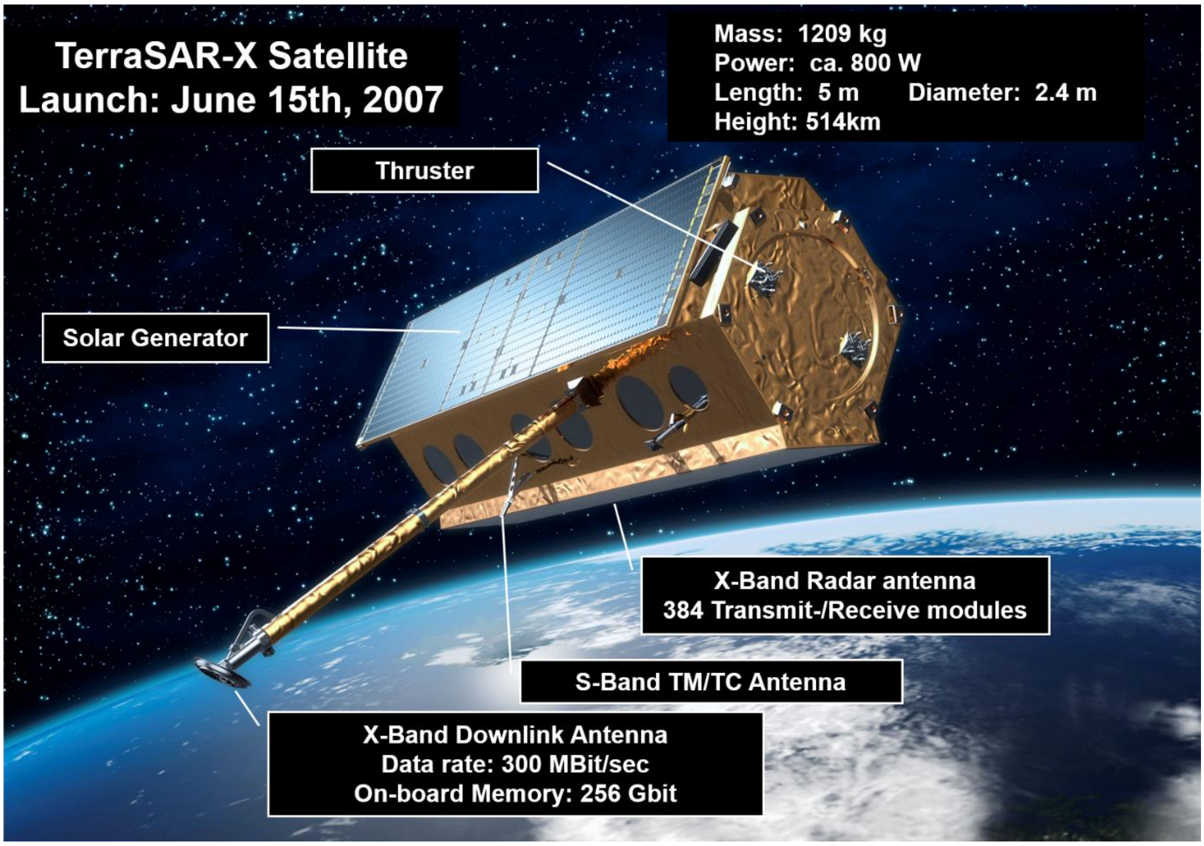

Figure 19: *The TerraSAR-X satellite*

Side looking Imaging Geometry and Imaging Modes:
A compromise between swath width and resolution

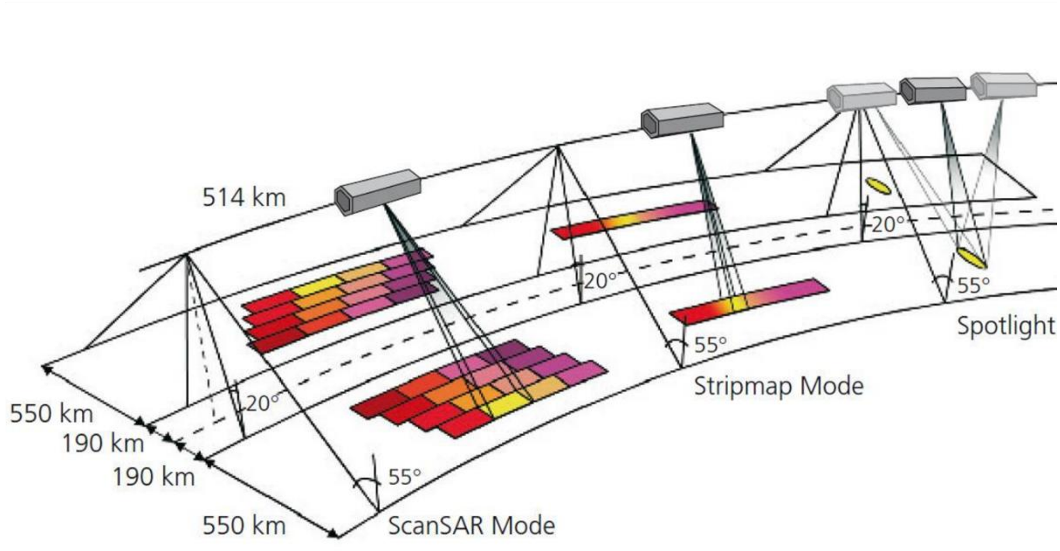

TerraSAR-X/TanDEM-X Imaging Modes:

- ScanSAR: Swath width 100-200km, Resolution 12-20m
- StripMap: Swath width 15-20km, Resolution 2.1 – 3.5m
- Spotlight: Swath width -8km, resolution 1-2m, Variants: High Resolution Spotlight, Staring Spotlight

Figure 20*: TerraSAR-X imaging geometry and imaging modes*

The tasking of the satellites acquisitions was performed on board the ship by DLR operators via a web based interface (https://eoweb.dlr.de/egp/). Ordering has to be done latest 17 hours before the planned UTC acquisition time. During the whole expedition time about 61 scenes were ordered from and received on the ship; 55 were successfully acquired, six orders failed due to technical problems, e.g. during downlink or due to system maintenance (Success rate was at ~90%). The majority of the data sets were downlinked at the DLR receiving station in Neustrelitz (NSG), but also at DLR partner stations in Svalbard (SGS) and Inuvik (INU). The data was ordered with a high priority (6 or 7) with a so-called predicted orbit. This assures a fast processing and delivery through the ingesting of the SAR raw data in the near real time processing chain in Neustrelitz. The delivery time from acquisition over download and processing to the DLR delivery server took between 3 and 12 hours. The download to the ship was performed via the Inmarsat satellite internet connection of AgulhasII, either via FTP, or via direct copy from DLR ground segment server via VPN. The nominal data rate of this internet connection is on AgulhasII in the range of 8 MBsec and was increased for the Expedition to 15Mb/sec (at additional cost of the expedition organizer). The DLR operators got a privileged internet connection for download, the true download rate was typically via FTP at ~0.7MB/sec, and via VPN/direct copy at ~0.3MB/sec. Data rate during night and early morning was clearly faster than during business hours. It is worthwhile to note that the TerraSAR-X data was downloaded and transferred to the vessel for the first time in its original L1B format (with all annotations and axillary files), means without any additional compression and resolution reduction (quicklook format) for ship transfer, in order to utilize the full spatial resolution for the ship navigation in dense pack ice. Main imaging mode for the majority of the data sets was 4beam ScanSAR (SC) with a swatch width of 100 km and a swath length of 150 km, in order to always cover the complete search box with some margin to East and West. Some data sets were acquired in 6beam WideScanSAR, StripMap (SM), as well as in Spotlight Mode (SL). Polarisation mode was always single pol VV (=vertical transmit, vertical receive), with one exception, as one Stripmap scene was acquired in Dual Polarisation mode. The total size of all TerraSAR-X images transferred to the vessel during the whole expedition is in the range of 200GB.

After downloading the radar data undergo the following processing steps on board:

- Reprojection: The data was reprojected from a geographic coordinate sytem to a cartesian coordinate system, the map projection used was UTM 22 South (EPSG code 32722
- Mosaicking: Due to the length of the data sets, the delivery unit for a single acquisition contains several subscenes; depending of the North-South extension and the imaging mode, the number of subscenes was in the order of 2-4.
- Byte scaling: The original 16bit data was scaled to an 8bit representation in order to allow display on normal monitors (which run on 8bit). This step comes with a contrast stretch a better representation in the GIS
- Final Transfer to shared folder: The final scenes were transferred on a shared folder, where the sea ice operations team was able to load the data into a GIS. Arrivals of new scenes were announced via WhatsApp notice

Please note: The TerraSAR-X images in the data section of this report are processed towards a good visual representation in the GIS. However, the bytes scaling alter the grey value statistics of the original file. No meaningful physical quantity can be derived from that modified grey values. If you need the data for a comparison between the original backscatter (so called sigma nought) value of the SAR and in situ measurements (e.g sea ice thickness), access to the original files is needed. Please contact DLR (see contact section), the original data sets can be provided on request.

Image Examples:

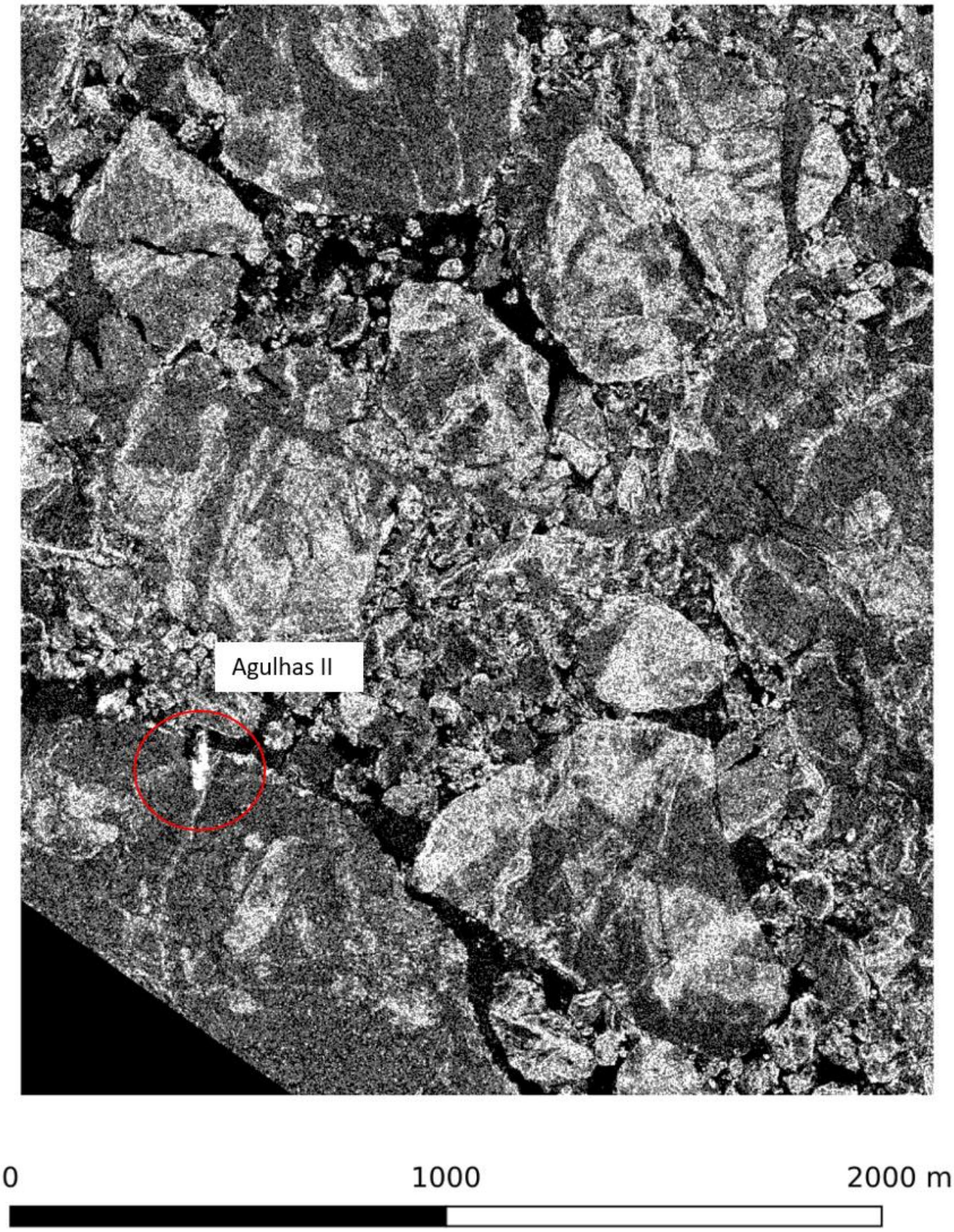

Figure 21: *TerraSAR-X Spotlight scene acquired on 20220220T070827 UTC, subset with Agulhas II, anchored at an ice floe.© 2022 German Aerospace Center (DLR)*

***Figure 22**: Agulhas II anchored at a sea ice floe. drone image, at the position where it was captured by the TerraSAR-X satellite on 20220220T070827 UTC. Image courtesy of Dmitrii Murashkin, DLR, 2022.*

Sentinel-1

Sentinel 1 is a constellation of two Synthetic aperture Radar satellites, Sentinel-1A and Sentinel-1B, operated by the European Space Agency (ESA) in the frame of the COPERNICUS programme. The two satellites, launched in 2014, and 2016, are operating at C-band frequency (5.405 GHz, 5.55cm), and similar to TerraSAR-X and TanDEM-X, in a sun synchronous, near-polar orbit; flight altitude is 693km, repeat-cycle is 12 days. The satellite mission offers several imaging modes: A Stripmap mode (5x5m resolution, and swath width of 80km), and 2 Wide-Swatch Modes, all available in single or dual polarisation configurations. The Interferometric Wide-Swath Mode has a swath width of 250km (at a resolution of 20m), while the Extra-Wide-Swath Mode has a swath width of 400km at a resolution of 20x40m. The Sentinell-1b satellite is since December 2021 out of operation.

During the Endurance22 expedition 10 Extra-Wide-Swath Mode scenes could be received on Agulhas II through the Icy Sea App from Drift & Noise, with full or partial coverage of the wreck location. The scenes, downloaded through the app, do not need any further processing, and can be directly injected into the GIS system. Temporal coverage was due to the failure of the Sentinel-1b satellite not really sufficient, with an image every 3 to 5 days. Due to the coarser resolution of 20x40m and low temporal coverage of the target area the other SAR satellite sensors were preferred for ship navigation in the search box at the wreck location.

ICEYE

During the cruise the expedition received on no cost Synthetic Aperture Radar data for ship navigation from ICEYE. ICEYE is a Finnish startup and microsatellite manufacturer, and was founded in 2014 as a spin-off of Aalto University's University Radio Technology Department, and is based in Espoo. The company represents a new generation of private enterprises in the so called ‘New Space’ sector. The new generation of satellites are cost effective, and light weight. The first ICEYE radar satellite was launched in 2018. Until now the company has

launched a fleet and constellation of 14 satellites (status in 2021), more are still in the pipeline. ICEYE offers a customer service for tasking image acquisitions on request for all kind of commercial, scientific and military applications. The SAR satellites have a weight of around 100kg, a fraction of elder last generation SAR satellites operated by state-based satellite agencies. The SAR satellites operate at X-band frequency, flight altitude is between 560 to 580 km, the polarisation is single polarisation in VV configuration only. Imaging modes are comparable to TerraSAR-X, ScanSAR, StripMap and Spotlight mode are currently offered. The satellite constellation allows for each point on earth an unprecedented short revisit time, several images a day are possible.
During the Endurance22 expedition 32 ICEYE scenes were provided for no cost by the company, 28 in StripMap mode, 4 in Spotlight mode. The delivery package always contained a couple of images acquired over some days. Some of the images were used within the Ice Information System on the bridge. The SAR data was processed in a similar way as the TerraSAR-X scenes. Image quality was all over good, and the usability for ice navigation on the same level as TerraSAR-X.

Figure 23 and **Figure 24** show an ICEYE image example for a Stripmap scene acquired by the X7 satellite on 2022-03-04 at 02:56:38 UTC. The image shows a large ice floe with a diameter of 8-10km. The Agulhas II has “parked” during the night to the West of the floe. Incorporated in the ice floe is an iceberg.

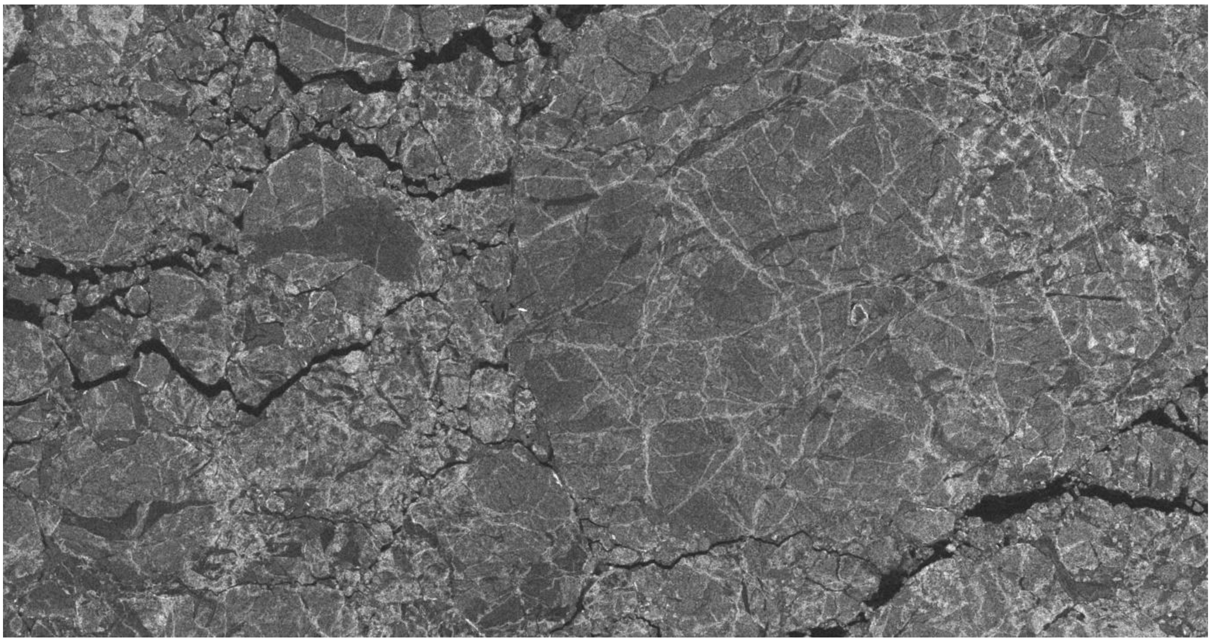

Figure 23: *ICEYE X7 Stripmap image subset, acquisition UTC start time 20220304T025638 2022 © ICEYE Oy. Copyright in all ICEYE Products and Derivatives is and will remain held by ICEYE Oy.*

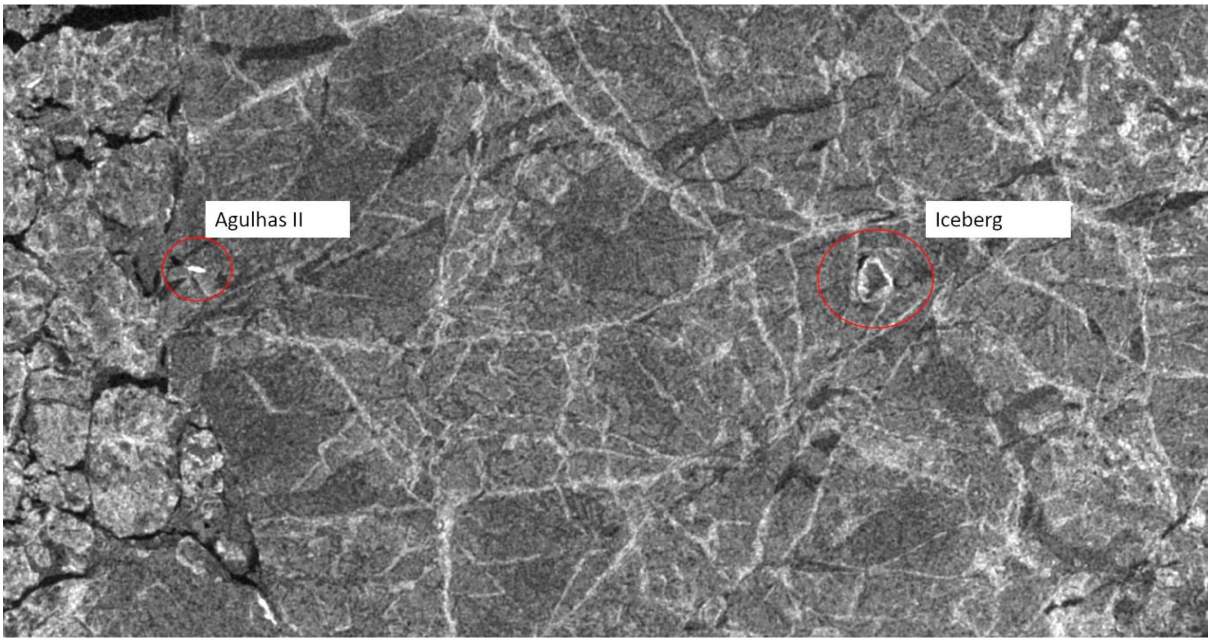

Figure 24: *Zoom in to ICEYE X7 Stripmap image subset, acquisition UTC start time 20220304T025638. 2022 © ICEYE Oy. Copyright in all ICEYE Products and Derivatives is and will remain held by ICEYE Oy.*

5.1.2. Optical images

Written by Lasse Rabenstein (DNPS)

Optical satellite images are passive recordings of the earth surface in the visual and infrared spectral bands. They provide an excellent additional information and interpretational help for SAR images of sea-ice. However, the biggest disadvantage is that optical images do not penetrate clouds and depend on sunlight. As a 10/10 cloud cover accompanied the Endurance 22 expedition in most days, the use of optical images was of less operational value compared to SAR images. Nevertheless, the few times a cloud free optical satellite image could be obtained, it excellently served to identify larger compact ice floes which the Agulhas II needed to avoid. Such images could even be used for the subsequent 10 days for tactical navigation, as with the known drift of the ice pack, they could be translated to the real time position. This only worked as long as the relative position of the larger ice floes to each other did not change significantly, which was luckily the case during Endurance 22.

MODIS

The expedition utilized the twice daily available MODIS optical true-colour images provided by NASA's EOSDIS and recorded by the two NASA satellites Terra and Aqua.

Planet Labs

The Expedition received an promotional image (at no cost) from planet labs, acquired on 2022-02-20 at 12:02 UTC at no cost.

Figure 25: *Optical satellite image (20220220T120200 UTC), subset showing the AgulhasII anchored to a sea ice floe , © Planet Labs, 2022.*

5.1.3. Level 3 Data

Classified Sentinel-3

Written by Thomas König (KuP) and Christine König (KuP)

The Endurance22 expedition provided the first opportunity to extensively test K&P's optical/thermal sea ice classification for practical use and to collect in-situ comparative data. For this purpose, classified data sets were created daily in near real time from up to 4 satellite overpasses and transmitted to the Drift & Noise Company, from where they were transferred to the expedition vessel S.A. Agulhas II in Antarctica via their mobile phone application IcySea. Delivered products contained a combination of up to four consecutive SLSTR scenes, covering more than 1400x1200 km^2 each. The ice classification preserves the original spatial resolution of SLSTR-images of app. 500 m. The type of classification-processing deals with measurements collected separately within 9 spectral channels, so that ice structures are represented without degradation in the classified products. In total, more than 80 products were provided before and during the expedition in order to make the ice situation in the near and far surroundings of the ship assessable for the expedition members. This allowed Drift & Noise to gather information on the development stage of sea ice and snow conditions in the cloud-free areas of the Weddell Sea and integrate this information into the research workflow and navigation support.

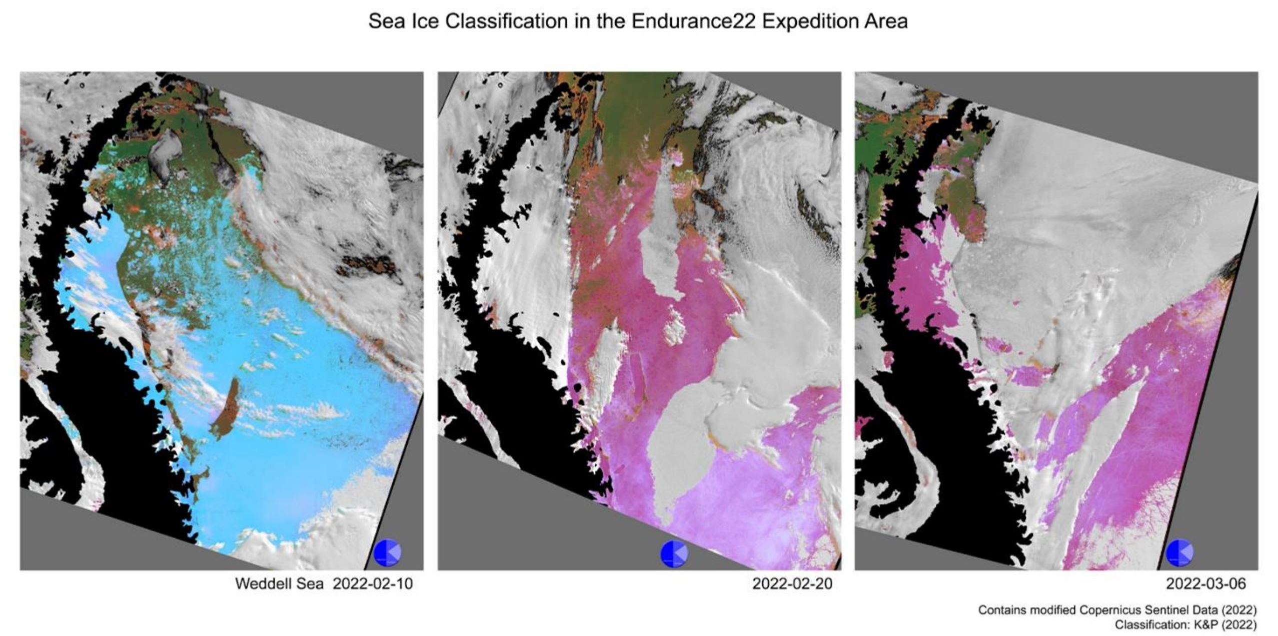

Figure 26: *Examples of sea ice classification products of K&P provided during Endurance22 expedition.*

K&P's sea ice classification is sensitive to sea ice thickness in case of (nearly) snow free ice up to approx. 40-50 cm. In case the ice is covered by snow, the information of this coverage is dominant. The classification of about 18000 Sentinel-3 (Arctic as well as Antarctica) scenes showed the following stable ice-classes:

Figure 27: *Legend explaining major ice class colours used for K&P's SLSTR based sea ice classification*

Sea-ice concentration

Written by Lasse Rabenstein

Sea-ice concentration was provided through the IcySea App (https://icysea.app) where it is generated automatically on the basis of satellite based passive microwave measurements provided by the Japanese Space Agencies AMSR2 sensor of the GCOM-W mission. The GCOM-W satellite circulates the earth 14.5 times a day (=14.5 revolutions per day). Due to its polar orbit, it crosses the poles during every revolution. The AMSR-E sensor records the passive microwave radiation on a stripe of 1450 km width (so called swath width). The data are thankfully provided by JAXA after every revolution, which enables so-called swath updates several times a day. The conversion from passive microwave data to sea-ice concentration uses the ARTIST sea-ice algorithm from Spreen et al. (2008).

Sea-ice concentration is a low-resolution information layer for strategic planning purposes and to assist the interpretation of SAR images. It is updated several times a day, automatically created and therefore to be used with care. During Endurance 22 sea-ice concentration was available with a pixel resolution of 6.25 x 6.25 km^2 or 3.125 x 3.125 km^2 , respectively, where each pixel shows the fractional area in percent (%) which is covered with ice. Sea-ice concentration was of limited use for operational purposes once the vessel was inside the closed sea-ice cover. However, it was still a useful data layer for strategic planning and to monitor the distance of S.A. Agulhas II to the ice edge. Example sea-ice concentration data are shown in **Figure 10**.

5.2. Met-ocean Forecasts and Observations

Written by Marc de Voss (SAWS) and Carla Ramjukadh (SAWS)

5.2.1. Wind forecasts and observations

As the primary driver of the ice drift, the bridge and sub-sea teams were kept appraised of predicted wind shifts in order to adjust their positioning and deployment plans accordingly. Since wind is implicitly included in the sea ice forecasts provided by the sea ice team, it was useful to compare projections and align advice to the operational teams in this regard.

5.2.2. Tide forecasts

Early in the cruise, the SAWS team was requested to provide a tide forecast for the search area. The TPXO 9.0 global tidal model was selected for this purpose. 11 harmonic constituents were extracted, and forecasts generated using these constituents. Tidal water levels were noted to affect the contraction/expansion of the ice pack, which affected ease of deployment and recovery of the AUV. Tidal information was thus utilized by the bridge and sub-sea teams to plan positioning and deployment. Initially, a 5-day forecast was provided, and extended upon request, with a forecast covering the entire operational period being provided. This lead time is made possible due to the high level of predictability of the tide and the harmonic reconstruction procedure use to generate the forecast. **Figure 28** shows the mixed semi-diurnal tidal signal which characterises the area.

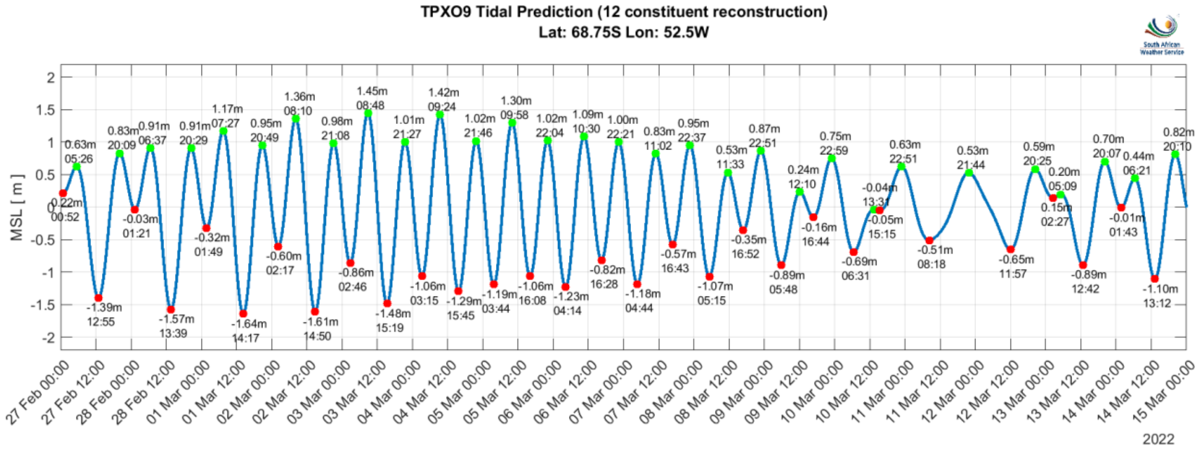

Figure 28*.Long-range tide forecast for the search area. Elevations are referenced to mean sea level.*

5.3. Ice Drift Forecasts

*5.3.1.*PRIIMA

Written by Panagiotis Kountouris (DNPS)

What is PRIIMA

PRIIMA (PRedicted Ice IMAges) is an algorithm developed in 2018 during an ESA Kickstart program, and since then it is continuously maintained and further developed by Drift + Noise. It merges ice drift or wind forecasts as driving forcing, with static Synthetic Aperture Radar (SAR) images, in order to produce high resolution sea ice forecasts, and ice drift trajectories. The unique points of PRIIMA are a) converts static satellite images into “real-time” sea-ice forecast information and b) converts ambiguous and cumbersome forecast data into actionable and easy to understand information.

Figure 29 describes in detail the system architecture, showing the input and output streams as well as the different processors and methodology implemented into PRIIMA.

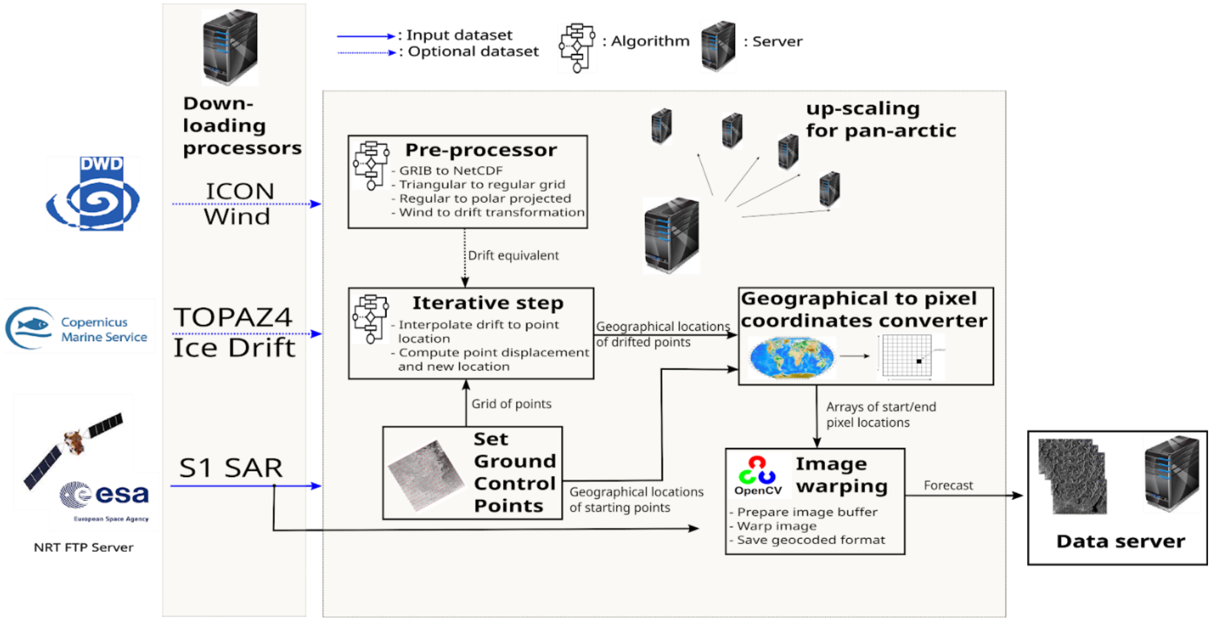

Figure 29*: PRIIMA system architecture*

Input data and parameters

For the Endurance22 expedition we used the following data products as input to PRIIMA:

1. Synthetic Aperture Radar images (SAR) from the Sentinel-1 satellite at 30m spatial resolution, operated by the European Space Agency (ESA).

2. Wind fields from the global weather prediction model ICON operated by the German weather service (Deutsche Wetter Dienst, DWD) which comes with a native grid resolution of 13km and a temporal resolution of 1 hour. In particular we have used the 10m u, v horizontal wind velocities at an hourly temporal resolution.

Data delivered on board for Endurance22

PRIIMA was delivering 4 times a day, updates of sea-ice drift trajectories, with a 72h timespan, for the area of operations, and using a predefined grid of points (see also **Figure 30**). Data were delivered in the form of an ESRI Shapefile spatial data format. Apart from the geographical location information, metadata information was also included within the Shapefile such as: 1) timestamp information, 2) speed and distance information for every subsequent pair of points.

Figure 30: *Ice drift trajectories*

Operational forecasts

A dedicated server was set up and provisioned to a) run PRIIMA and b) run the preprocessor responsible to acquire the input data. Dedicated software and “in house” scripts ensure the service automation. DWD is releasing wind updates 4 times a day. We have aligned the preprocessor and PRIIMA to run when an update was available, and in more specific some minutes after: 04, 10, 16, 22 UTC hours.

Forecast accuracy

The forecast accuracy/uncertainty was derived using a limited number of cases (14). For each case the distance and angular misfit were calculated, and results are summarized in **Figure 31**. A perfect fit should be located at the very centre of the circles. For the majority of the cases ICON forecasts manage to predict the final point position in less than 30 degrees angular misfit and within 10 km distance from its true position. The average misfit was found to be 26.12 degrees and 9.12 km.

Summarising, PRIIMA forecasts using ICON as drift forcing and for time spans between 48h and 72h, show a probability of 12% to have a distance error less than 5 km, 56% probability for a distance error between 5 and 10 km, and 32% probability for an error larger than 10 km.

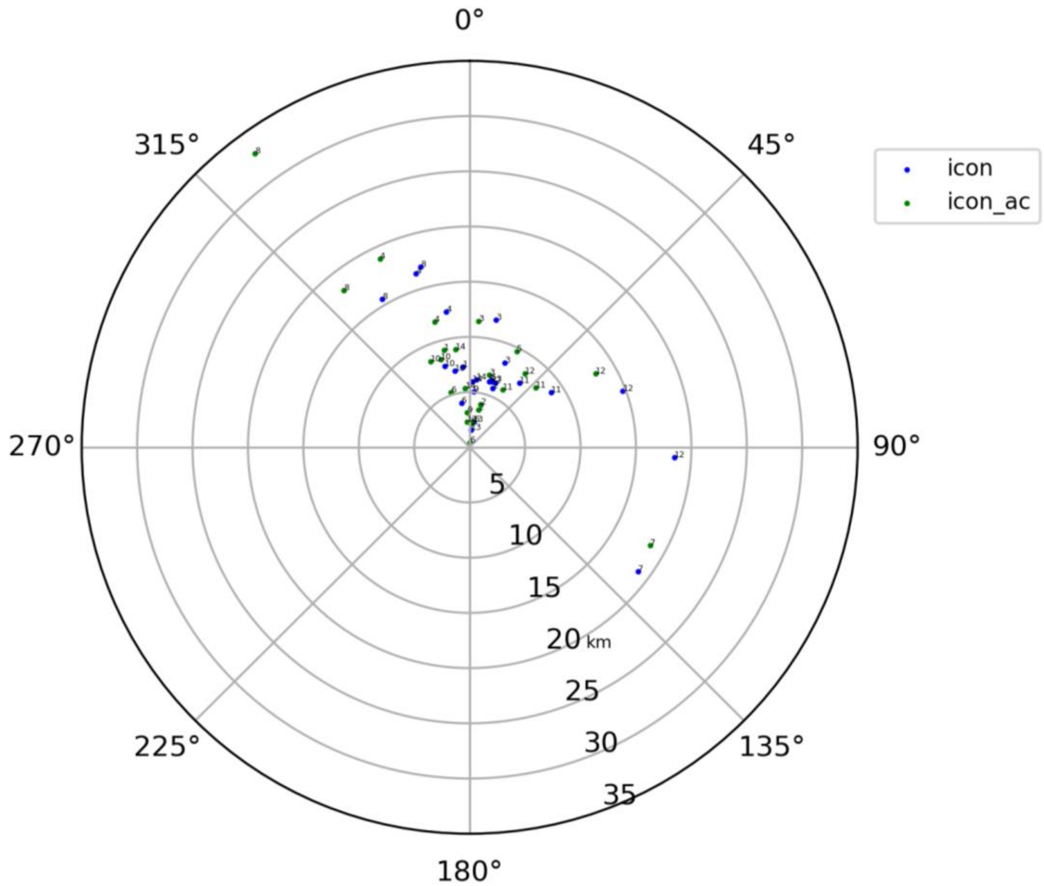

Figure 31: *Overview of forecast performance. Concentric circles show distances from the final true position in km. Bearings show angular error in degrees.*

5.3.2. SIDFEx

Written by Helge Goessling (AWI) & Valentin Ludwig (AWI)

The Sea Ice Drift Forecast Experiment (SIDFEx) is a community effort to utilise and foster sea-ice drift forecast capabilities at lead times from days to a year. SIDFEx collects, processes, and analyses forecasts that are made with various methods, largely for drifting sea-ice buoys of the International Arctic Buoy Program (IABP), but also for campaigns such as the Multidisciplinary drifting Observatory for the Study of Arctic Climate (MOSAiC) and now the Endurance22 campaign. SIDFEx is part of the World Meteorological Organization's Year of Polar Prediction (YOPP) and inspired by increasing research and operational needs to forecast future positions of assets drifting in Arctic sea ice. Two publications describing SIDFEx in detail are in preparation, but since they are not yet available, the most relevant information is provided here.

Since the launch of SIDFEx in 2017, thirteen groups have been contributing drift forecasts. Some forecasts are based on free drift or on drift observed from satellites during past years, but most groups (and that holds for all that were used for Endurance22) derive their days-to-seasonal-range forecasts by means of diagnostic Lagrangian tracking based on predicted sea-ice drift fields of coupled or uncoupled general circulation models. Some groups submit ensembles of drift trajectories instead of single (deterministic) trajectories, and several groups submit their forecasts in (near-)real-time (which, obviously, holds for all forecasts that were used for Endurance22).

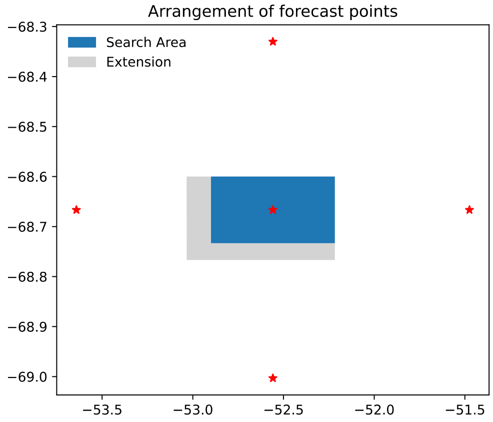

Figure 32: *SX1: SIDFEx forecast points (trajectory starting positions; red stars) in comparison to the Endurance search area (blue and grey boxes).*

For the Endurance22 campaign we have produced a dedicated consensus forecast product, building on the experience gained during the MOSAiC expedition. We provided forecast trajectories for five fixed starting points (**Figure 32**). For the consensus, we used near-real-time forecasts from three systems of the UK Met Office (handled by Ed Blockley), one system of Environment and Climate Change Canada (handled by Yukie Hata), one system of the US Naval Research Laboratory (handled by Joseph Metzger and Michael Phelps), and one system of the ECMWF (handled by Steffen Tietsche). The last of these is a seasonal system providing a large ensemble of forecasts only once per month; the other systems provide daily shorter-term forecasts with lead times between 7 and 10 days.

We updated the consensus forecast every 6 hours. At short lead times it was constructed as a multi-model-ensemble based on the short-term systems, always using the most recent available forecast of each system, truncating the obsolete part of the trajectories and repositioning the remaining trajectory such that a spatio-temporally consistent ensemble forecast was obtained. At longer lead times, ensemble members of the seasonal system (SEAS5) were used to extend individual forecasts that, due to the truncation, did not reach out to 7 days. We provided a graphical version of the forecast (example shown in ***Figure 33***) as well as corresponding shape files (for both the consensus mean and the individual systems) that could be used more easily by the Endurance22 team aboard the ship in GIS software to locate which ice was expected to drift into which locations by moving the shape files around. Upon request of the Endurance22 team, we added hourly positions and drift speeds in additional shape files to facilitate the usability further (although the underlying resolution remained effectively daily). The graphical product as well as the shape files were sent by email and also provided under a specific URL.

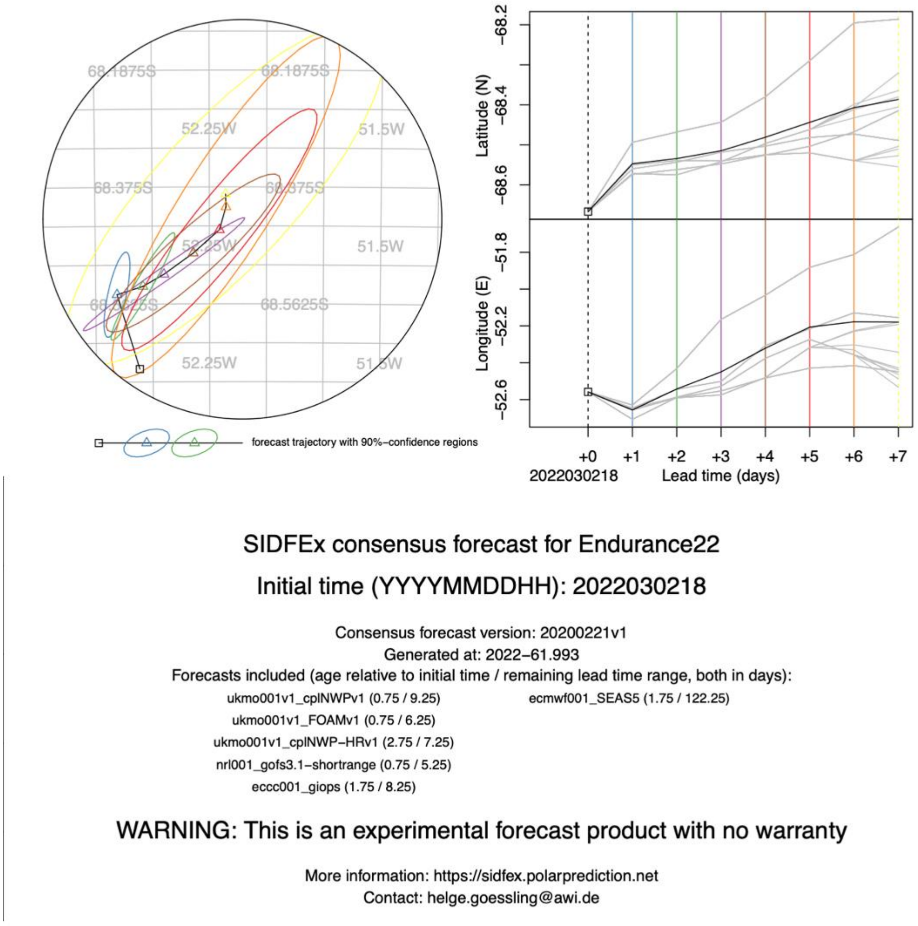

Figure 33: *SX2: SIDFEx graphical forecast product, example with initial time at 18UTC on March 2nd.*

On February 21st we provided the results of an evaluation to the Endurance22 team to enable an up-to-date assessment of the to-be-expected skill of the SIDFEx forecasts. To that end we evaluated SIDFEx forecasts for a buoy drifting about 200km to the south of the search area, using data since December 2021 and mimicking the same NRT conditions (assumed timeliness of the individual forecasts). The details are beyond the scope of this report, but **Figure 34** SX3 provides a high-level summary. Time permitting, we will use data from the buoys deployed by the Endurance22 team to repeat the evaluation for the actual Endurance22 forecasts. Finally, we are planning to present Endurance22 as one of several use cases of SIDFEx forecasts in an upcoming scientific publication.

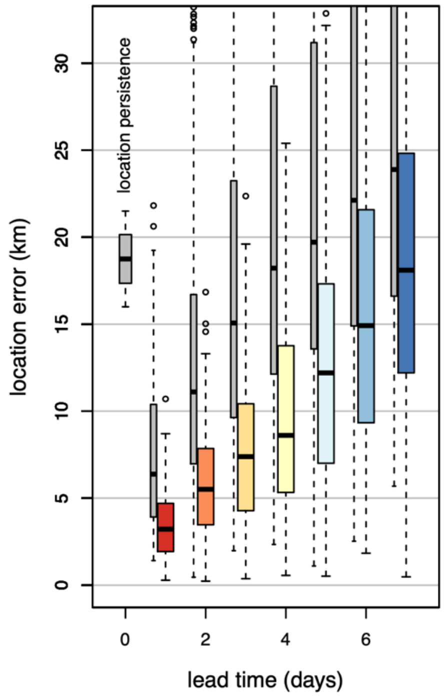

Figure 34: *SX3: Error statistics of the SIDFEx consensus forecast, evaluated for a drifting buoy close to the Endurance site between December 2021 and mid-February 2022.*

5.4. Integration into the navigation process

Written by Lasse Rabenstein (DNPS)

Shipping in sea-ice covered regions causes the vessel to progress slower, to consume more fuel, causes larger abrasion at the hull and bears the risk to get stuck in the ice entirely. There is a large potential to minimize those risks by skilled personnel on-board (e.g. trained ice pilots) and by a better level of ice relevant information. Over the last years the availability of relevant earth observation and weather model data has increased significantly. However, the incorporation of those data into the navigation process on board an ice going vessel is a big-data problem which no single nautical crew can solve alone. Concepts on how to turn sea-ice relevant data into information and eventually into navigational decisions are researched within the projects EisKlass2 and FastCast2, both financed by the German Ministry of Transportation and Digital Infrastructure. The participants DNPS, Koenig und Partner and DLR are consortium members of both projects and performed a case study during Endurance 22. They provided a set of continuously updated operational information via a 24/7 ice information desk on the bridge. The goals were to minimize the risk of ice navigation, to enable the Agulhas II to operate 24/7 even in the dark hours and to receive feedback from the bridge crew in order to design the ice information App of the future.

Data used

The following data were processed an displayed at the ice information desk:

Data	Type	Resolution	Delivery Frequency	Provider
Sentinel-1	SAR satellite image	30 m	Every 2-6 days	Copernicus

TerraSAR-X	SAR satellite image	3-12 m (depending on mode)	1-3 scenes per day	DLR
ICEYE	SAR satellite image	2.5 -12 m (depending on mode)	1-3 scenes per day	ICEYE
Sea-ice concentration	Level 3 satellite image	6 and 3 km	6 times a day	JAXA, DNPS
MODIS	Optical satellite image	250 m	2 times a day	NASA
LandSat	Optical satellite images	15 to 30 m	occasioanlly	NASA / US Geological Survey
Classified Sentinel-3 data	Level 3 satellite image	300 m	daily	Copernicus, KuP
Drift Buoy	Position data	Hourly	Hourly	AWI
PRIIMA	Sea-ice drift forecast	Hourly	Every 6 hours	DNPS
SIDFEX	Sea-ice drift forecast	Daily	Every 6 hours	AWI / SIDFEX

24/7 operations – shift plan

Once in the ice there was always one member of the science team at the ice information desk at the bridge. The task of that person was to keep the information on the screen up-to date and to be ready to provide information on demand to the subsea team and to the bridge crew. An ice information shift on the bridge lasted 4 hours.

Problems of data integration

Common problems to integrate ice information into the routine decision making process and their solutions during Endurance 22 and general solutions.

Problem	**Endurance 22 solution**	**General solution**
Low-bandwidth on-board	Very good geostationary satellite communication system, 15 Mbyte/sec, very expensive 30'000 USD for two months	Pre-process data to smaller file sizes
Too many different data, too much data handling	Dedicated person from the science team is responsible for data management	Automation, User friendly interface
Satellite images difficult to interprete	Experienced ice pilot and ice analysts on board, Automatically classified Sentinel-3 images	Automatic interpretation and classification in an App, Polar educated bridge crew
Data and images are too old	Specifically ordered SAR images for the search area (TerraSAR-X and ICEYE) up to 3 times a day,	Faster automatic data fetching and processing, integrate more satellite missions, hope for more openly available SAR missions

Data are too low resolution for tactical navigation	Access to high resolution SAR missions	Integrating an order process for commercial high-res SAR images into the ice information App
Mismatch between displayed data and reality due to ice drift which hampers tactical navigation	Manual and continuous adjustments of satellite images to the drift	Automatically adjust the satellite image do the drift, e.g. via pattern matching with the ship radar
Viewing systems of ice information do not include navigational planning tools	Ice analyst on the bridge did calculations manually in QGIS (distances, bearing etc)	Include navigation functions into an ice information App

Strategic & Tactical Navigation

The usage of ice information changed during the course of the Endurance 22 expedition from strategical planning in the beginning to tactical navigation once the vessel was in the ice. 3 months before the cruise DNPS started to monitor the sea-ice situation by the usage of sea-ice concentration information, ice charts of the US National Ice Centre and Cryosat-2 based ice thickness data provided by AWI.

A couple of days before Agulhas II entered the Weddell Sea sea-ice additional moderate resolution satellite images were used such as MODIS, classified Sentinel-3 or Sentinel-1. Those data helped to depict an optimal point to enter the ice cover and a rough route to the search box.

Once in the sea-ice pack additional high resolution Terra-SAR-X and ICEYE SAR images were used and continuously displayed on the bridge. Those types of images are in the same resolution range as the ship radar and are the perfect supplement for tactical navigation. On SAR images open or refrozen leads can be identified beyond the range of the ship radar and even ice types and pressure ridges. A crucial requirement to use SAR satellite images for tactical navigation is a continuous adaptation and shifting of the image according to the ice drift. Otherwise the displayed ship position would not match the true situation on the ship radar. The shifting of the satellite radar image according to ice drift was a continuous task for the ice analyst at the bridge. For a future tactical ice navigation system this needs to be automated based on drift information.

Acceptance of ice information by the nautical crew

The integration of earth observation and ice drift information into the navigational process on board needs to be accepted by the bridge crew and it demands from the crew to learn and acquire new skills about data interpretation of SAR satellite images. The Endurance 22 had a skilled ice navigator on-board who was familiar with a wide range of satellite information. We observed that also the remaining bridge crew incorporated the high resolution ice information into the tactical navigation with an increasing intensity towards the end of the period in sea-ice.

Determination of Dive position

Of particular importance was the process to park the vessel in the right position to start an AUV survey dive. The strategy of the subsea team changed during the course of the expedition. The first strategy to plan a survey line as close as possible aligned to the predicted ice drift trajectory included a lot of data handling, complex planning and recalculations of median lines of the drift etc. It also included too much non-routine information and data exchange between the subsea and the ice team. Furthermore, the true ice drift was rarely close enough to the predicted trajectory. The strategy was changed after a couple of days. The more successful strategy was to subdivide the search area into smaller boxes of precalculated survey lines. The only information exchange needed between the ice team and the subsea team was the direction and speed of the forecasted ice drift for the next 6-12 hours. The ship was repositioned after every AUV dive of 5-8 hours next to one of the planned survey boxes. This was possible due to favourable ice conditions and high level of ice information on-board for tactical navigation.

Description of QGIS System on the bridge

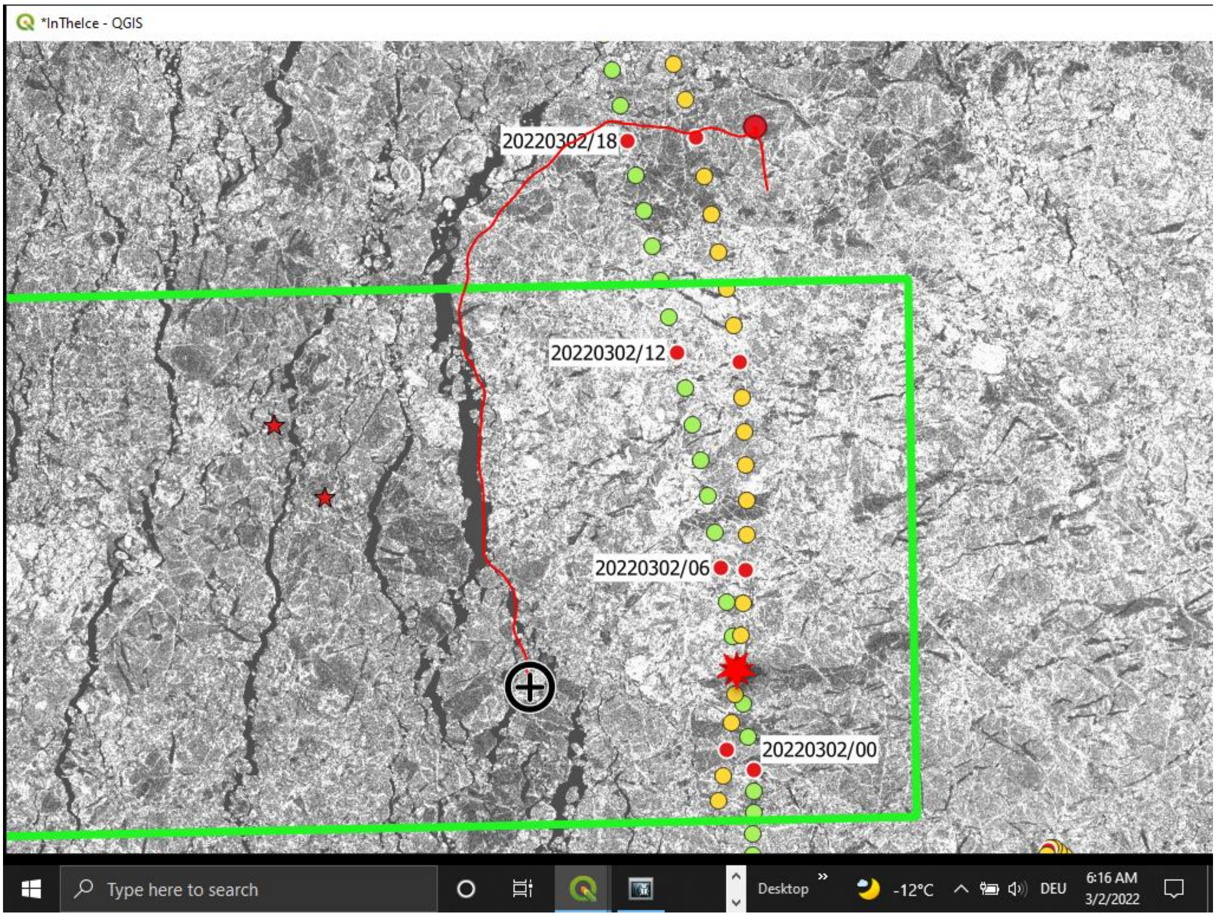

Figure 35: *Screenshot of the Q-GIS experiment on the ice information desk at the bridge. On top of a Terra-SAR-X image are information layers about the current GPS track (red line), current position (black crosshair), navigation points (red dots and stars) and the latest drift forecast trajectories (yellow PRIIMA, green SIDFEX) labelled every six hours with a timestamp. In this image the Agulhas II travelled southward through an open lead (black elongated structure). In the northern part it appears as if Agulhas II transited through ice instead through the open lead, however, this mismatch is due to the ice drift.*

Figure 36*: One of the ice analysts on-board keeps the information in the QGIS up-to-date.*

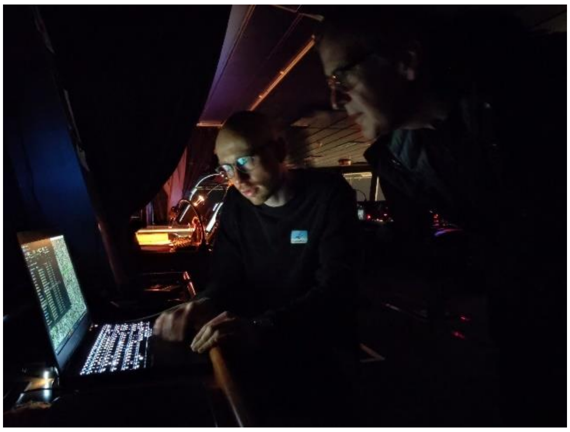

Figure 37 *Two ice analysts working on the ice information QGIS at the bridge during the night. One issue was to reduce the light intensity of the Laptop screen to night mode (darker colours for the QGIS interface).*

The downloaded and processed satellite images and drift forecasts were stored on a ship's internal shared drive. The Q-GIS experiment directly accessed those data and displayed it on the bridge. In addition a GPS receiving antenna was plugged into the bridge Laptop's USB port to continuously display ship's position and track on the screen (see **Figure 35**). Access to the ship's internal GPS stream was unfortunately not possible due to regulative hurdles.

Q-GIS is a powerful analysis tool for geospatial data but not a lightweight and easy to use navigation software. For instance during Endurance 22 it needed skilled personnel with a geodata background and sometimes it took several minutes of frontend usage before an information could be displayed on-demand. This delay could be reduced after bridge crew and ice analysts got aware of the most important data layers and could establish routine processes. However, it was very obvious that in general ice navigation needs a software with less but more targeted functionality.

Nevertheless, the Endurance 22 ice information system was unprecedented in its use of near-real time very high resolution SAR imagery and ice drift forecasts integrated into the tactical navigation process especially in difficult periods of dark hours and snowfall.

Lessons learned

- Do not include more satellite image layer than necessary, Q-GIS can become increasingly slow which hampers the decision making on the bridge
- A very useful feature of Q-GIS was the freehand raster georeferencer plugin. It was used continuously to shift satellite images to the latest positions of the drifting ice regime
- Correct and clear labelling of the drift forecast trajectories was important. We used a point shape file layer with an hourly sampling rate. Every 6^{th} point was marked red and labelled with day and time.
- Ice drift forecast trajectories were moved and aligned to the next planned surveying box to determine the next parking position for the ship
- Display of the drift path and up to date position of a nearby drift buoy within QGIS was used to align satellite images according to predominant ice drift.

- Whenever a parking position was reached to start an AUV dive, a screenshot was taken and shared with the other analysts. The screenshot had to show the true position relative to the ice structures on the latest satellite image. That way ice analyst of the subsequent shifts had a reference for the next freehand georeferencing to adjust for ice drift.

The IcySea App

DNPS is developing the Progressive Web App (=PWA) IcySea https://icysea.app (see **Figure 38**) with the ultimate goal to deliver an easy-to-use ice information system for nautical crews on board ice going vessels. It is especially designed for low-bandwidth connections. During Endurance 22 the latest version of IcySea (2.2.0). was tested and its usability for ice navigation evaluated. The latest version of the IcySea App was developed within the EisKlass2 (http://eisklass.org) project and included the display of classified Sentinel-3 images provided by Koenig und Partner. The first version of IcySea was financed by the Copernicus Marine Service User Uptake Project with the same name "IcySea" in 2020.

Generally the IcySea App worked as planned and could be used for semi-strategic semi-tactical navigational decisions. The ice navigator on-board installed it via https://icysea.app within minutes on his Smartphone. The positioning function worked without internet connection, on the Laptop as well as on the Smartphone, and all layers could be loaded in and displayed. Problematic was the reduced Sentinel-1 image update rate due to the failure of Sentinel-1B just before Christmas 2021. The longest period to wait for a new image was more than 7 days, which is way out of scope for an operational sea-ice information app. Once the expedition reached the search box the higher resolution Terra-SAR-X and ICEYE images were of greater importance than the information displayed within IcySea. The classified Sentinel-3 images only provided relevant information during cloud free days, which happened only in 1.5 out of 21 days within the search period. However, on the way out of the ice, IcySea was again being used.

The following ideas for improvement of IcySea could be identified during Endurance 22:

- Push messages or indications on the screen about whether a new Sentinel-1 image tile is available
- Option to download multiple radar tiles
- Option to delete individual tiles
- Add transparency to layers
- Animated sea-ice concentrations to display the current momentum of the ice cover
- Show gps track, not only position
- Increase the backend processing speed for S1 images to become more near-real time
- Display the bearing of the current GPS track
- Option to shift (on the fly re-georeferencing) of satellite image, either manually, or better automatically
- Customize order of layers
- Display hourly forecast time steps

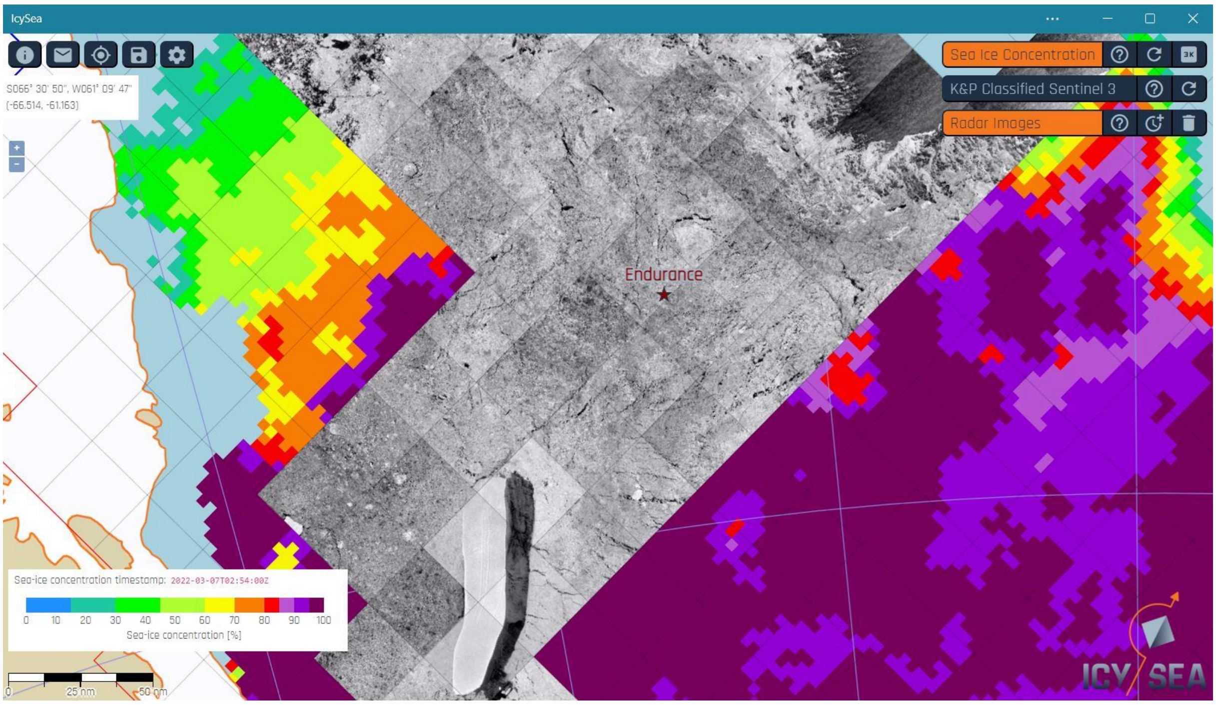

Figure 38: *Screenshot of the IcySea progressive web app (=PWA) version 2.2.0 (https://icysea.app).*

6. Sea-ice observations from the ship

6.1. Manual observations from the bridge

Written by Jukka Tuhkuri

Visual observations of ice were made continuously from the bridge when the ship was encountering any type of ice. A team member was standing on the port side of the bridge with a laptop computer and wrote down observation into a log file every ten minutes. For an estimate of the ice thickness, a yardstick, fixed to the railing on the port side of the main deck and visible to the bridge, was utilised. The logs include also notes on ice conditions, ice load events, and ship operation.

6.2. Optical camera systems – visual band

Written by Jukka Tuhkuri (Aalto University)

A camera setup (a machine vision system) was placed on the crow's nest, watching over the front of the ship (**Figure 39**). A laptop collecting the data was placed inside the crow's nest while the camera itself was outside. The camera was set into a time-laps mode taking an image every 5 seconds. The raw images were transferred into jpg-images every 30 seconds. In addition, a GoPro camera was attached at the ship railing at Deck 5 and looking down, thus capturing the ship-ice interaction events. The GoPro camera was set into a time-laps mode taking images every 2 second. Examples of the camera recordings are shown in **Figure 40** and **Figure 41**.

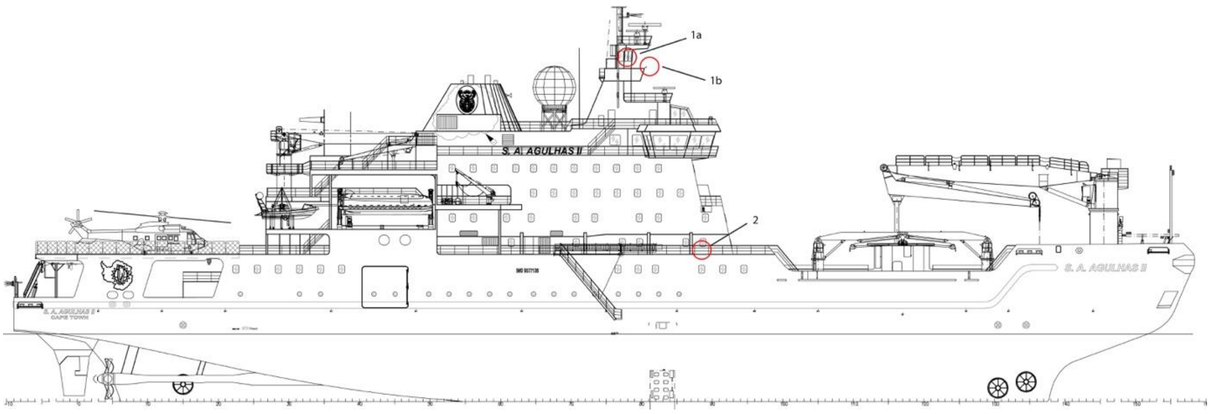

Figure 39: *The crow's nest (1a) was used to operate a camera (1b) looking forward. Another camera (2) was looking at the ice broken by the ship bow.*

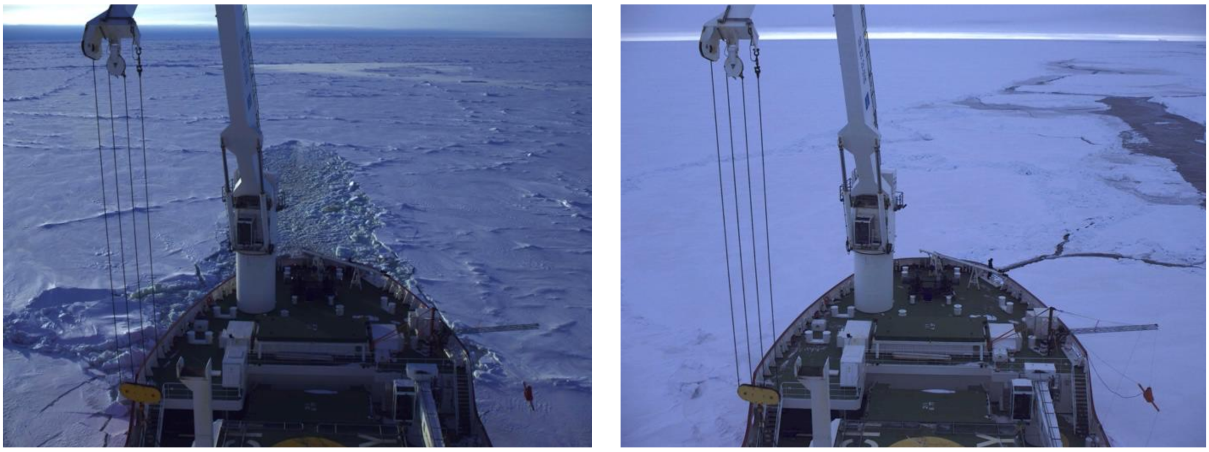

Figure 40: *Two examples of photos taken every 30 seconds from the crow's nest*

Figure 41: *A sequence of images showing the ice failure process at the SB side of the ship bow.*

6.3. Optical camera systems – infrared band

Written by Dmitrii Murashkin (DLR)

Thermal Infrared Images

Airborne and satellite borne thermal infrared imagery if often used for sea ice conditions observations in polar areas, especially during winter time, when visible imagery is not available. During the expedition a thermal infrared camera provided by the University of Bremen has been installed on board of the vessel on the upper deck (Monkey island, **Figure 42**). The side-way looking camera was located on the starboard side of the vessel under 30 deg angle to the horizon (**Figure 43**). Images were taken every two seconds during the ship transfer through sea ice. Image resolution is 640 by 480 pixels.

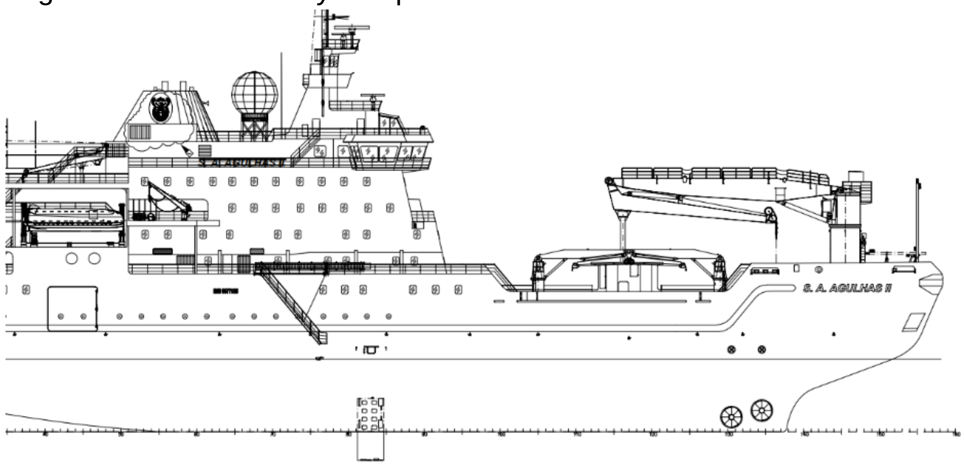

Figure 42. *Scheme of the ship. The location of the IR camera is shown in red.*

***Figure 43**. Photo of the infrared camera set up. The camera is set at 30 deg angle to the horizon.*

The camera measures brightness temperature of objects (surface of sea ice and open water). The brightness temperature can be related to the real object temperature via emissivity.

$$Tb = E * T$$

Since surface temperature and emissivity of the snow, sea ice, and water surfaces varies, infrared images can be used to map ice conditions in the vicinity of the ship. Apart from observations in the visible spectrum, infrared images can provide the information during night hours.

Image examples are shown in **Figure 44**, **Figure 45**, and **Figure 46**. **Figure 44** shows thicker snow-covered ice floes in blue, newly formed think ice in green, and open water areas in red. It should be noticed that the scale on the infrared images correspond to object brightness temperatures, not the true object temperatures. **Figure 45** shows an opened crack with open water (in red). Blue colors corresponding to -22 deg C represent level thick sea ice. Lower temperatures and darker blue colors show a ridge on the ice floe. **Figure 46** presents an infrared image of an ice floe (in blue) surrounded with thin ice (in yellow and orange). Cracks with open water are shown in red and pink colors.

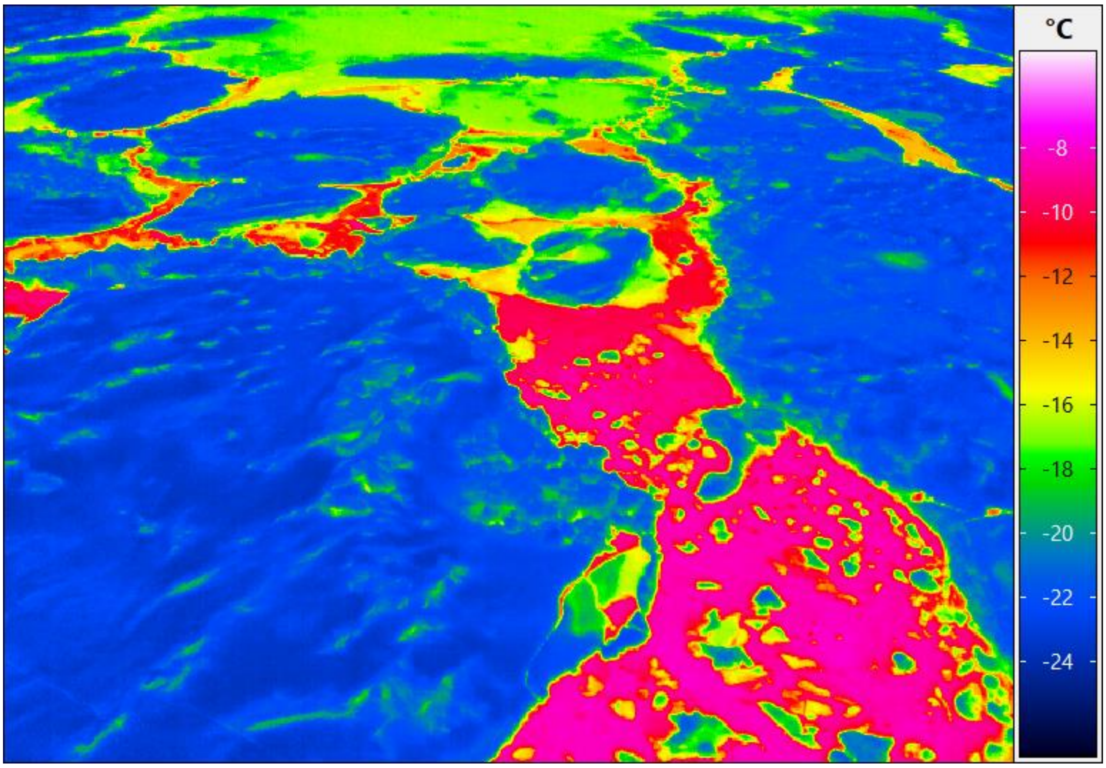

Figure 44*. Infrared image of sea ice and open water. Warm colors show warmer areas of open water. Green is thin ice, Blue is thicker ice.*

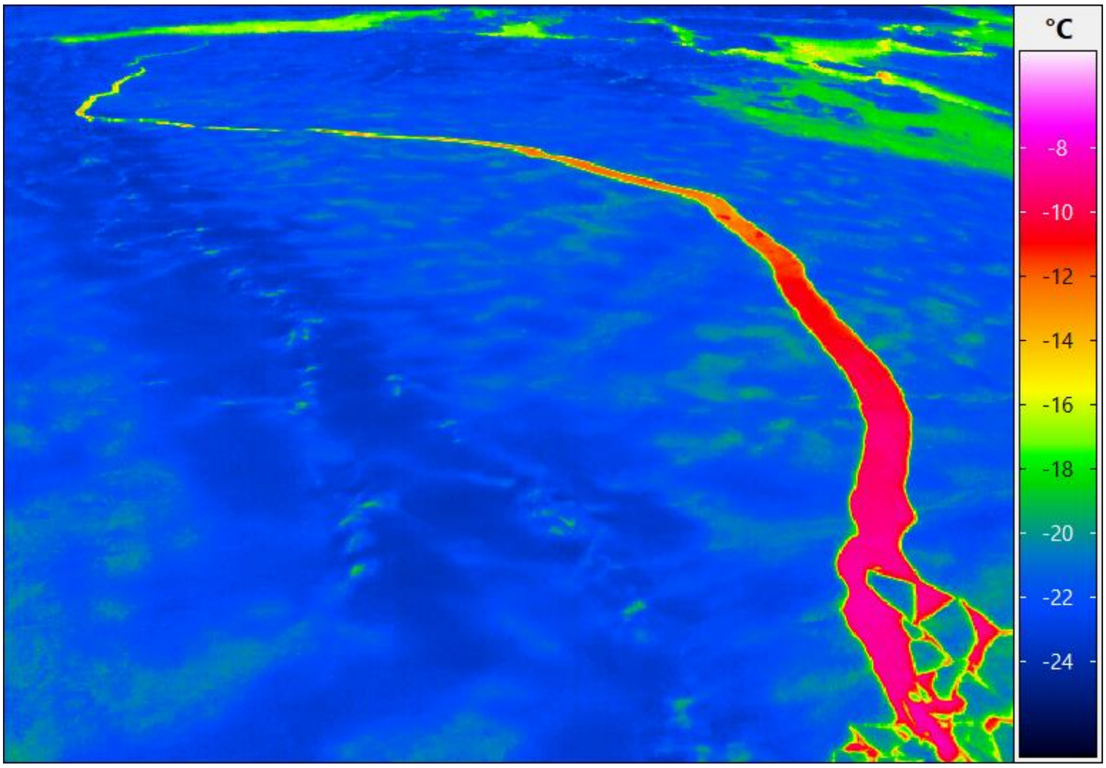

Figure 45. *Thermal infrared image of sea ice. Blue ice has a brightness temperature of about -22C, darker colors show a ridge going through the ice flow (brightness temperature differs due to varience in incidence angle to the camera). Red is newly open crack.*

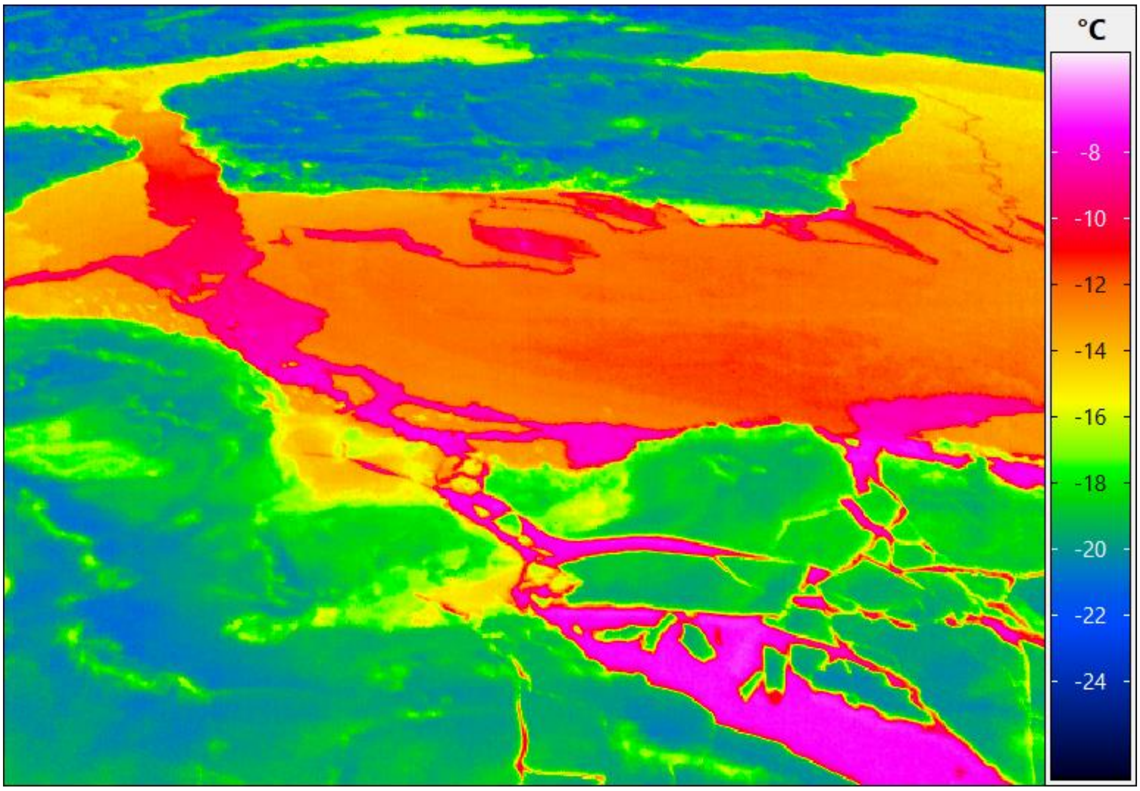

Figure 46. *Thermal infrared image of a sea ice floe (in blue) surrounded with thin ice (nilas). Open water areas (in pink) appear warmer then the thin ice.*

6.4. Ship based EM ice thickness measurements

Written by Mira Suhrhoff (DNPS)

Ice thickness measurements were taken for the period between 15 Feb and 08 Mar 2022 alongside the SA Agulhas II using an electromagnetic induction instrument (EM) as part of the AWI objective to obtain physical sea-ice properties during the expedition. This is a widely used method that combines electromagnetic induction sounding with laser altimetry (e.g., Haas et al., 1997; Kovacs and Morey, 1991; Worby et al., 1999) and relies on a large difference in electrical conductivity between sea ice and water. The electrical conductivity is measured by a Geonics EM-31 instrument with two antenna coils spaced 3.66 m apart and operating at a frequency of 9.8 kHz. It measures the distance between the instrument and the ice-water interface, i.e., the underside of the ice. First, a transmitting coil generates a primary alternating electromagnetic field that induces small eddy currents in the seawater beneath the ice. These currents generate a secondary magnetic field, which is measured by the second, receiving coil. The relationship between this primary and secondary field is related to the height of the instrument above the ice-water interface, or else the underside of the ice. The measurement is made within a lateral distance of several meters (=footprint), over which the distance to the underside of the ice is averaged. Therefore, the maximum thickness is always underestimated, especially in areas with large features such as pressure ridges. In addition, the distance to the ice or snow surface is measured with a downward looking ultrasound altimeter with a footprint of a few centimetres. The total ice thickness can be calculated as the difference between the height above the underside of the ice and the distance to the snow or ice surface. It is the sum of snow and ice thickness. The ice thickness measurement series is accompanied by the GPS position and can be determined with a time resolution of 2 Hz. To avoid influences of the ship's hull in the conductivity measurements, the instrument was suspended under a beam on the starboard side of the foreship, about 4 m above the water level and 5 m away from the ship (**Figure 47**).

Figure 47: *Image of the SA Agulhas II with the mounted AWI EM ice thickness sensor. Copyright Esther Horvath.*

The EM was calibrated twice (02/15/2022 and 02/19/2022) by measuring incremental changes in the height of the instrument above open water. The second calibration of 19/03/2022 was used for the processing of the raw data. The complete dataset consists of the passage in and out of the ice, during the 15-16/02/2022 and 07-08/03/2022, and the time in between when we were in the search area of Sir Ernest Shackleton's shipwreck. Therefore, the distribution of ice thickness varies for different days (see **Appendix**). Time periods when the ship was stationary in the ice were removed from the data set.

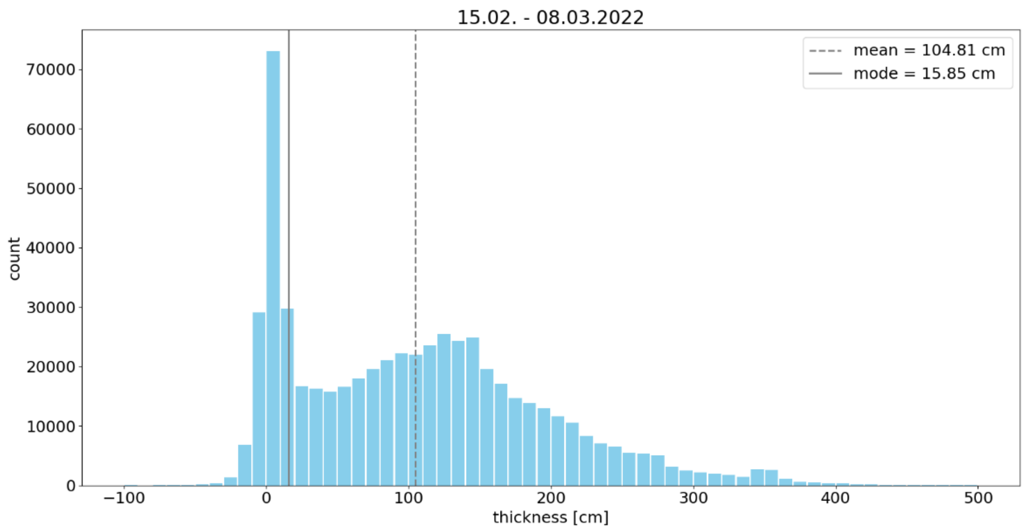

Figure 48: *The ice thickness distribution measured by a shipborne EM instrument during the Endurance 22 Expedition*

The overall distribution of ice thickness is shown in **Figure 48**, with a mode around 16 cm, indicating to open water and thin ice areas, and a mean of 104 cm. We expect a slight bias toward thinner ice compared to the true ice thickness distribution of the area, as we often chose routes with easy to navigate ice conditions, which means more open water and thin ice areas.

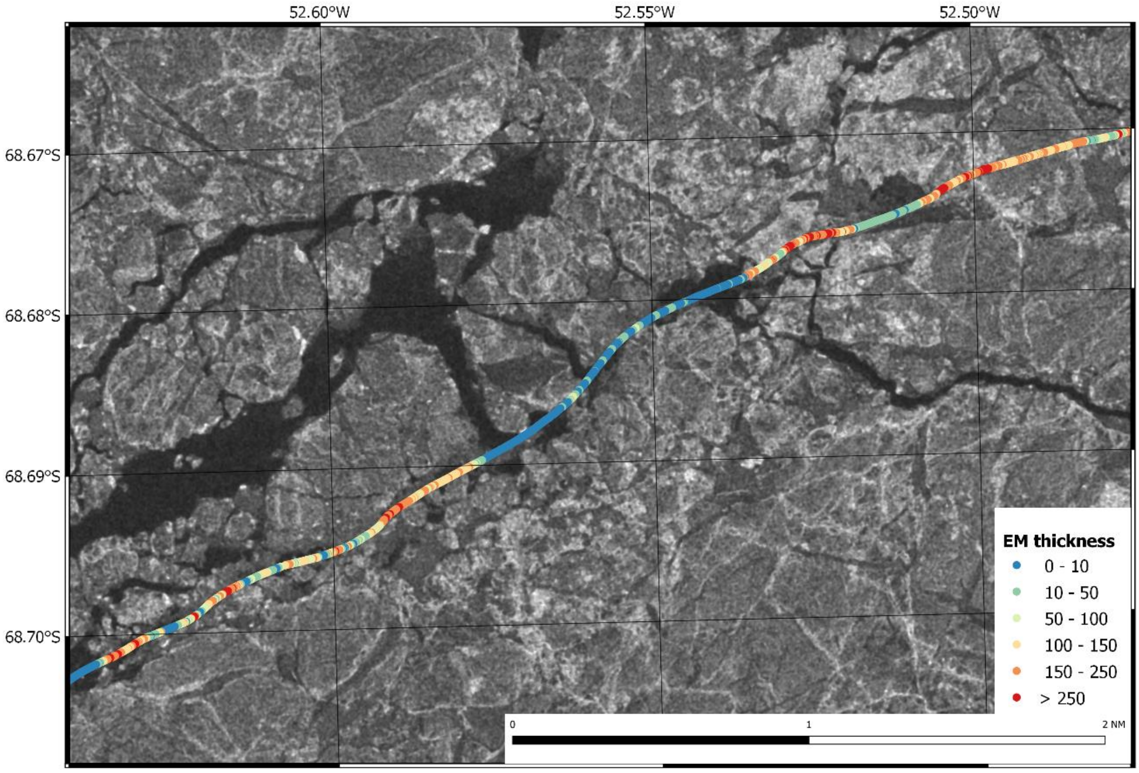

Figure 49: *SAR satellite image (© 2022 ICEYE Oy.) from 04/03/2022, shifted to EM thickness track from 03/03/ 2022.*

Figure 49 shows a section of the route on 03/03/2022 within the search area where we moved the ship to a different position together with ice thickness measurements along the route that ranged from open water to ice thicknesses of more than 2.5 m.

The ice thickness information was displayed in real time on the bridge and complemented the information from the satellite imagery well. It improved decision making and on-site navigation through the ice cover. In addition, the measurements will be used for the FAST-CAST 2 project, which aims to optimize route suggestions through ice-covered areas and will play a role in linking ship performance to ice loads.

7. Measurements during Ice Stations

7.1. Ice stations overview

Written by Stefanie Arndt (AWI)

Station	Date	Time (UTC), start	Latitude (deg), start	Longitude (deg), start	Time (UTC), end	Means of floe access	Gear
E22_20220216_1	2022-02-16	11:50	68°49.539'W	51°56.966'W	15:30	Helicopter	SIT, SPIT, SDMP, GEM, CORE, SBUOY-D
E22_20220218_2	2022-02-18	10:00	68°40.550'W	52°18.550'W	15:35	Mummy Chair	SIT, SPIT, SDMP, GEM, CORE
E22_20220219_3	2022-02-19	22:05	68°41.410'W	52°26.667'W	00:10	Mummy Chair	SIT, SPIT, SDMP, GEM, CORE
E22_20220220_4	2022-02-20	14:25	69°31.950'S	50°59.083'W	18:00	Helicopter	SIT, SPIT, SDMP, GEM, CORE
E22_20220221_5	2022-02-21	16:20	68°40.733'S	52°24.450'W	18:20	Mummy Chair	SIT, SPIT, SDMP (failed), GEM, CORE
E22_20220222_6	2022-02-22	10:10	68°39.917'S	52°24.700'W	12:25	Mummy Chair	SIT, SPIT, SDMP, GEM, CORE
E22_20220222_7	2022-02-22	18:10	68°40.150'S	52°20.250'W	20:00	Mummy Chair	GEM,SDMP
E22_20220223_8	2022-02-23	16:20	68°40.983'S	52°20.000'W	18:50	Mummy Chair	SPIT, SDMP, GEM, CORE
E22_20220225_9	2022-02-25	11:40	68°41.533'S	52°28.767'W	13:55	Mummy Chair	SIT, SPIT, SDMP, GEM, CORE
E22_20220226_10	2022-02-26	10:15	68°40.933'S	52°28.667'W	12:20	Mummy Chair	SIT, SPIT, SDMP, GEM, CORE
E22_20220227_11	2022-02-27	09:15	68°37.183'S	52°12.033'W	11:20	Mummy Chair	SIT, SPIT, SDMP, GEM, CORE
E22_20220228_12	2022-02-28	16:10	68°42.483'S	52°10.467'W	18:20	Mummy Chair	SIT, SPIT, SDMP, GEM, CORE
E22_20220301_13	2022-03-01	19:40	68°39.350'S	52°06.250'W	21:35	Mummy Chair	SIT, SPIT, SDMP, GEM, CORE
E22_20220303_14	2022-03-03	13:10	68°40.367'S	52°08.100'W	15:45	Mummy Chair	SIT, SPIT, SDMP, GEM, CORE
E22_20220304_15	2022-03-04	14:15	68°44.067'S	52°29.567'W	17:30	Mummy Chair	SIT, SPIT, SDMP, GEM, CORE
E22_20220305_16	2022-03-05	13:45	68°44.650'S	52°19.767'W	16:30	Mummy Chair	SIT, SPIT, SDMP, GEM, CORE
E22_20220306_17	2022-03-06	13:40	68°44.533'S	52°19.333'W	16:30	Mummy Chair	SIT, SPIT, SDMP, GEM, CORE

Table 1: *Overview of all sampled ice stations, including the used gear on-site. SIT: manual sea ice thickness measurements, SPIT: Snow pit, SDMP: Snow depth with Magna Probe, GEM: Sea ice thickness from GEM-2 device, CORE: ice coring, SBUOY-D: Deployment of Snow Buoy.*

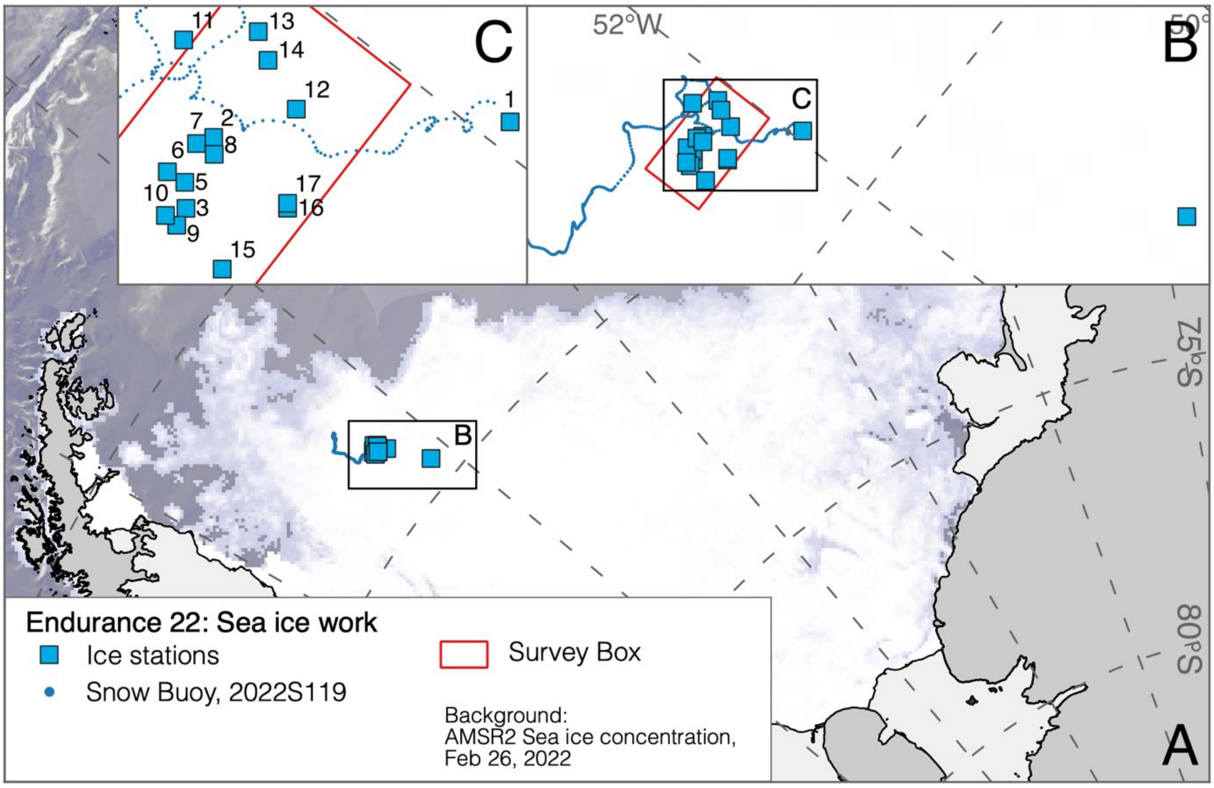

***Figure 50:** Overview of all sampled ice stations during Endurance22. Numbers in panel C are related to station numbers from **Table 1**.*

7.2. Floe based EM ice thickness measurements

Written by Jakob Belter (AWI)

Objectives

Sea ice thickness and snow depth are among the most important parameters describing the total mass and energy balance of the Antarctic sea ice cover. Despite their importance, in situ measurements of both parameters are sparse and usually limited spatially. In order to increase coverage and distinguish between ice and snow cover, snow depth and sea ice thickness are measured simultaneously along transect lines on selected ice floes. High resolution data sets of ice thickness and snow depth are gathered to complement characterisation of ice floe properties and are valuable for validation of satellite remote sensing products.

Work at sea

Total sea ice thickness (ice thickness plus snow cover) was measured along triangular transects using a ground-based multi-frequency electromagnetic induction sounding device (GEM-2, Geophex Ltd). The GEM-2 was pulled over the ice on a modified plastic sledge (instrument about 20 cm above the snow-air interface) and recorded its GPS position simultaneously. A GPS-equipped instrument, called MagnaProbe (Snow Hydro, Fairbanks, AK, USA), measured snow depth and was operated along the same transect lines as the GEM-2. In order to correct for the drift of the ice floe during the sampling period a small GPS tracker was installed at the start of the transect and positions of both GEM-2 and MagnaProbe measurements were corrected during processing. Snow depth was measured every 1.5 to 2.5 m along the track, while distance between individual GEM-2 measurements was dependent on the speed at which the sledge was moved over the ice.

GEM-2 and MagnaProbe surveys were conducted on a total of 17 stations. During a number of stations two GEM-2 were used for surveying, while the MagnaProbe was usually used along only one of the GEM-2 surveys. During the expedition problems occurred with the MagnaProbe, which is why only GEM-2 total sea ice thickness is available for station E22_20220221_5. Further details and a summary of all transect measurements is given in section 7.1. **Table 1**. Separate GEM-2 transects were conducted around the hull of the SA Agulhas II to support the work of the Engineering group from Stellenbosch University (stations E22_20220220_4, E22_20220222_6, E22_20220228_12).

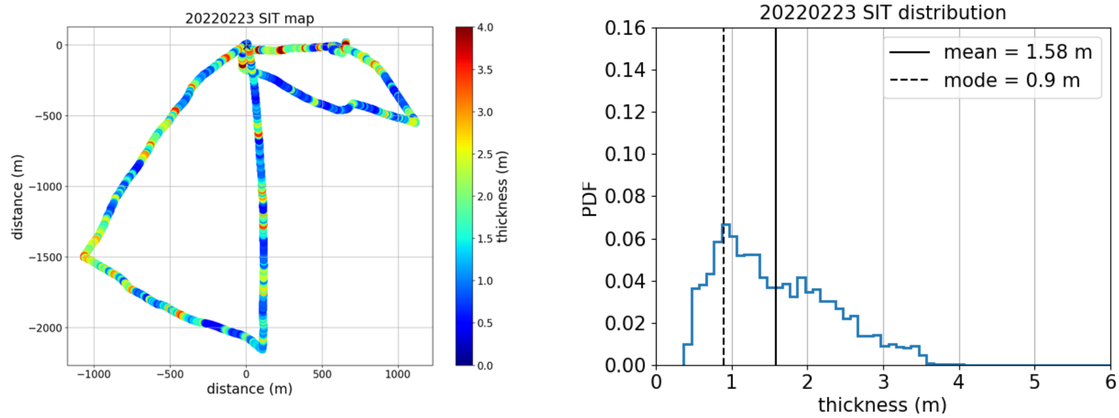

Figure 51: *Map of total sea ice thickness measured by GEM-2 (left) and corresponding distribution of total ice thickness values (right) from station E22_20220223_8*

Preliminary results

Mean (modal) total sea ice thickness measured on the 17 stations range from 1.18 to 1.72 m (0.8 to 1.7 m). Mean snow depth (MagnaProbe) varied from 9 to 23 cm. Foggy conditions limited the spatial extent of the surveys on stations E22_20220227_11 and E22_20220228_12. **Figure 51** shows an example of GEM-2 sea ice thickness data collected at station E22_20220223_8. The distribution given in the right panel shows a mode at approximately 0.9 m and less pronounced modes at approximately 1.9 and 3 m. Similar distributions were observed on most of the sampled ice floes, indicating that the floes consisted of conglomerates of ice patches of different ages. The next step is to analyse total ice thickness distributions in more detail, relate the sampled floes to their source regions, and distinguish between level and ridged ice regimes to increase the quality of these first preliminary statistics.

Data management

Sea ice thickness and snow depth transect data will be released after final processing and quality assessment. Data will. be submitted to the PANGAEA data archive.

7.3. Ice cores for studying mechanical vessel load

Written by Jukka Tuhkuri (Aalto University)

During the expedition altogether 17 ice stations were established and 40 ice cores were drilled and studied by AWI and Aalto University (see section 7.1.)

Aalto University, supported by Stellenbosch University and other members of the science team, collected 16 ice cores from 15 different floes. All the cores were taken close to SA

Agulhas II and many of them at the SB side of the bow. The cores were taken both from level ice and from ridges. The longest core was 2.9 m. From each core, the temperature, salinity and density profiles through the ice were measured. This data is important in determining the sea ice strength, which has a key role in ice loads on the vessel.

The procedure of measuring the properties was as follows: First, the ice temperatures were measured by drilling small holes into the cores and in this way measuring the temperature inside the cores. Second, the density was measured by cutting the ice cores into about 200 mm long pieces and measuring the dimensions and mass of the pieces. Third, the salinity was measured by taking parts of the same ice pieces back onboard and after the ice had melted, the salinity was measured with a salinometer.

Based on the ice cores studied, the ice in the search box was very warm late summer ice and many cores included rotten ice. The ice temperature was mainly above -1.8 C, except at the top 20 cm where the ice temperature reflected the air temperature and was at some cores lower. The coldest ice temperature measured was -8.7 C, but that was at the depth of 2 cm from the top. At 1 m depth, the ice temperature was typically between -1 C and -1.5 C. Density of the top 50 cm of the cores was low, typically less than 800 kg/m^3, but such low densities were also measured deeper in the ice. Higher densities, reaching 850 kg/m^3 and more, were measured at the bottom of the ice cores.

For the salinity measurements, the procedure described above was not ideal. The measured salinity was typically zero at the top 20 cm and between about 2 ppt and 3 ppt below that. These values are much lower than those measured by AWI from the same floes. The same salinometer was used by both groups, so we assume that during the procedure used by Aalto, brine drainage was fast enough to disturb the salinity measurements. All the ice cores were very warm and also the air temperature during the ice stations was often warm, making brine drainage fast.

7.4. Ice cores for studying sea-ice processes

Written by Stefanie Arndt (AWI)

Objectives

Summer thaw-freeze cycles in the snow and upper ice layers result in strong, destructive snow metamorphism, and eventually in the formation of superimposed ice and gap layers. While metamorphic snow was studied in snow pits and with lateral profiling methods (Section 7.4), different ice types indicative of specific ice developmental histories including the transformation from snow to ice, and the porosity and state of ice deterioration can only be observed from ice cores.

Work at sea

Station	Label	Date	SIT (cm)	SD (cm)	IFB (cm)	Core length (cm)	Full (F)/ Surface (S) core	Number of samples
E22_20220216_1	E22_20220216_1-5_CORES01	2022-02-16	163,0	10,0	11,0	175,0	F	26
E22_20220216_1	E22_20220216_1-5_CORES02	2022-02-16	113,0	13,0	4,0	73,0	S	15
E22_20220216_1	E22_20220216_1-5_CORES03	2022-02-16	122,0	10,0	7,0	101,0	S	25
E22_20220218_2	E22_20220218_2-5_CORES01	2022-02-18	123,0	2,0	24,0	90,0	S	23
E22_20220218_2	E22_20220218_2-5_CORES02	2022-02-18	154,0	5,0	25,0	70,0	S	18
E22_20220218_2	E22_20220218_2-5_CORES03	2022-02-18	141,0	2,0	21,0	143,0	F	22
E22_20220219_3	E22_20220219_3-5_CORES01	2022-02-19	63,0	7,0	3,0	63,0	F	20
E22_20220219_3	E22_20220219_3-5_CORES01	2022-02-19	52,0	5,0	4,0	52,0	F	14
E22_20220220_4	E22_20220220_4-5_CORES01	2022-02-20	72,0	2,0	5,0	72,0	F	20
E22_20220220_4	E22_20220220_4-5_CORES02	2022-02-20	160,0	7,0	8,0	167,0	F	34
E22_20220221_5	E22_20220221_5-5_CORES01	2022-02-21	182,0	7,0	28,0	189,0	F	36
E22_20220221_5	E22_20220221_5-5_CORES02	2022-02-21	68,0	5,0	6,0	68,0	F	19
E22_20220222_6	E22_20220222_6-5_CORES02	2022-02-22	187,0	9,0	19,0	196,0	F	34
E22_20220223_8	E22_20220223_8-5_CORES01	2022-02-23	35,0	3,0	3,0	38,0	F	9
E22_20220223_8	E22_20220223_8-5_CORES02	2022-02-23	345,0	8,0	24,0	353,0	F	49
E22_20220225_9	E22_20220225_9-5_CORES02	2022-02-25	82,0	13,0	12,0	95,0	F	21
E22_20220226_10	E22_20220226_10-5_CORES01	2022-02-26	142,0	3,0	13,0	145,0	F	37
E22_20220227_11	E22_20220227_11-5_CORES01	2022-02-27	252,0	10,0	22,0	262,0	F	39
E22_20220228_12	E22_20220228_12-5_CORES01	2022-02-28	163,0	17,0	13,0	180,0	F	28
E22_20220301_13	E22_20220301_13-5_CORES01	2022-03-01	124,0	13,0	11,0	137,0	F	25
E22_20220303_14	E22_20220303_14-5_CORES01	2022-03-03	212,0	21,0	22,0	233,0	F	32
E22_20220304_15	E22_20220304_15-5_CORES01	2022-03-04	131,0	5,0	18,0	136,0	F	29
E22_20220305_16	E22_20220305_16-5_CORES01	2022-03-05	180,0	14,0	38,0	187,0	F	34
E22_20220306_17	E22_20220306_17-5_CORES01	2022-03-06	125,0	9,0	11,0	134,0	F	33

Table 2: *Overview of all sampled ice cores during Endurance22, including the information on the sea ice thickness (SIT), snow depth (SD) and ice freeboard (IFB) at the drilling site.*

Physical ice properties were analyzed on all 17 sampled pack ice floes by means of ice cores. Therefore, a total of 21 ice cores with a diameter of 0.09m were taken, with 4 surface ice cores of at least 70 cm of the ice and the remaining ones covering the entire ice column. All ice cores were sliced on-site based on the apparent crystal structure and color of the ice. Based on this, the upper part of the ice core was usually cut into 2-cm-thick slices. Towards the bottom, the sections became up to 15 cm thick. The sectioning resulted in 642 individual ice samples. Table **Table 2** summarizes all ice core properties.

All sections were melted for the following analysis of vertical salt (on board) and isotope profiles (in laboratory back home). Salinities were determined with a conductivity meter (pocket conductivity meter WTW 3110) with a stated accuracy of 0.5% for each measurement.
The melted samples were poured into sampling vials that were filled completely and tightly sealed. The vials will be shipped at 4°C to the AWI ISOLAB Facility in Potsdam, where they will be analyzed for stable water isotopes.

Preliminary (expected) results

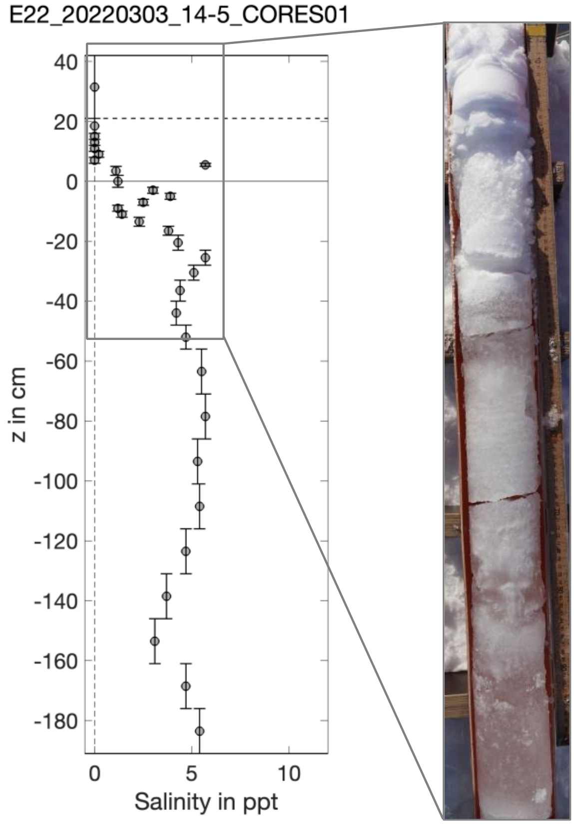

Figure 52: *Example of an ice core from station E22_20220303_14. (left) Salinity profile of the whole ice core. The bars indicate the individual sampled slices of the ice core. The vertical dashed line denotes the snow/ice interface, the solid black line the water level. (right) Picture of the top part of the ice core in the field.*

In total, 24 cores have been sampled for salinity, with 4 surface ice cores of at least 70 cm of the ice and the remaining ones covering the entire ice column. The ice core length range between 38 and 353 cm, including the snow cover on top. This wide range indicates the variety of the samples, including young first-year ice, first-year, and second-year ice. A subsequent more detailed analysis of the region of origin of each sampled ice floe will help to distinguish between different drift paths and ice age regimes.

Measured salinity profiles indicating an averaged thickness of rather salt-free sea ice of 10 ± 5 cm, ranging from 1 to 16 cm. Salt-free ice can be attributed to superimposed ice and was appeared in the field often as crystal clear ice layer. However, the distinction between snow and ice was not always clear. It is therefore proposed that all large-grained polygonal granular textures, i.e. melt-freeze clusters and superimposed ice, be summed up for later analysis.

For some cores, a thin, high-salinity layer is observed beneath the superimposed ice, followed by another, rather fresh layer. This suggests that two cycles of snow ice and superimposed ice formation took part, indicating at least second-year ice for these ice cores.

A fairly degraded salty layer was frequently observed beneath the superimposed ice layer, which is most likely snow ice, i.e., snow that has been flooded and refrozen. In order to certainly quantify the relative and absolute proportion of the snow ice layer, additional oxygen isotope analysis will be performed in the lab back home.

Rotten ice was regularly observed in the middle and lower parts of the ice cores, which is consistent with the relatively warm temperatures measured in the ice cores by our colleagues (see Chapter 7.3).

Data management

All ice core data will be released following its analysis in the home laboratories after the cruise or depending on the completion of competing obligations (e.g. PhD projects), upon publication as soon as the data are available and quality-assessed. Data submission will be to the PANGAEA database.

7.5. Snow properties

Written by Stefanie Arndt (AWI)

Objectives

Physical snow properties are highly variable even on small horizontal scales. These spatial and temporal variations in the snow pack characteristics (e.g., temperature, density, stratigraphy) and their dimension have a crucial impact on the energy and mass budget of Antarctic sea ice. Therefore, the snow pack on different ice floes was characterized in detail. Snow stratigraphy will be used as ground truth for the interpretation of retrieved snowmelt signatures from passive and active microwave data.

Work at sea

Physical snow properties were analyzed on all 17 sampled pack ice floes by means of so-called snow pits to describe key physical snow parameters and their stratigraphy of the prevailing snowpack.

Snow pit measurements were taken on the undisturbed shaded working wall of the snow pit. At first, the temperature was measured every 1 to 5 cm from the top (snow-air interface) to the bottom (snow-ice interface) with a hand-held thermometer (Testo). In a next step the different layers in the snow pack and their stratigraphic parameters were described. For each layer the snow grain size and type (e.g., rounded crystals, facetted crystals, depth hoar) is determined with a magnifying glass and a 1-to-3-mm grid card. In addition, every layer was characterized by its hardness with the following categories: fist (F), 4 fingers (4F), 1 finger (1F), pencil (P), and knife (K). Afterwards, the density of each snow layer was measured volumetrically by removing a defined snow block with a density cutter from each layer and weighing it with a digital scale. The snow samples from each density measurement were bagged on site to then be measured for salinity on board the ship. Table 7.4.1 summarizes the specific measurements conducted in each snow pit.

Station	Label	Date	Snow depth (cm)	Measurements				Location
				TEMP	DENS	STRAT	SAL/ISO	
E22_20220216_1	E22_20220216_1-1_SPIT01	2022-02-16	8,0	X	X	X	X	Coring site 3
E22_20220218_2	E22_20220218_2-1_SPIT01	2022-02-18	10,0	X	X	X	X	Coring site 1
E22_20220219_3	E22_20220219_3-1_SPIT01	2022-02-19	10,0	X	X	X	X	Coring site 1
E22_20220220_4	E22_20220220_4-1_SPIT01	2022-02-20	7,0	X	X	X	X	Coring site 2
E22_20220221_5	E22_20220221_5-1_SPIT01	2022-02-21	14,0	X	X	X	X	Coring site 1
E22_20220222_6	E22_20220222_6-1_SPIT01	2022-02-22	14,0	X	X	X	X	Coring site 1
E22_20220223_8	E22_20220223_8-1_SPIT01	2022-02-23	8,0	X		X		Coring site 2
E22_20220225_9	E22_20220225_9-1_SPIT01	2022-02-25	9,0	X	X	X	X	Coring site 1
E22_20220226_10	E22_20220226_10-1_SPIT01	2022-02-26	9,0	X	X	X	X	Coring site 1
E22_20220227_11	E22_20220227_11-1_SPIT01	2022-02-27	14,5	X	X	X	X	Coring site 1
E22_20220228_12	E22_20220228_12-1_SPIT01	2022-02-28	14,0	X	X	X	X	Coring site 1
E22_20220301_13	E22_20220301_13-1_SPIT01	2022-03-01	16,0	X	X	X	X	Coring site 1
E22_20220303_14	E22_20220303_14-1_SPIT01	2022-03-03	21,0	X	X	X	X	Coring site 1
E22_20220304_15	E22_20220304_15-1_SPIT01	2022-03-04	9,0	X	X	X	X	Coring site 1
E22_20220305_16	E22_20220305_16-1_SPIT01	2022-03-05	9,0	X	X	X	X	Coring site 1
E22_20220306_17	E22_20220306_17-1_SPIT01	2022-03-06	10,0	X	X	X	X	Coring site 1

Table 3: *Overview of all sampled snow pits. Possible measurements are: temperature (TEMP), density (DENS), stratigraphy (STR), and samples for salinity and oxygen isotopes (SAL/ISO).*

Preliminary (expected) results

Figure 53 shows two typical snow pit data sets during the expedition: on the one hand, at the beginning of the expedition with hardly any fresh snow, as from station E22_20220220_4, and on the other hand, a typical profile after periodic snow showers, as that from station E22_20220301_13.

Starting with the snowpack analysis from February 20, the snow pit was sampled in a representative area of the floe with a snow depth of 7 cm. The snowpack contained 5 different layers (from top to bottom): a thin layer of wind-compacted fresh snow, so-called wind slab, (1), followed by a rather loose layer of facetted crystals (2). Below, a loose layer of poorly layered depth hoar crystals was identified (3). The lower part of the snowpack is characterized by two consecutive layers of melt-freeze forms, while the upper one (4) is not yet as hard and compacted as the lower one (5) at the interface between snow and ice. However, it must be stated that the transition from snow to ice is not explicit for all snow pits, but the transition from melt-freeze form to superimposed ice is rather gradual.

Snowpack characteristics in the second half of the sampling period differ significantly from those in the first half. The snow pit analysis of March 01 is a representative example of this. The 16 cm thick snow pack contained 5 different layers (from top to bottom): a compacted hard crust at the top (1), followed by a 10.5-cm thick uniform layer of small-grained angular crystals of medium hardness (1 finger) (2). Below, a loose layer of layered depth hoar crystals was identified (3), whereas the bottom of the snowpack was again characterized by a layer of melt-freeze forms (4).

Throughout the sampled snowpack the grain sizes increase, which correlated with the medium-range temperature gradient from top to bottom throughout all snow pit analysis. The given grain type distribution throughout the snowpack is typical for all sampled snow pits during Endurance22. Thus, melt-freeze forms were the dominant grain type in all snow pits with an averaged relative proportion of 32% (**Figure 54**) caused by an early beginning and frequently recurrence of thaw-freeze events in the northern Weddell Sea. The second-most prevalent grain type, with an averaged relative proportion of 23%, is wind slab, as snowfall events were accompanied by strong winds forming that rather compacted layer.

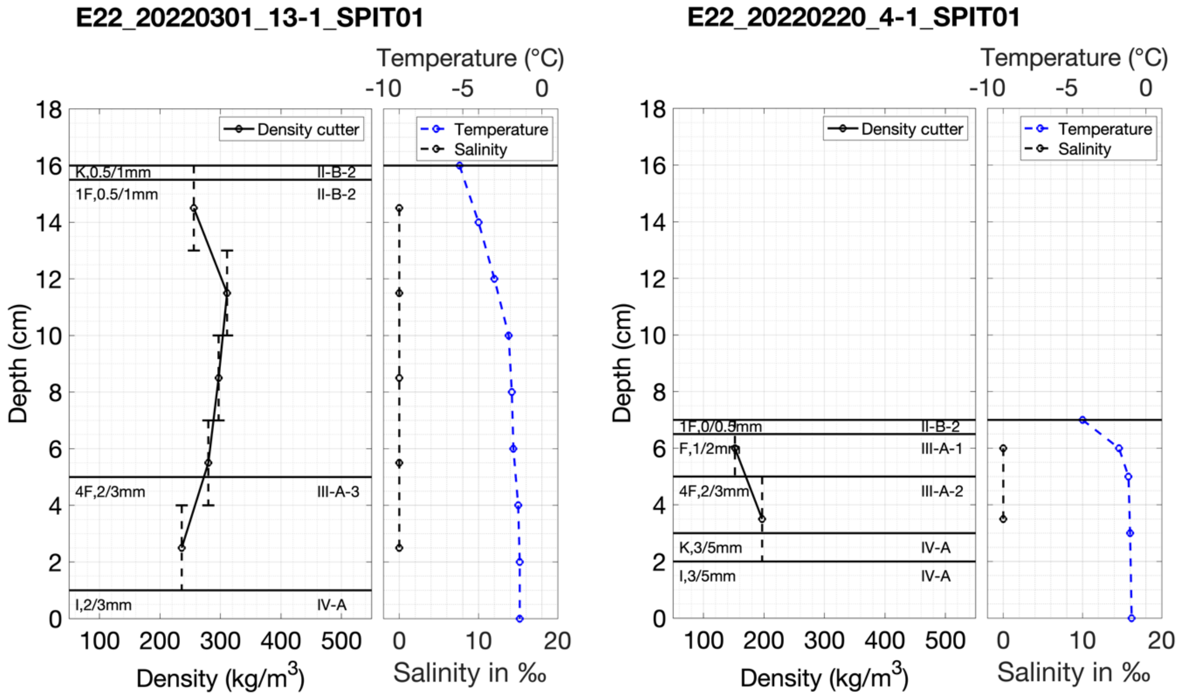

Figure 53: *Example of snow pit analysis from station (left) E22_20220220_4 and (right) E22_20220301_13. Respectively, the left panel shows the density measurements with the density cutter marked as black line, while vertical dashed lines mark the vertical range of the cutter (3cm). Horizontal lines indicate the different layer interfaces. Below the lines grain type classifications for the respective layer are given. The right panel shows the vertical profiles of snow temperature (blue) and salinity (black).*

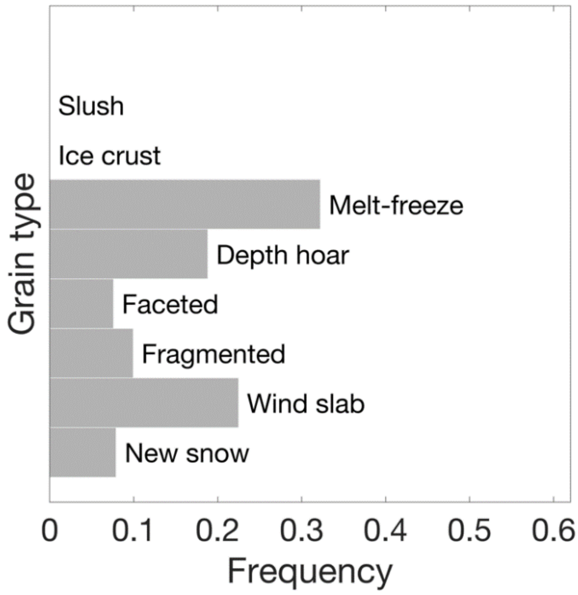

Figure 54: *Overview of relative occurrence of grain types within all sampled snow pits during the Endurance22 expedition.*

Data management

Data from all snow pit measurements will be delivered to PANGAEA within two years after the cruise.

7.6. Deployments of autonomous ice tethered platforms (buoys)

Written by Stefanie Arndt (AWI)

Objectives

In-situ snow measurements only provide snap-shot observations of snow properties. In order to also obtain information about the seasonal and inter-annual variability and evolution of the observed ice floes, we deploy autonomous ice tethered platforms (buoys), which measure snow characteristics also after the cruise. During Endurance22, one Snow (depth) Buoy was deployed measuring the snow accumulation over the course of the year. In addition, the buoy is equipped with sensors measuring air and/or body temperature and sea level pressure.
Combining all long-term data from these autonomous sensors, we will be able to better observe sea-ice processes and feedback mechanisms in the ice-covered Weddell Sea.
Beyond the immediate value for our sea ice mass balance research, the Snow Buoys report their position together with measurements of surface temperature and partially atmospheric sea level pressure directly into the Global Telecommunication System (GTS) used by weather prediction and atmospheric reanalysis systems. This activity is a contribution to the International Programme for Antarctic Buoys (IPAB) which is coordinated by AWI.

Work at sea

During Endurance22 one Snow Buoy, system 2022S119, was deployed during the first ice station on February 16, 2022 (see **Table 1**).

Preliminary (expected) results

Snow Buoys measure the snow accumulation at four spots by sonar sensors. **Figure 55** shows the snow accumulation of Snow Depth Buoy 2022S119 for the time period from February 16 to March 15, 2022. During this, a total snow accumulation of approx. 15 cm is recorded. Overall, the time series is characterized by small-scale changes of snow depth, shown by highly variable snow readings from the single sensors. Even though temperatures remained around 0°C between March 05 and March 10, no significant surface melt is evident.

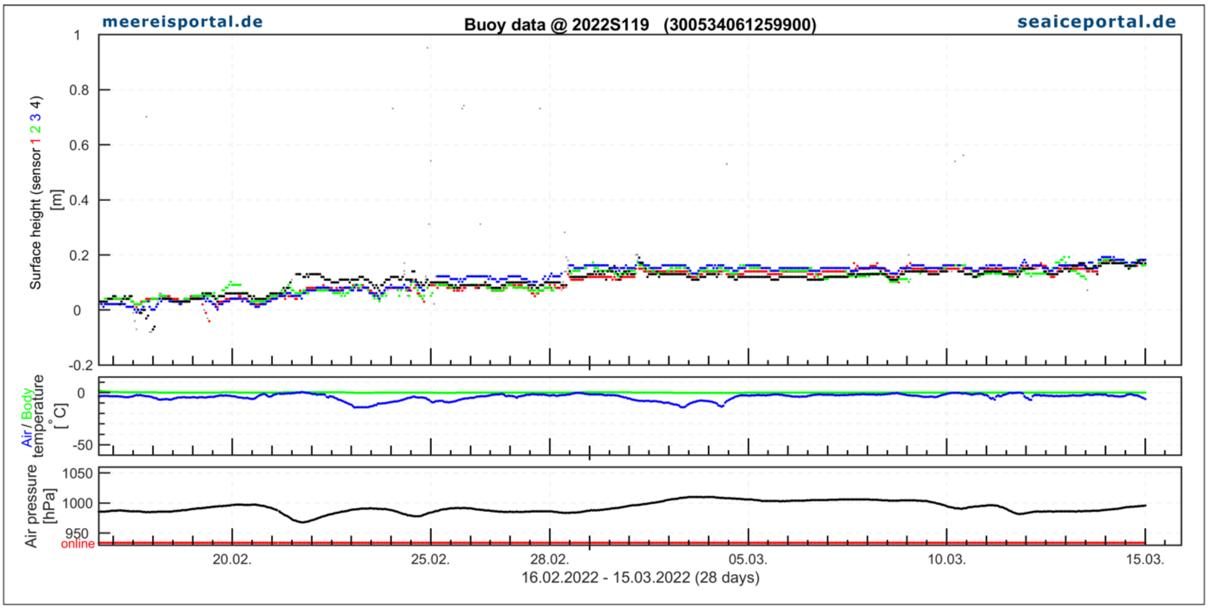

Figure 55: *Time series of snow accumulation along with respective meteorological conditions for Snow Buoy 2022S119, deployed on February 16, 2022.*

Data management

All buoy positions and raw data are available in near real time through the sea-ice data portal www.meereisportal.de. At the end of their lifetime (end of transmission of data) all data will be finally processed and made available in PANGAEA. All Snow Buoys report their position and atmospheric pressure directly into the Global Telecommunication System (GTS). Furthermore, all data are exchanged with international partners through the International Program for Antarctic Buoys.

8. Ice mechanics and ship response

Written by Anriëtte Bekker (Stellenbosch University)

Polar supply and research vessels operate in some of the harshest dynamic environments on earth. Knowledge of sea ice, its properties and resultant loading on vessels is far from complete and as such the safety of ships operating in these environments is based on the extrapolation of engineering data with reasonable assumptions from scale model tests in ice tanks and simulation models. An international research consortium comprising the University Stellenbosch, Aalto University, Aker Arctic, DNV GL, Rolls-Royce, STX Finland, University of Oulu, Wärtsilä and the Department of Environmental Affairs South Africa initiated a full-scale measurement program on the SAA II for her ice-trails in the Baltic Sea in March 2012 (Bekker *et al.*, 2014, 2018). Subsequently, Stellenbosch University and Aalto University have expanded on this effort, resulting in a one-of-a-kind full-scale measurement campaign to capture long term data. The measurements on the Endurance22 Expedition focus on structural ship responses. In particular, the measurement of ice loads on the ship hull and propulsion system from appropriate strain measurements as well as structural vibration of the ship hull with a focus on wave-induced vibration from wave slamming.

An overview of the measurement infrastructure, number of channels and sample rate of the full-scale measurements is presented in **Table 4**.

Measurement	Variables	Equipment	Number of channels	Sample rate
Ship vibration response (hull and super-structure)	Acceleration (Rigid body motion and flexure)	DC accelerometers,	10	2048 Hz
		ICP accelerometers	20	2048 Hz
Ship - shaft-line torsional and thrust vibration	Thrust, Torque,	Strain gauges, V-links and Quantum data acquisition units	2	600 Hz
	Bearing acceleration	Accelerometers to Quantum data acquisition units	6	2048 Hz
	Bearing acoustic emissions	Acoustic emission sensors, Qass measurement system	2	6 MHz
Ship - hull ice loading	Bow, bow shoulder and stern shoulder loads	Strain gauges, Central measurement unit	56 (+ 9)	200 Hz
Ship – AIS data	Various sensors and ship central measurement unit	Time, latitude, longitude, SOG, COG, HDT, relative wind direction, wind speed, depth	9	1 Hz
Ship machine control {This system did not operate correctly on the present voyage}		Propeller motor current, speed and voltage for starboard propeller. Rudder order, position and pitch for port- and starboard shaft, rpm.	26	0.5 Hz

Table 4: . *Full-scale ship-based measurement instrumentation on the SA Agulhas II.*

8.1. Ice-induced propeller moments on SA Agulhas II

Written by Anriëtte Bekker (Stellenbosch University)

The aim of full-scale propulsion measurements on the Endurance22 Expedition is to capture data for the EU MARTERA project, Life Prediction and Health Monitoring of Marine Propulsion System under Ice Impact (HealthPROP). In this project, Stellenbosch University is partnering with academia and industry in Norway and Germany to develop a digital twin platform towards monitoring the propulsion system and drive line of ships in Arctic and Antarctic operations. Here, the combination of intelligent sensors, data acquisition systems and fault detection algorithms will be used to improve the reliability and operational safety of ship propulsion systems in harsh environmental conditions. The project is funded through the EU MARTERA Programme with the funding for the participation of Stellenbosch provided by the Department of Science and Innovation.

Shaft-line measurements (***Figure 56***) entailed strain gauges on the port side shaft line of the SAA II to determine the shear and axial strain as described in De Waal et al. (2017). These measurements enable the calculation of the instantaneous torque and thrust at the measurement location in the shaft. Measurements on the shaft-line have a three-fold purpose:

1. The strain analysis enables determination of the stress cycles in the shaft from where shaft fatigue can be determined using rainflow counting.
2. The transient torque and high-resolution speed enable the determination of the ice-induced propeller moments.
3. The potential exists to provide estimates of global resistance forces through concurrent analysis of the shaft thrust and ship speed.

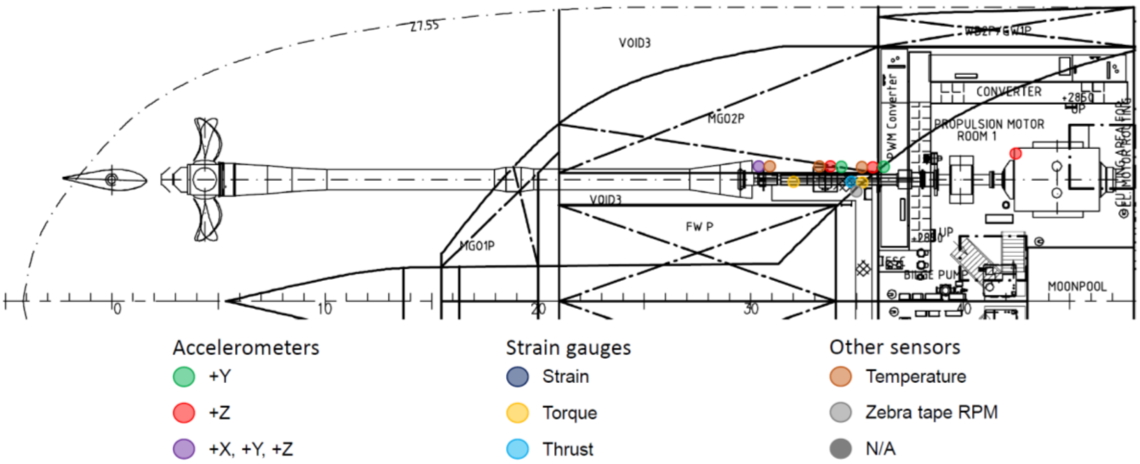

Figure 56 *Overview of measurement infrastructure on the port side shaft of SAAII.*

8.1.1 Sample result of inverse ice-induced propeller moment calculations

Stellenbosch University is leading research in the determination of ice-induced propeller loads from full-scale measurements. The steps to achieve this are outlined in ***Figure 57***.

First, indirect measurements of shear strain on the shaft are used to determine the torque in the shaft at the measurement location. Next, A modal superposition algorithm (Nickerson and Bekker, 2022) is used to calculate the ice-induced propeller torque. The advantages of this model include that it does not require regularization and that near real-time calculation is possible owing to the short processing time involved.

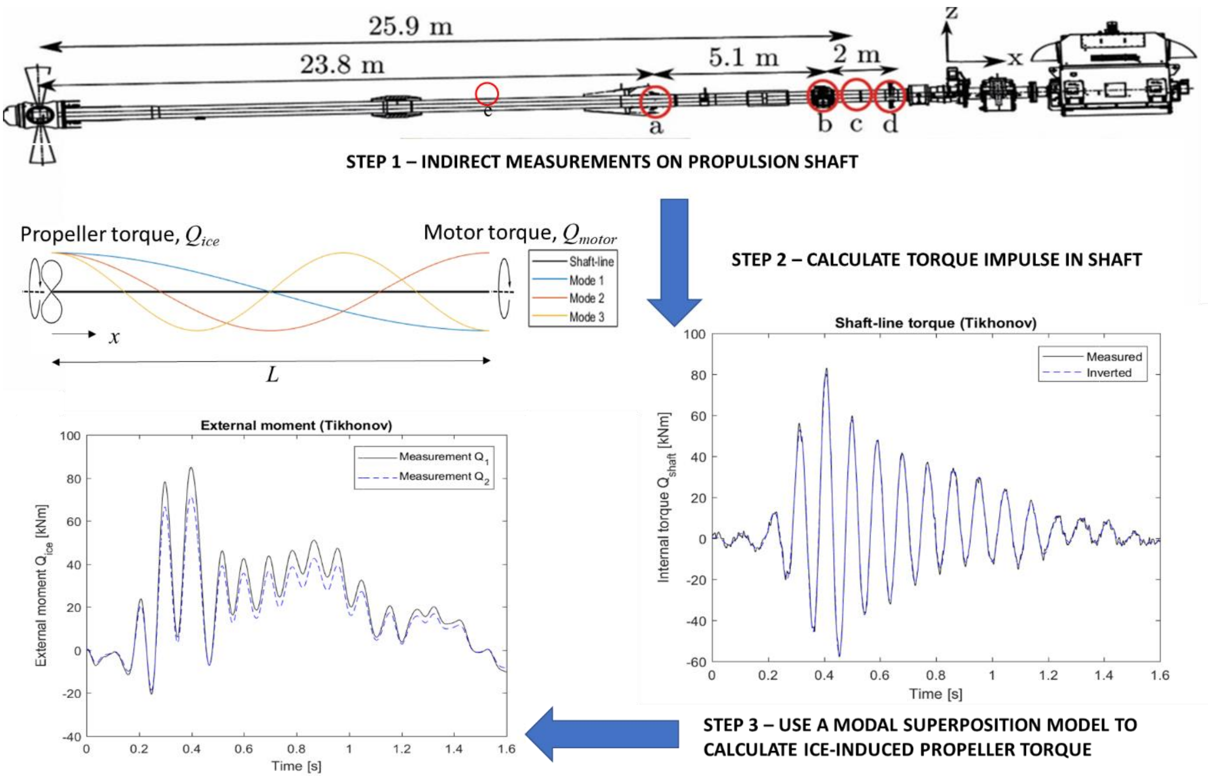

Figure 57: *A diagram depicting the methods involved with determining the inverse- ice-induced propeller moment.*

The investigation onboard pursued the determination ice-induced propeller moments. Sample time histories of the portside shaft torque depict the intermittent ice navigation of the vessel in the Weddell Sea to relocate the vessel to new stations in the sea ice. It is apparent (see ***Figure 58***) that the shaft torque exceeded the Maximum Continuous Rating (MCR) of 307 Nm for short intervals in ice. The calculation of the ice-induced propeller moment results in peak loads that exceed those observed in the shaft as presented in **Table 5** and ***Figure 58***. The peak loads do not exceed the design load limit of 1009.9 kNm (DNVGL, 2015) but reach about 88% of this value.

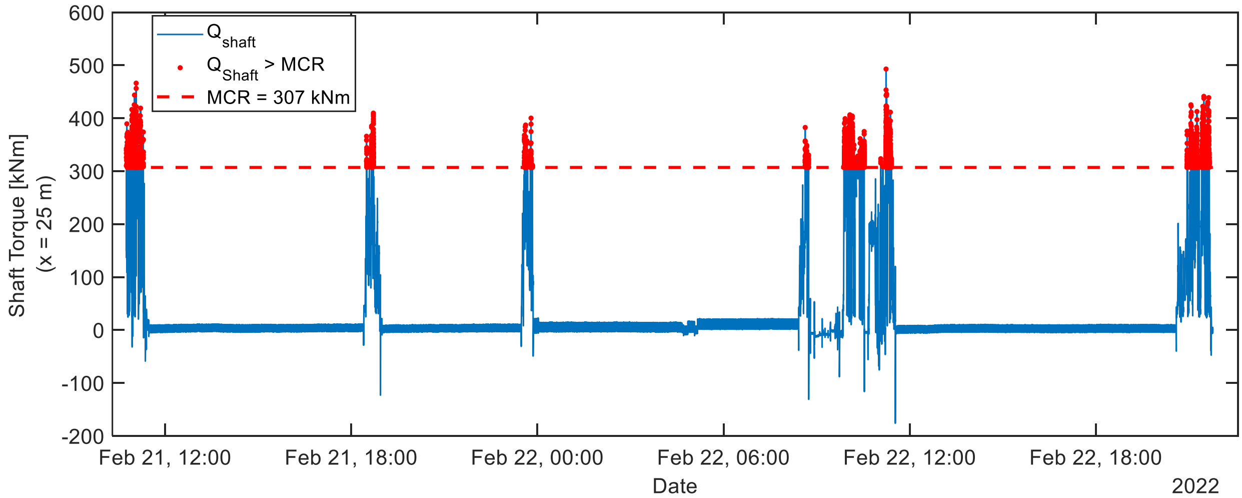

Figure 58: *Port side shaft torque of the SA Agulhas II during ice navigation in the Weddell Sea. The values are reflected against the maximum continuous rating of the shaft.*

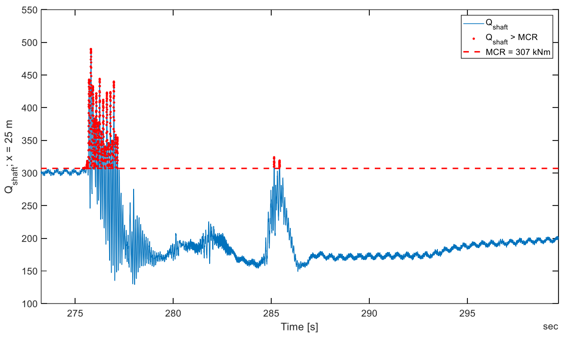

(a) Case A - Q_{shaft}

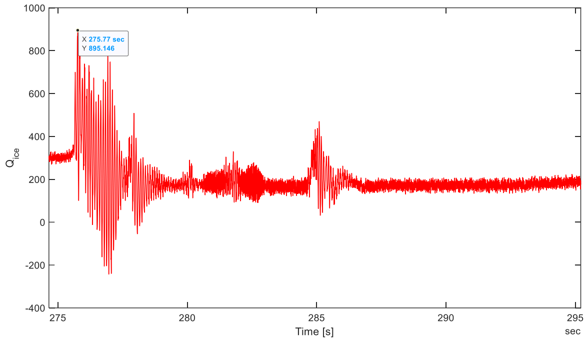

(b) Case A - Q_{ice}

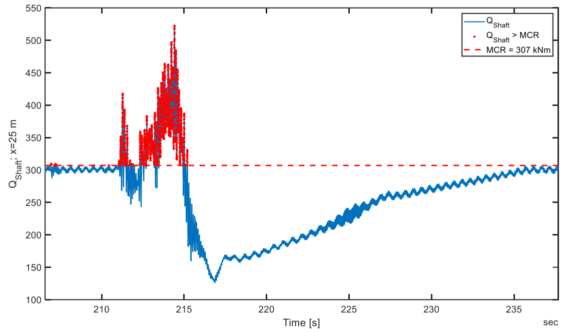

(c) Case B - Q_{shaft}

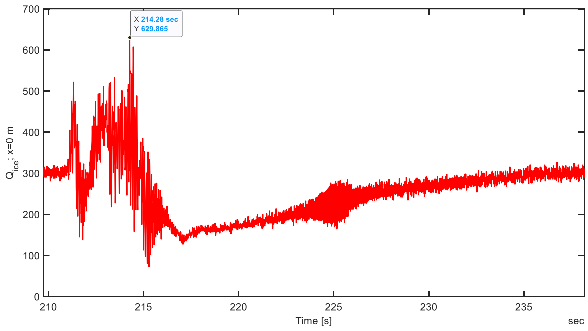

(d) Case B - Q_{ice}

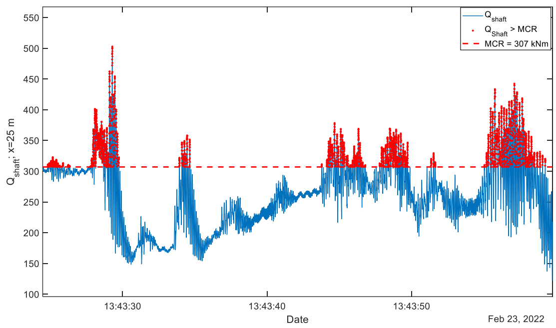

(e) Case C - Q_{shaft}

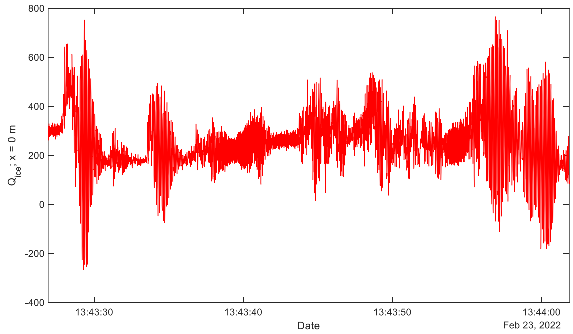

(f) Case C - Q_{ice}

Figure 59: *Examples of shaft torque measurements and ice-induced propeller moment calculations.*

.#	Load case description	Maximum shaft torque Q_{shaft} [kNm]	Maximum propeller moment load Q_{ice} [kNm]
		MCR=*307* kNm	Qice,max=*1009.9* kNm
A	Milling, ship moving astern	606.9	950.0
B	Single impact and milling, moving astern	575.7	764.2
C	Multiple impacts whilst speed recovers, astern	547.2	686.3
D	Single impact, moving ahead	545.8	887.5
E	Single impact and milling, moving astern	533.5	674.0
F	Multiple impacts, moving ahead	530.3	839.7
G	Single impact, moving astern	529.7	852.9
H	Single impact and milling, moving astern	522.5	629.9
J	Multiple impacts, moving ahead	521.5	901.1
K	Milling, moving astern	518.9	786.0

Table 5: *Examples of prominent ice-propeller impact cases during Endurance22 ice navigation.*

8.1.2 Preliminary insights from propulsion measurements

The measurement campaign of Endurance22 represents the first meaningful investigation of Stellenbosch University into bearing temperature variation during ice navigation. It is interesting to observe the intermittent rise in bearing temperatures that correspond to periods of ice navigation as shown in ***Figure 60(a)***. The coolest temperatures are also associated with the most outboard locations of the temperature probes. The locations of the probes are indicated on the ship technical drawings in ***Figure 60(b).***

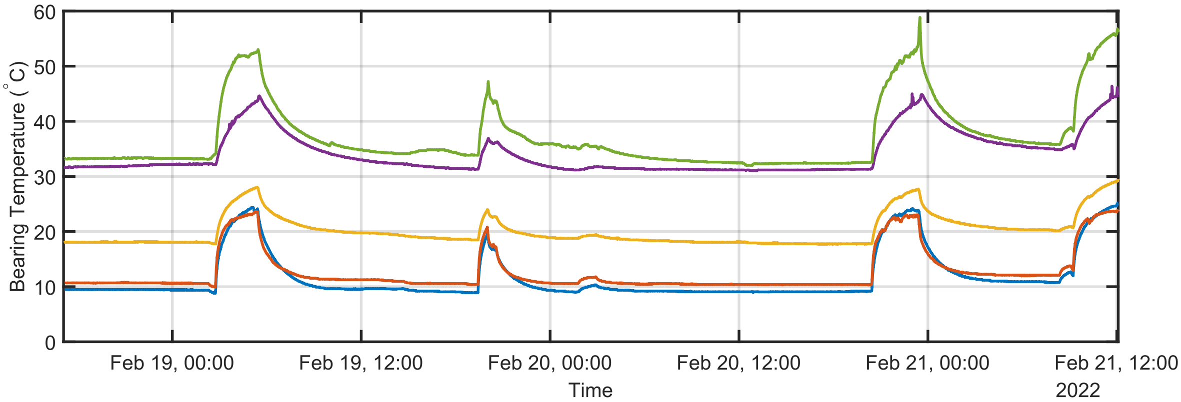

(a)

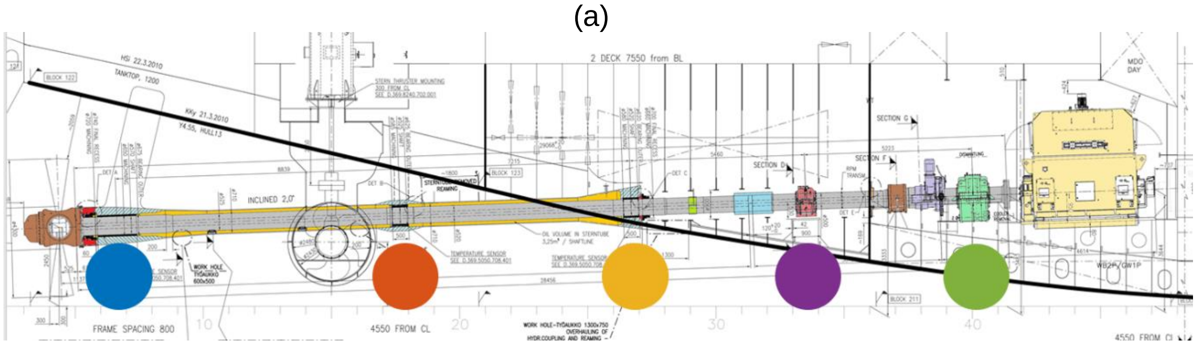

(b)

Figure 60: *Preliminary results from bearing measurements on five bearings along the port side shaft of the SAAII during ice navigation.*

The ship propulsion system presented with some issues during the voyage in that the crew found it challenging to retain navigation using the ice mode of the vessel. These issues are reportedly associated with the tripping of a converter unit. As such not all four converters were available to allow full utilization of the ship power. The tripping incidents are visible in the recorded data. ***Figure 61(a)*** shows the drop in the port side torque, thrust and shaft rpm. A spectrogram of the motor acceleration in ***Figure 61(b)*** signal shows the abrupt loss of the electrical signature of the motor. No final conclusions are possible yet, however these features may prove promising in the detection of tripping events and associated data after the fact. Such analysis could benefit a root cause investigation into the causes of converter tripping.

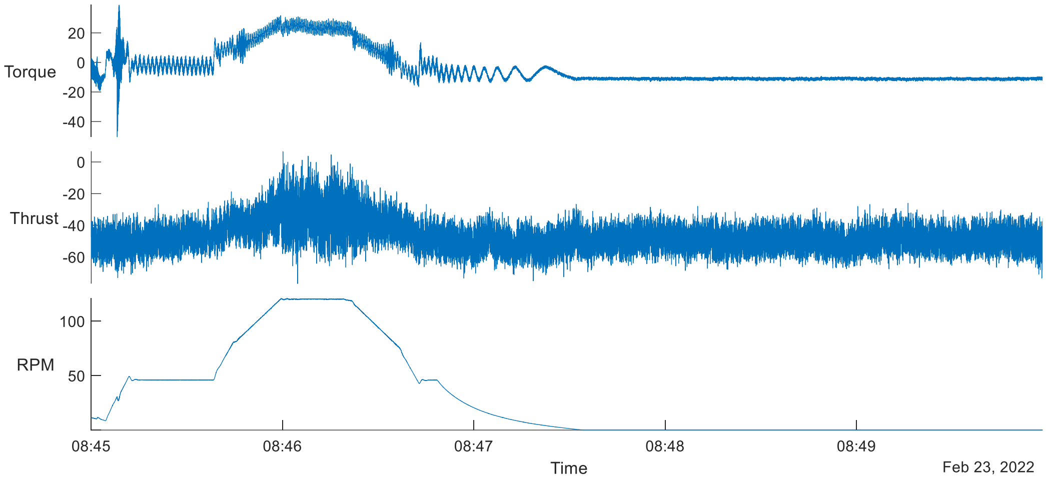

(a) Torque, thrust and rpm of the port side propulsion shaft.

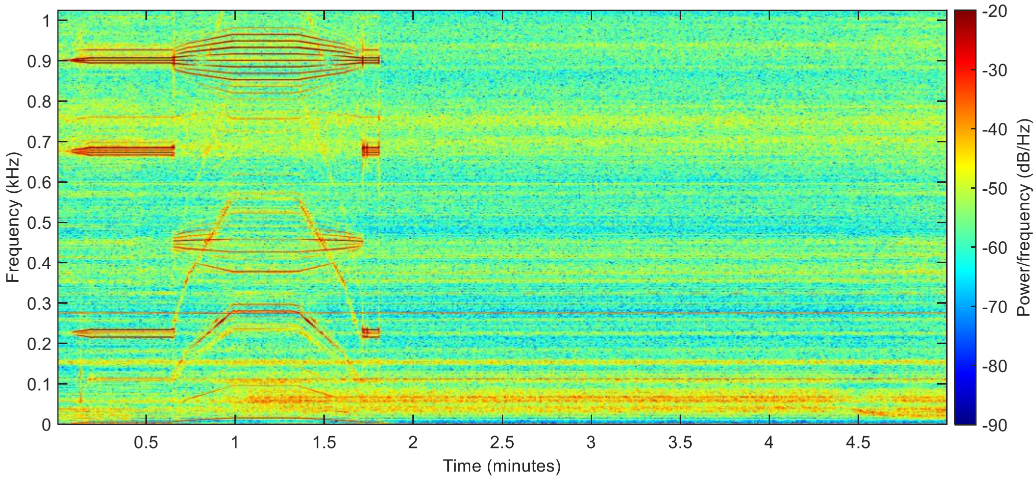

(b) A spectrogram of the acceleration on the motor housing.

Figure 61: *Indicative propulsion measurements during a converter tripping event on 23 February 2022.*

8.2. Ice-induced loads on SA Agulhas II

Written by Jukka Tuhkuri (Aalto University)

Aalto University and Stellenbosch University jointly measured ice loads on the hull of SA Agulhas II and conducted parallel observations about ice conditions. Data was recorded continuously when the ship was in ice. We monitored sea ice concentration, thickness and floe size continuously when in ice. For our research goals, it is important to obtain both the loads on the ship and the ice data at the same location with high resolution. The ice conditions were monitored the by using (1) visual observations, (2) cameras, and (3) an electromagnetic (EM) device provided by AWI and operated by D&N. In addition to monitoring sea ice conditions, small scale ice properties were studied by collecting sea ice samples from 15 ice floes and the salinity, temperature, and density profiles of the ice were measured. In addition to the Endurance22 expedition organised by the FMHT, the work by Aalto was supported by the Academy of Finland and the Finnish Antarctic Research Program (FINNARP)

Ice loads on the ship hull were be measured with strain gauges mounted on the hull (**Figure 62**) and with a measurement system located in the engine storage room on Deck 2. The measurement computer recorded also the navigational and operational data. The system was installed in 2011 when the ship was under construction in Rauma, Finland. The system has been operating since, and has given us very valuable data on ice loads on a ship. Indeed, this data set is the most extensive ship ice load data that exists. ***Figure 63*** shows the ice load on two bow frames during the Endurance22 expedition. It is noteworthy that event though the ice conditions during the expedition can be considered easy, compared with the 2019 Weddell Sea expedition, a number of high ice load events were recorded. The detailed mechanics of these events remains to the analysed.

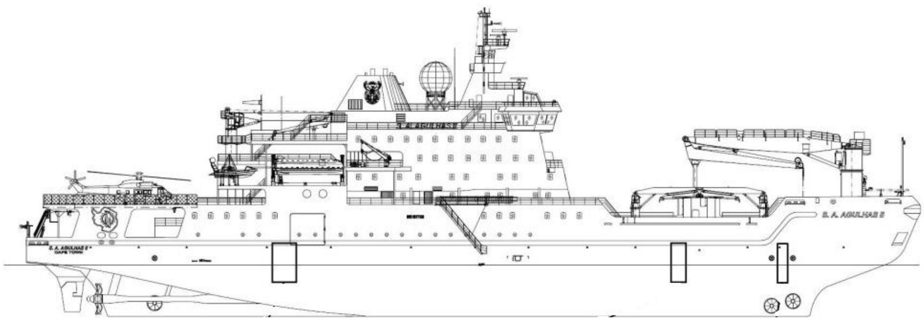

Figure 62: *SA Agulhas II. The three rectangles on the hull show locations where ice loads are measured.*

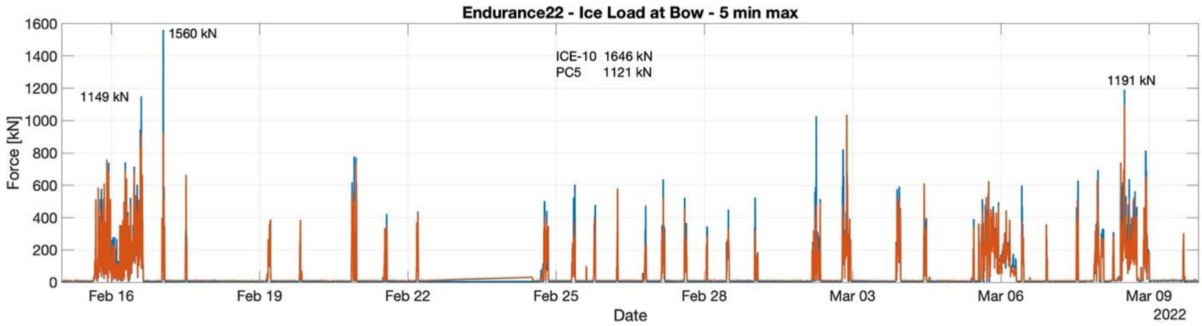

***Figure 63**: The ice loads measured from two frames at the bow. Also shown are the design ice loads for PC5 and ICE-10.*

8.3. Wave-induced hull vibration on SA Agulhas II

Written by Anriëtte Bekker (Stellenbosch University)

For the Endurance22 expedition an accelerometer network of 30 accelerometers was utilized and referenced to a vessel-centric coordinate system, where the respective axes, xyz refer to fore-aft, lateral- and vertical acceleration. All measurements were sampled at 2048 Hz by this accelerometer network which is suitable to capture rigid body and flexural motion. Measurement locations are presented in **Figure 64**. The global response of the ship hull is captured by six pairs of accelerometers on the port- and starboard sides of the vessel hull. Lateral motion is measured by two sensors, one on the starboard side at the stern and one on the vessel centre line in the bow chain locker.

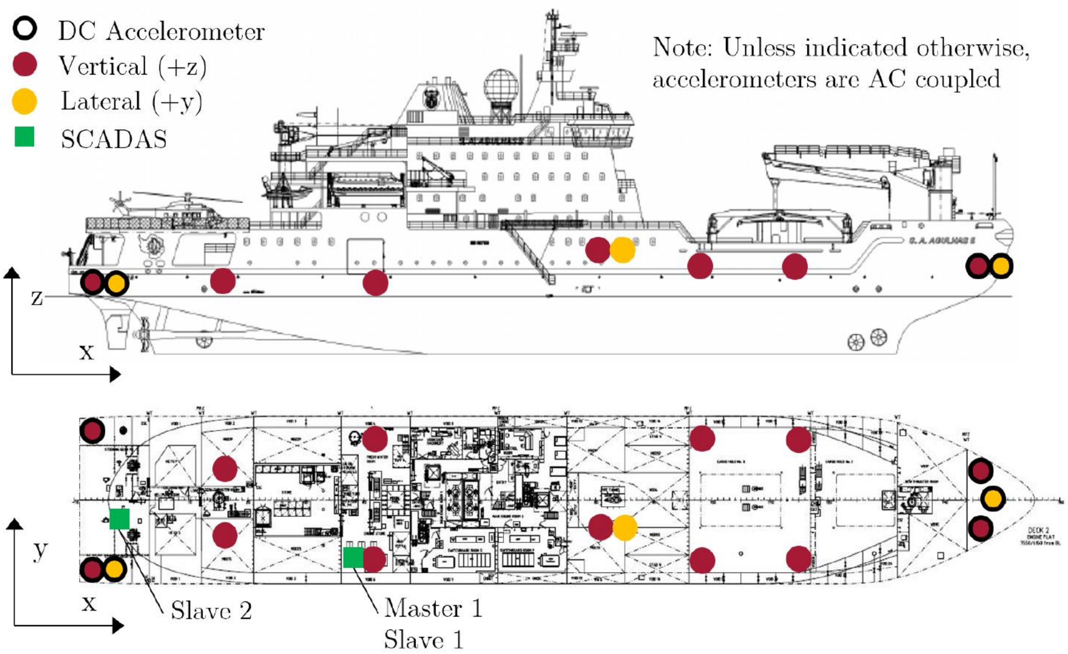

***Figure 64:** Overview of accelerometer measurements throughout the hull structure of the SAAII.*

In order to enable a full-scale fatigue calculation, strain sensors were installed amidship at the transition between the bow and the superstructure. The sensor configuration in this was updated and installed in Void 16 and Void 17 prior to Endurance22. For this reason, the results from this will enjoy focus in the future analysis of voyage data. Improvements involve the relocation of the measuring point within the void and the application of a long base strain gauge making use of previously installed measurement cables. The full-scale hull measurement project is funded by the National Research Foundation through the South African National Antarctic Programme.

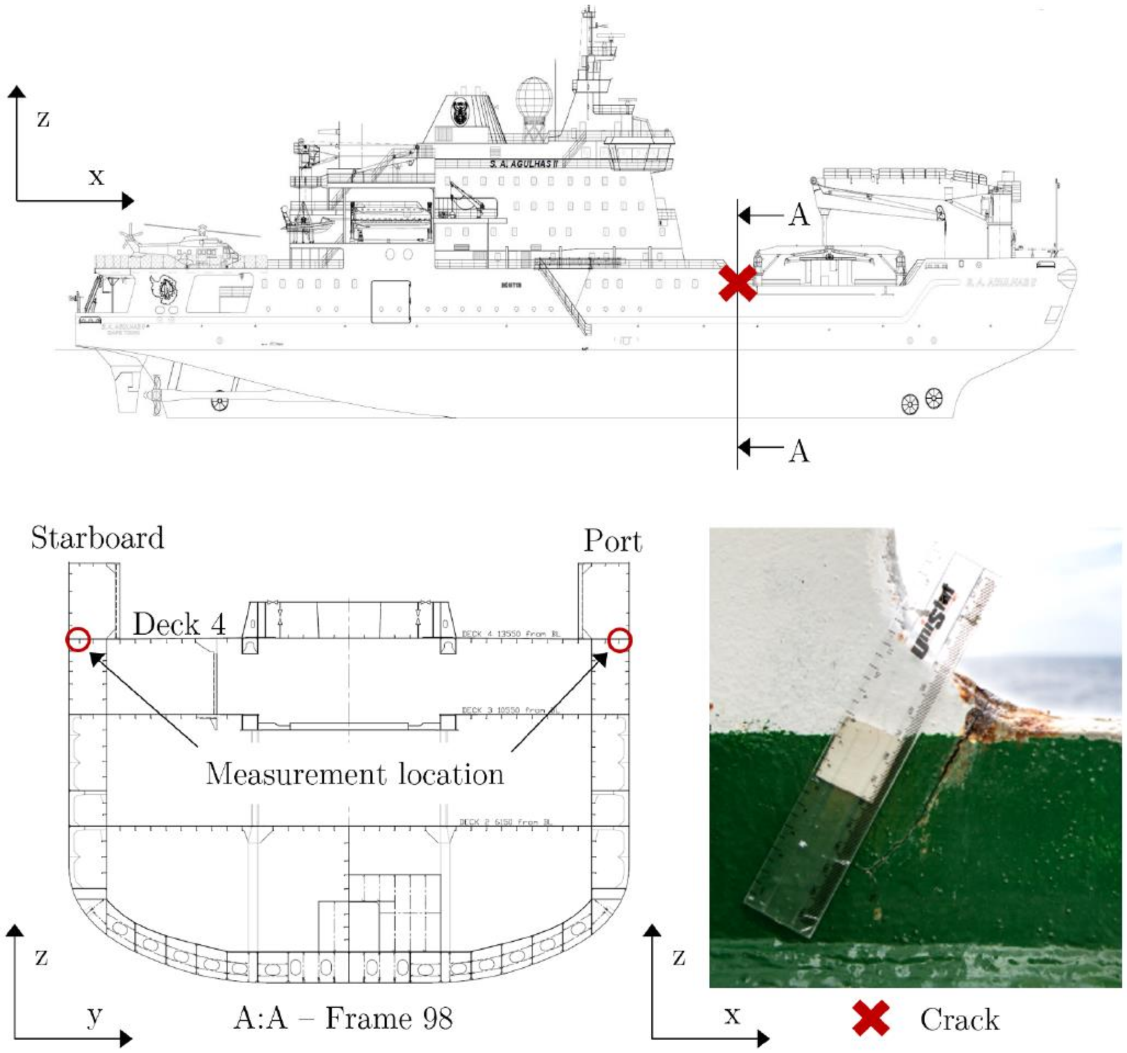

Figure 65: *Strain measurement locations and nearby cracking.*

8.3.1. Sample calculation of full-scale fatigue

Figure 66 presents an overview of the workflow for full-scale fatigue damage Quantification (Pferdekämper and Bekker, 2022). The structural detail of interest is to be identified to determine the appropriate Stress Concentration Factor (SCF). Additionally the appropriate S-N curve should be retrieved from class rules (Bureau Veritas, 2016). The recorded strain-time series are then loaded and converted to the stress-time equivalent. This series is down sampled and cleaned, before the different frequency components are isolated. Rainflow cycle counting and Miner's accumulative damage theory can then be used to quantify the fatigue damage.

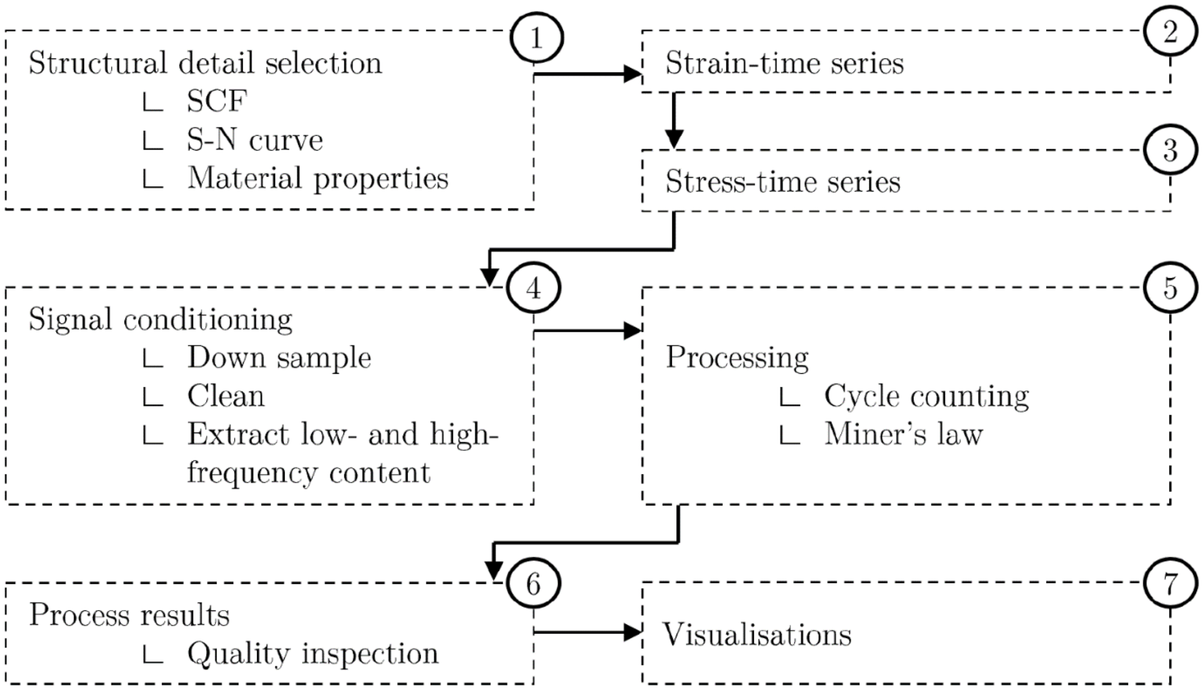

Figure 66: *Steps of the full-scale fatigue calculation.*

The connection of a longitudinal deck stiffener to a transverse web frame represents the selected structural detail used in example calculations. More specifically, fatigue cracks are common at the weld joining the tripping bracket to the flange of the stiffener (Pferdekämper and Bekker, 2022). This detail is shown in **Figure 67** for the SAAII.

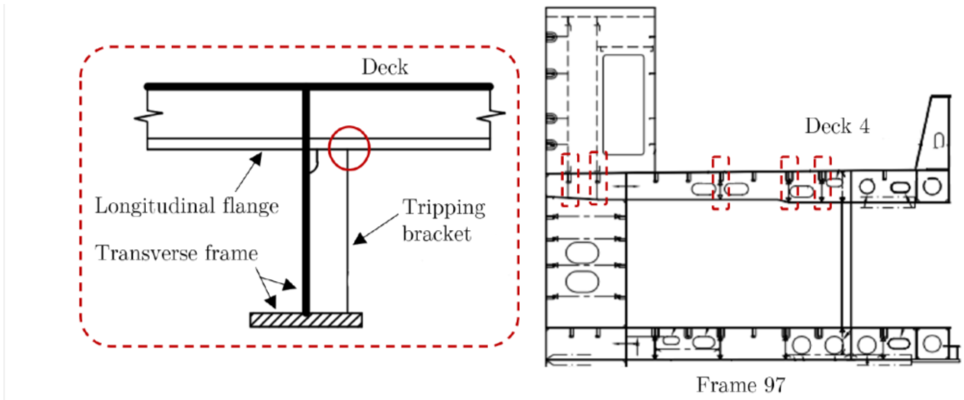

Figure 67: *Longitudinal deck stiffener to a transverse web frame connection.*

Bureau Veritas specifies that a SCF of 1.67 is applicable to this geometry. This SCF effectively transfers the global frame stress (measured by the strain gauge), to a hotspot stress experienced by the welded connection. Additionally, Bureau Veritas provides the applicable S-N curve for the selected detail and loading condition. The P⊥ curve is used as the hotspot stress acts perpendicular to the joint. The selected detail is not expected to be in direct contact with seawater. Therefore, a two-slope P⊥ S-N curve for welded steel joints in air is selected. This curve is plotted in Figure 68. The hull girders of the SAAII are constructed from DH-36 marine steel. This material has a modulus of elasticity $E = 210\ MPa$ and a Poisson's ratio $\nu = 0.3$.

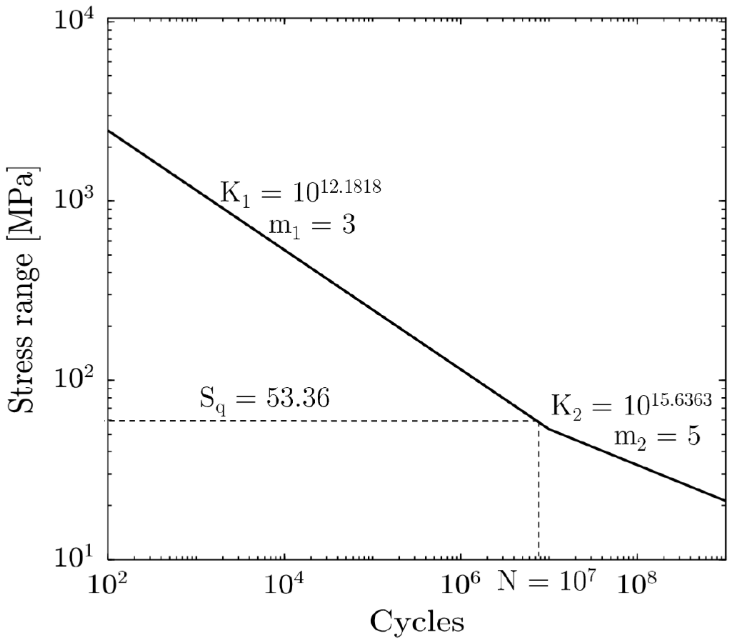

Figure 68: *A S-N curve for steel welded joints in air plotted on logarithmic axes.*

Fatigue damage can be deconstructed into two components (**Figure 69**). The low frequency component stems from the hogging and sagging bending moments. These are caused by the weight distribution of a vessel tending to bend the hull girder depending on the location of support provided by passing waves . The component due to wave induced vibrations, hereafter referred to as the high frequency component, is caused by the excitation of structural bending modes. These modes can be excited through springing and whipping. For the purposes of the present voyage, the determination of the vibration-induced fatigue damage will enjoy significant focus in future analysis efforts.

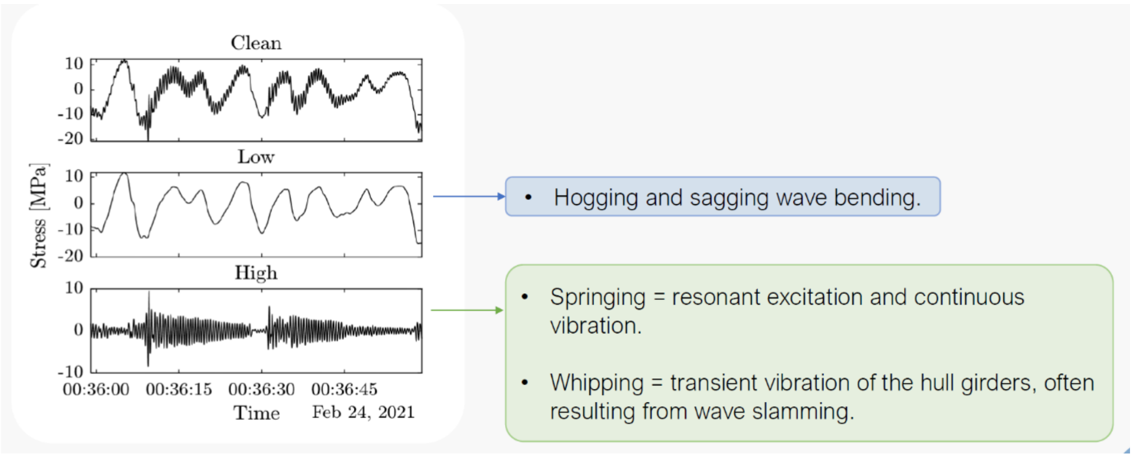

Figure 69*: The high and low frequency components of fatigue.*

A preliminary analysis was conducted during an open water storm on 13 February 2022. From **Figure 70** it can be seen that the high frequency fatigue exceeds that of the low frequency by one to two orders of magnitude. As such the further investigation of wave-induced vibration on the SAAII is warranted.

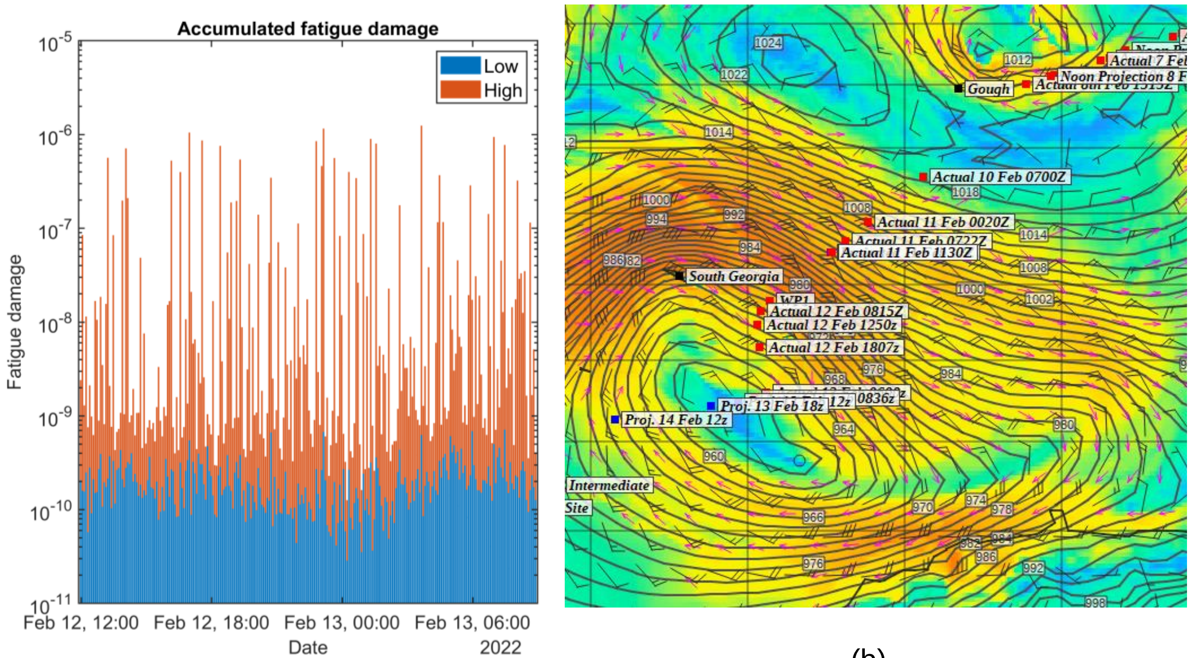

(a) (b)

Figure 70*: (a) A sample analysis of high and low frequency fatigue damage in the context of the (b) open water transit of the SAAII on 13 February 2022 (Courtesy of the South African Weather Service).*

8.4. Route prediction based of historic ship data

Written by James-John Matthee (Stellenbosch University)

A routing algorithm is currently in development at Stellenbosch University, that utilizes ship data like Speed Over Ground and Propeller Motor Power as prior inputs to optimize for various objectives.

The collected data from the 2019 Weddell Sea Expedition was used to develop the first iteration of the algorithm. The basic method uses AMSR-2 satellite images (https://seaice.uni-bremen.de/data/amsr2/) of the 3.125km grid ice concentration, together with the previous responses of the SA Agulhas II during ice navigation. It is possible to create different weighted arrays based on specific objectives that you want to optimize the route for. This is the first attempt to develop a suite of possible navigational services that can aid in decision-making onboard.

On the 15th of February 2022, the SA Agulhas II approached the ice edge. Ice navigation was unavoidable, and a strategic path had to be selected. The initial route selected by the captain, was a low-risk, ice avoidance route in an L-shape (see **Figure 71**). The Sentinel 1 and TerraSAR X images were also used to make this decision, but from the AMSR-2 image below, the reasoning behind the route is clear.

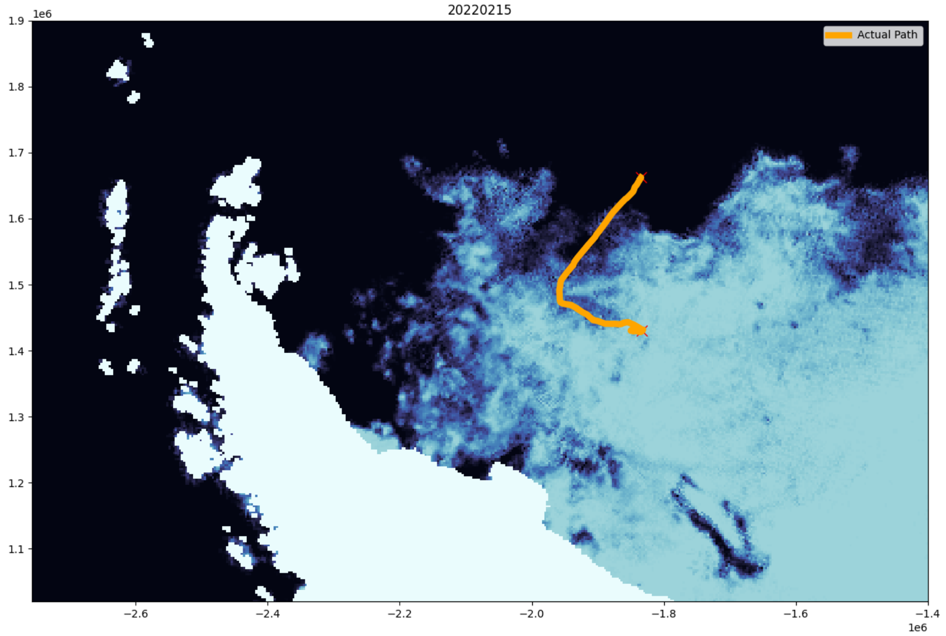

Figure 71: *Route travelled on 15 March 2022.*

Using the historic data from the vessel in navigating ice, it was possible to create two alternative routes, one that optimizes for speed (time) and the other for power (fuel consumption). These routes look similar to each other and are plotted in **Figure 72**.

It took approximately 24 hours (2022-02-15 15:00 to 2022-02-16 15:00) to move from the ice edge waypoint selected, to the search box.

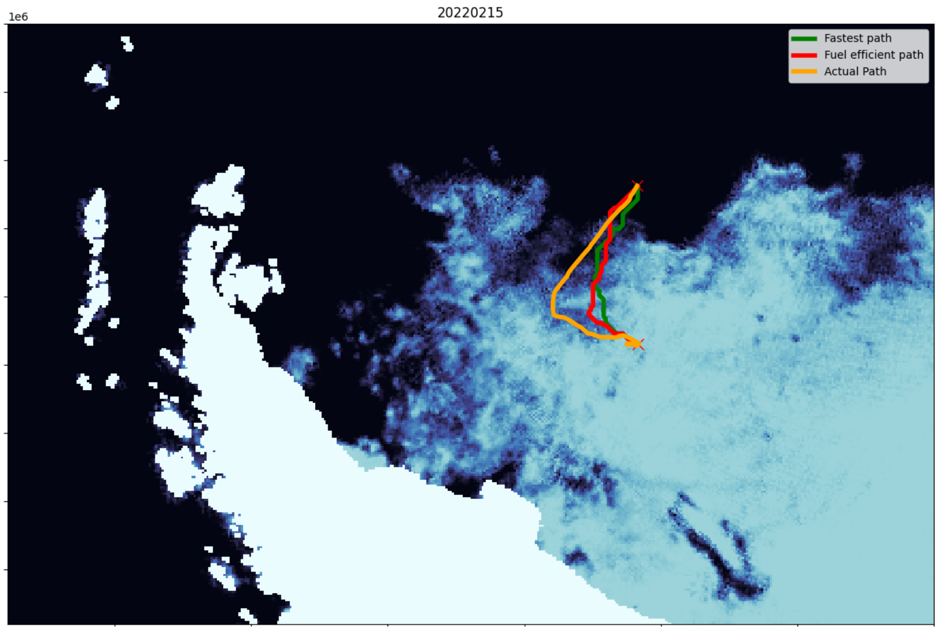

Figure 72: *Predicted routes based on time and fuel consumption optimization.*

The historic data of the ship was used to calculate the average speed of the vessel during certain ice regimes. It is possible to reverse engineer an ETA for the predicted paths, based on the prior knowledge of the possible average speeds attainable. For *time* optimization, the total distance traveled was 156 NM and for *power consumption* optimization, the total distance was 162 NM. When optimized for time, the algorithm predicts an estimated travel time of 22 hours, with a minimum time of 19 hours and a maximum time of 1 day and 2 hours. This is calculated by including the 99 percent confidence band of the historic ship speeds. When optimized for power consumption, the algorithm predicts an estimated travel time of 23 hours, with a minimum predicted time of 20 hours and a maximum time of 1 day and 5 hours. Results are plotted in **Figure 73**.

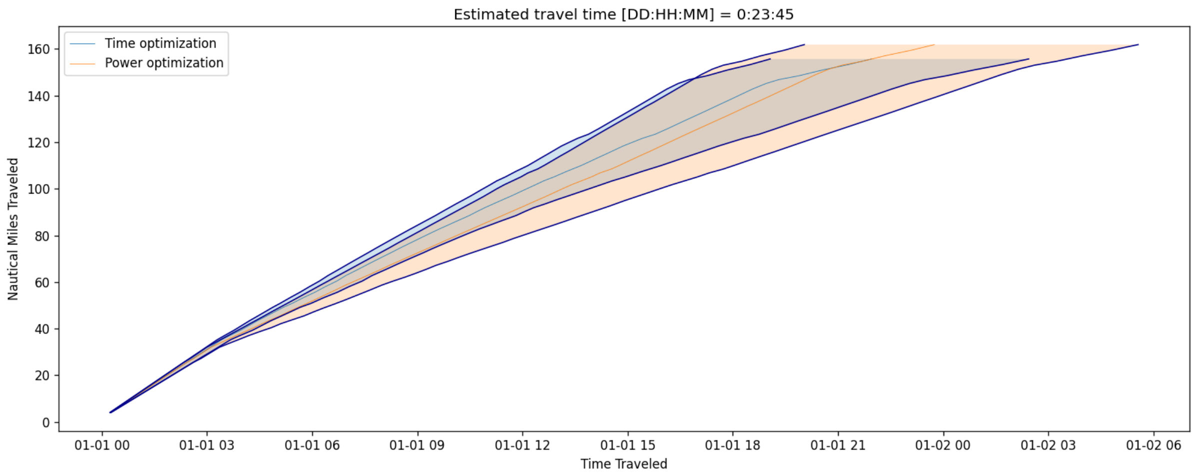

Figure 73: *Predicted travel times for the two optimization objectives.*

The Endurance22 navigational data will be used to improve these estimated travel features. The same algorithm was run for the 8th of March 2022 for our route out of the ice. Although the actual vs predicted routes are not exactly the same, the algorithm gives an objective direction of exit, that looks similar to the actual route (i.e., Northeast instead of Northwest) (see **Figure 74**).

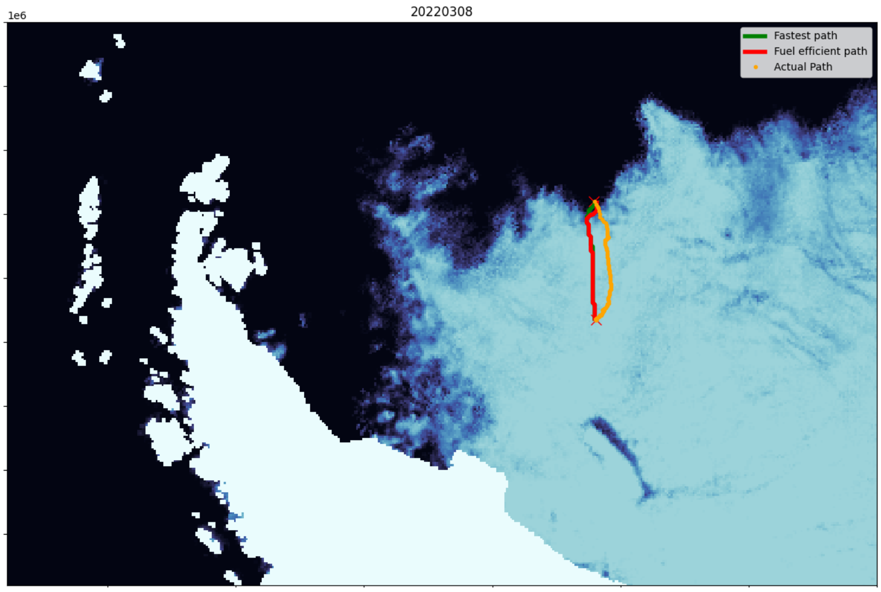

Figure 74: *Predicted route and actual route out of ice regime.*

The algorithm falls short on our route out and just predicts a straight line, because the ice concentration according to the ASMR-2 images is almost 100% all the way out. A higher resolution image is needed to estimate a more realistic path.

8.4.1 High-resolution blue-sky work

TerraSAR-X images that were already processed by DLR were provided during the expedition. This was crucial for tactical decision-making on the bridge and was even used during night navigation, which speaks volumes of how effective this service was.

Without taking drift into account, the 8-bit GeoTIFF files were converted to binary threshold images, which classifies all pixels smaller than a certain intensity as an open lead (**Figure 75**). This is a very preliminary proof of concept and an oversimplification of leader-line classification.

By tweaking the algorithm of the low-resolution data, it was possible to predict routes from point A to point B on a higher resolution.

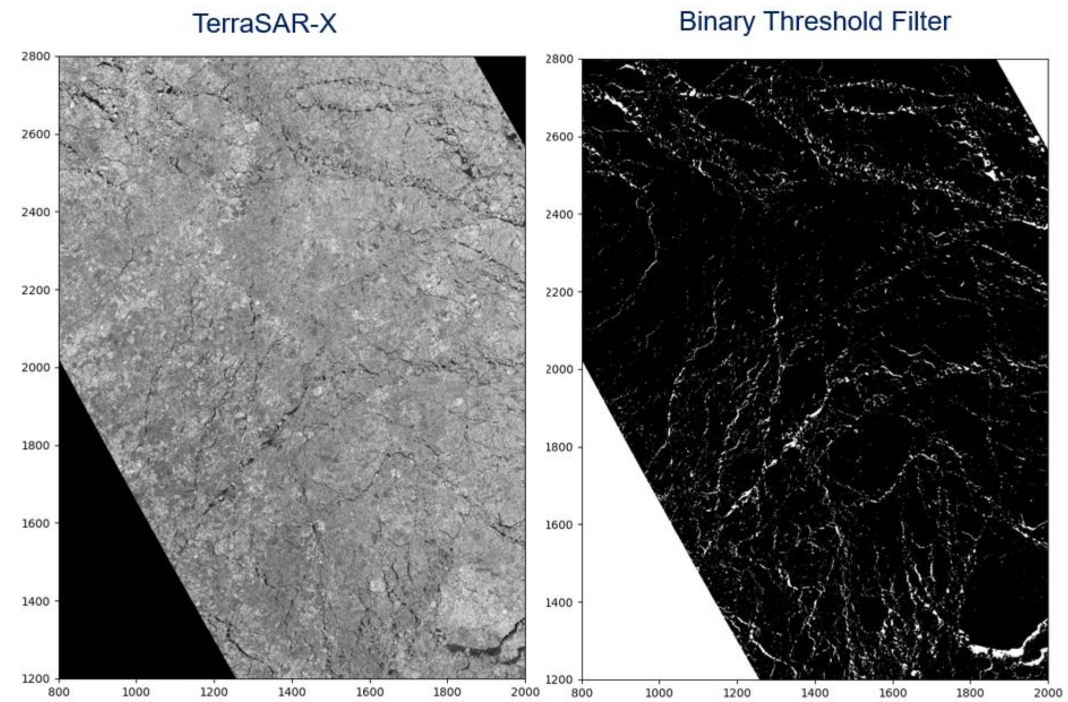

Figure 75: *TerraSAR-X image(left) with the binary threshold filter (right).*

4 Waypoints (info received from Alexandra on bridge) was plotted as a (green) line in **Figure 76**, with a predicted route in red[1]. When zoomed in, it is clear that the algorithm looks for the

[1] Remark from the editor: The TSX images were continuously re-georeferenced for purpose of tactical navigation. It appears that the green line (planned route corridor) does not match the shown TSX image in the background but belongs to another shifted version of the TSX image in Fig. xx. So the green line does not fulfill the criterion of being a planned route relative to the red one.

leader lines and follows them. It is not yet at a maturity level where different optimization objectives can be used for this algorithm.

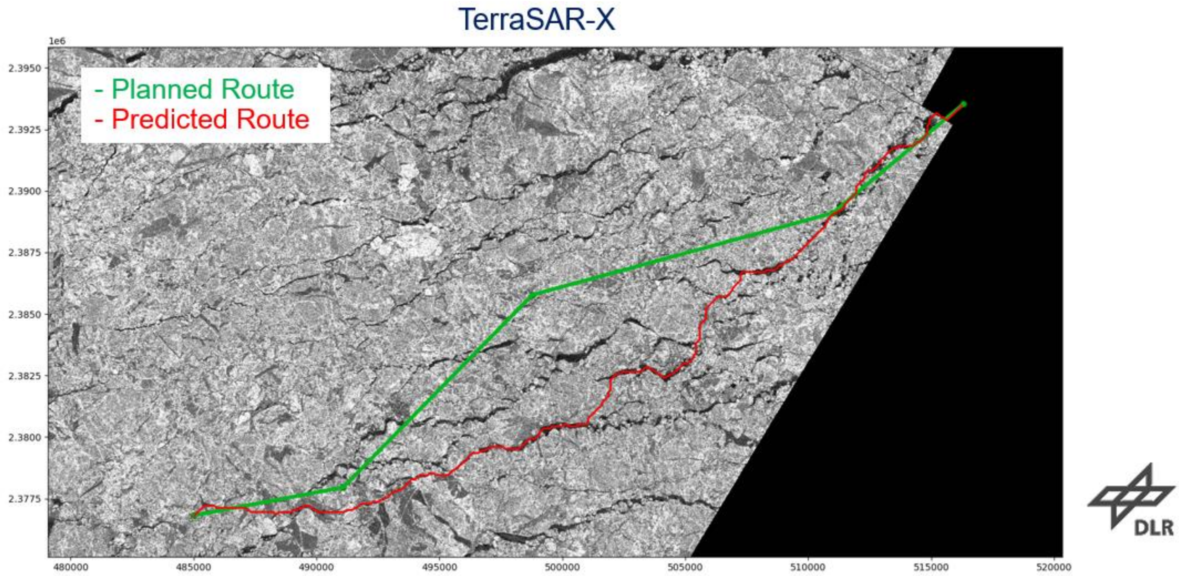

Figure 76:

Various remarks regarding the route planning algorithm with regards to the Endurance22 expedition:

1. Low resolution 3.125 km grid ice concentration maps can aid in strategic decision making, suggesting waypoints and a point-of-entry into the ice.
2. Ice concentration is one of the biggest factors to be considered during ice navigation.
3. Other features became apparently important during the ice navigation of Endurance22. This includes, but is not limited to ice thickness, type of ice, tidal information, drift information, visibility, and temperature changes.
4. To incorporate this into the model is possible but will require a lot more resources and time. We also run the risk of adding more variability and uncertainty to the model by adding these features, as each feature also comes with its own variability and uncertainty factors.
5. During tactical decision-making, the critical role of high-resolution radar images became apparent. As the classification of these TerraSAR X images (DLR) is also a project on its own, it is not wise for us to investigate this to the n^{th} degree. It was possible to put a simple threshold filter on the images, to detect leader lines. With the same algorithm as the lower-resolution AMSR-2 images, it is possible for the algorithm to follow leader lines from point A to point B.
6. The algorithm could be adjusted to more accurately simulate the decisions made on the bridge. It seemed as if the main priority was to reduce risk, by avoiding heavy ice as far as possible, instead of a trade-off between distance and time.
7. The data from this voyage would be used to further develop the weights of the algorithm to get better insights into the decision-making process, to hopefully one day assist captains during ice navigation.

9. Meteorology and Oceanography

Written by Marc de Voss and Carla Ramjukadh

The meteorological and oceanographic (met-ocean) work package consisted of an observational and forecasting (modelled) component. Forecasting and observation was primarily used to assist for operational support to bridge and sub-sea teams. Passengers were also kept appraised of current and predicted met-ocean conditions via daily weather briefings and various graphical forecast printouts posted in common areas. A dedicated, low-bandwidth data and information interface was built prior to departure to facilitate easy access onboard. **Figure 77** shows a sketch of the kind of information made available via the interface.

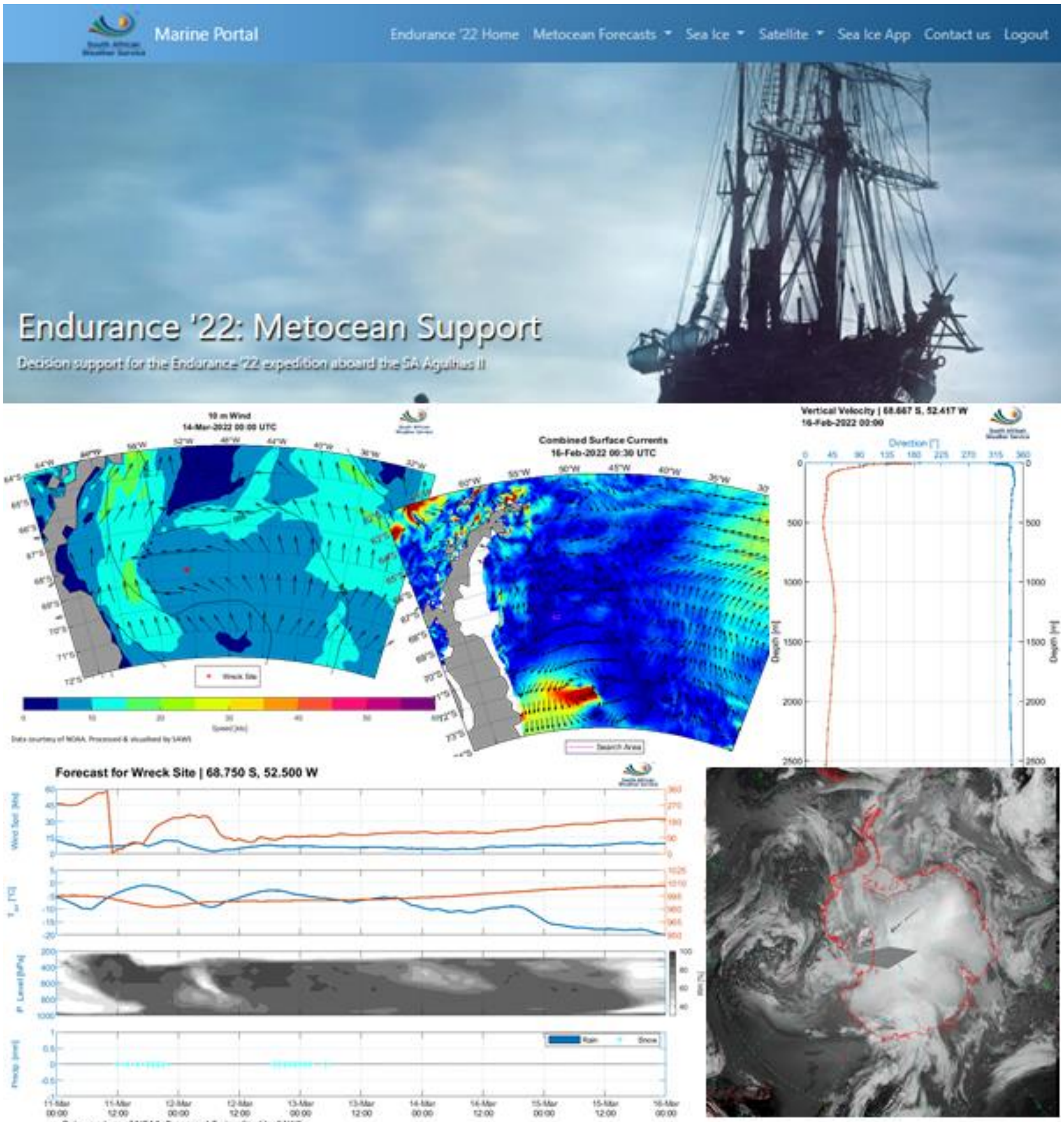

Figure 77. *The SAWS Endurance22 interface provided customised data and information products to support operations onboard with a low bandwidth overhead.*

9.1. Forecasting

A range of global numerical weather and ocean forecasting products was prepared for use onboard. Preparation included the establishment of subset and download protocols to the Cape Town office and scripting for processing and visualisation as required for the expedition. Low bandwidth imagery was then supplied to the vessel to minimize bandwidth requirements. A summary of the model products, variables acquired, and their producers is given in **Table 6**.

Model	**Variables/derived information**	**Producer**	**Onboard Use**
South African Wave and Storm Surge Forecast System (SWaSS)	Wave parameters, wind speeds and direction, tide and water level.	South African Weather Service Marine Research Unit	Port forecasts prior to departure and arrival at Cape Town. Regional deep sea forecast during transits.
Global Forecasting System (GFS)	Wave parameters, wind speeds and direction, surface temperature, cloud cover at various levels, rain and snow.	National Oceanic and Atmospheric Administration (NOAA)/National Centers for Environmental Prediction (NCEP)	General forecasting including 2D (map) graphics of a range of variables, and timeseries forecasts for the search area.
Icosahedral Nonhydrostatic Model (ICON)	Wave parameters, wind speeds and direction, surface temperature, rain and snow.	Deutscher Wetterdienst	General forecasting including 2D (map) graphics of a range of variables, and timeseries forecasts for the search area.
Integrated Forecast System (IFS)	Wave parameters, wind speeds and direction, surface temperature,	European Consortium for Medium Range Weather Forecasting (ECMWF)	General forecasting including 2D (map) graphics of a range of variables, and timeseries forecasts for the search area.
Mercator Global Analysis and Forecast Systems (GAFS)	Total (eulerian mean, wave and tide driven) surface currents, vertical current profiles for points of interest, sea ice concentration and drift.	Mercator Ocean/E.U. Copernicus Marine Service Information	2D maps and vertical profiles of ocean currents for use by sub-sea team as required.
Global Ice-Ocean Prediction System (GIOPS)	Sea ice concentration, sea ice drift, sea-ice internal pressure.	Environment and Climate Change Canada (ECCC)	Basic assessment of internal ice pressure to supplement through-ice navigation.
TPXO 9.0	Tidal constituents at wreck site and resulting tide-induced sea-level.	Oregon State University (OSU) TPXO	Assessment of likelihood of tide-controlled convergence/divergence of sea ice field in

			respect of timing of AUV deployment and recovery and/or through-ice navigation.

Table 6: *Summary of numerical model forecast products utilised during Endurance22*

9.2. Observation

Various observations were used to supplement forecast information for real-time reference and to ground-truth models (**Table 7**).

Observation Type/Activity	**Instrument/method**	**Variables/derived information**	**Onboard Use**
Surface synoptic observations	Automatic weather station and visual.	• Wind speed and direction • Wind wave/swell height/period/direction • Cloud type, coverage and height • Temperature, pressure, humidity • Precipitation and visibility • Sea ice type, coverage and navigability • Weather phenomena	1) Real-time reference for onboard operations. 2) 6-hourly assembly of visual and automatic (instrument) observations into coded FM12 weather messaged. Transmission to GTS for ingestion into global weather prediction models to constrain model forecast error.
Upper Air Soundings	Radiosondes and weather balloons	Temperature, pressure, humidity, position and various derived quantities.	Real-time assessment of upper air stability, cloud bases etc. Transmission to GTS for data assimilation into global NWP models.
Wave observations	Sofar Ocean Wave Spotter	Wave height, period, direction.	Ground-truthing of global wave forecasts during transit.
General marine weather	SVP drifters and voluntary observing ships belonging to the Global Ocean Observing System	Sea level pressure (SVP drifters) and SYNOP (see above) information from ships.	Ground truthing of forecast models during transit. NRT assessment of conditions in areas of interest.
Satellite meteorological imagery	NOAA 15,18 & 19, EUMETSAT Meteosat infrared, optical and microwave radiometers.	Cloud cover, fog, sea ice.	General assessment of atmosphere above search area. Observation of storms during transit.

Table 7: *. Summary of observation products utilised during Endurance22*

9.3. Research

Aside from instrumentation deployed in support of operations during Endurance22 (see section 9.2), a number of Argo floats were deployed in support of the global Argo program. Argo floats are profiling ocean investments which collect data such as temperature, salinity and ocean current data in the water column. These data are invaluable to the oceanographic research community, which uses them for direct observation-based research as well as for ingestion into and ground-truthing of ocean models. The 12 Argo float deployments were done together with the Reach the World foundation and the Adopt a Float programme, to involve children around the world in oceanographic science. Each float was "adopted" and named by one of various schools around the world. Student are then able to track their instrument in real time and watch as it collects data. **Table 8** summarises all ARGO deployments as well as operational instruments deployed (data from which will ultimately form part of research datasets). **Figure 78** shows deployments in space and time.

Outbound Leg			
Latitude	**Longitude**	**Instrument**	**Date deployed**
42° 00.0' S	005° 59.2' W	Argo float, Wave spotter buoy	09 February 2022
45° 00.0' S	010° 02.0' W	Argo float, Wave spotter buoy	09 February 2022
50° 00.0' S	029° 00.4' W	Argo float, Wave spotter buoy	10 February 2022
52° 00.0' S	020° 49.7' W	Argo float, Wave spotter buoy, SVP drifting buoy	11 February 2022
55° 00.0' S	025° 58.1' W	Argo float, Wave spotter buoy, SVP drifting buoy	11 February 2022
57° 00.0' S	029° 05.7' W	Argo float, Wave spotter buoy, SVP drifting buoy	12 February 2022
62° 00.2' S	028° 14.6' W	Argo float x 2	13 February 2022
63° 00.0' S	032° 27.0' W	Argo float	13 February 2022
64° 00.0' S	036° 11.5' W	Argo float	13 February 2022
65° 01.3' S	039° 47.4' W	Argo float	14 February 2022
66° 01.3' S	043° 01.1' W	Argo float	14 February 2022

Inbound Leg			
Latitude	**Longitude**	**Instrument**	**Date deployed**
59° 00.3' S	039° 52.3' W	Wave spotter buoy, SVP drifting buoy	10 March 2022
61° 00.9' S	040° 48.6' W	Wave spotter buoy, SVP drifting buoy	10 March 2022
53° 00.5' S	035° 09.8' W	Wave spotter buoy	12 March 2022
50° 59.3' S	033° 04.2' W	Wave spotter buoy	12 March 2022
50° 00.3' S	032° 05.8' W	Wave spotter buoy	12 March 2022
48° 59.3' S	031° 07.3' W	Wave spotter buoy	12 March 2022
48° 00.4' S	030° 10.0' W	Wave spotter buoy	13 March 2022
47° 00.1' S	029° 11.8' W	Wave spotter buoy	13 March 2022
46° 00.1' S	027° 45.2' W	Wave spotter buoy	13 March 2022
45° 00.3' S	026° 12.0' W	Wave spotter buoy	13 March 2022
43° 59.9' S	024° 37.9' W	Wave spotter buoy	13 March 2022
43° 00.6' S	022° 12.1' W	Wave spotter buoy	14 March 2022
42° 00.1' S	018° 42.9' W	Wave spotter buoy	14 March 2022
41° 00.1' S	015° 19.7' W	Wave spotter buoy	15 March 2022

***Table 8**: Summary of ocean research instrumentation deployed during Endurance22. Note: Due to bad weather conditions on the outbound leg the instrument intended to be deployed at 59° S and 61° S could not be carried out due to safety concerns on the aft deck. These deployments were rescheduled and were deployed on the inbound leg back to Cape Town.*

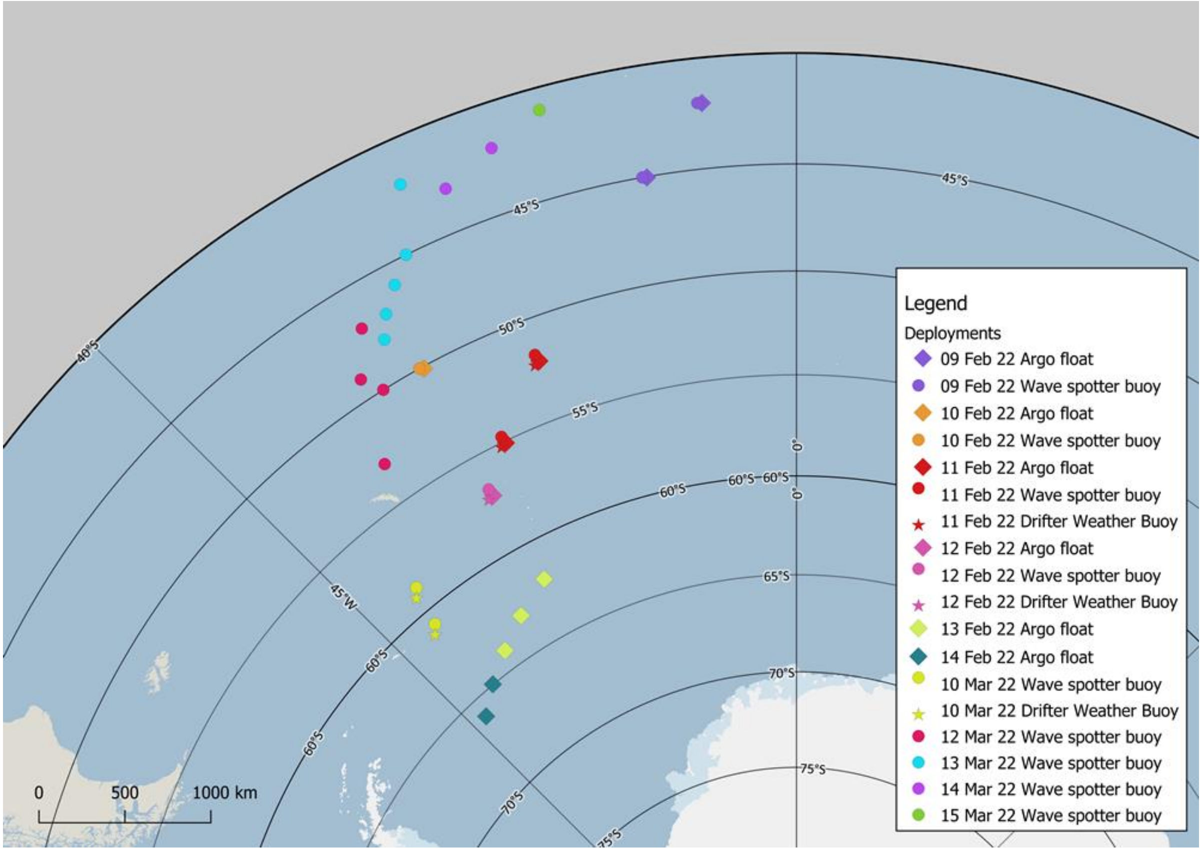

Figure 78:*.Map showing deployment locations of oceanographic instruments.*

10. Science Education and Outreach

Written by Timothy Jacob (Reach the World)

Reach the World's Endurance22 Education & Outreach program began in August 2021 and will run through the end of the academic year (approximately June 2022). One of the primary goals of the multi-disciplinary virtual exchange program was to give K-12 students (ages 5-18) around the world real-time access to the extraordinary Science team aboard the S.A. Agulhas II, thereby amplifying the important work performed by the Science team and highlighting careers in STEM fields. We achieved this goal in the following ways:

1. <u>Adopt-a-Buoy Project</u>: In partnership with Dr. Tamaryn Morris and Thomas Mtontsi from the South African Weather Service, Reach the World matched 11 schools in North America with 11 schools in South Africa and Namibia to name and "adopt" an Argo smart buoy and collaborate on classroom projects using the data collected by those buoys in the weeks following deployment. Each participating classroom received a video of their buoy being dedicated and deployed from the S.A. Agulhas II en route to the Weddell Sea. Dr. Morris produced a series of short videos teaching classrooms focused on how smart buoys help oceanographers monitor ocean health, how classrooms can track their buoys online, and how educators can integrate oceanographic data into their lesson plans.

2. <u>Livestream Events</u>: Reach the World hosted four, 45-minute live educational events from the S.A. Agulhas II with members of the Science team. Each event featured a different sub-section of the greater Science team and spotlighted a unique area of the ship so that students gained a broad understanding of participants' jobs and work environments. Hundreds of students participated live in each event, and thousands more around the world watched the event recordings in their classrooms during the days and weeks that followed.

E22 Participant(s)	**Topic**	**Location**	**Link**
1. Marc De Vos, South African Weather Service 2. Carla Ramjukadh, South African Weather Service	Meteorology, oceanography, and using models to predict weather	South African Weather Service office aboard the S.A. Agulhas II	Full recording available here
1. Alexandra Stocker, Drift + Noise	Remote-sensing tools and ice floe drift forecasting	Remote-sensing data processing	Full recording available here

2. Christian Katlein, Alfred Wegner Institute		room aboard the S.A. Agulhas II	
1. Dr. Annie Bekker, University of Stellenbosch 2. Dr. Jukka Tuhkuri, Aalto University	Mechanical engineering and monitoring ship health/performance	3rd deck laboratory aboard the S.A. Agulhas II	Full recording available here
1. Dr. Stefanie Arndt, Alfred Wegner Institute	All about sea ice, including how it forms and why it is important to study	Top-deck observation area aboard the S.A. Agulhas II	Full recording available here



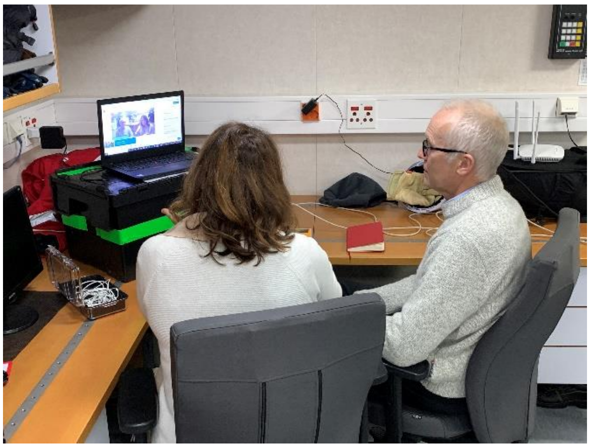


3. Written articles for students: Reach the World published four student-friendly articles describing unique aspects of the Endurance22 Expedition Science program. Each article shared first-person accounts of STEM jobs in action, preparing student audiences for their opportunity to speak to (and ask face-to-face questions of) expedition Science team members during livestream events.

Article Title	Topic	Link
Putting (Very) Smart Buoys to Work (by Dr. Tamaryn Morris; South African Weather Service)	What are smart buoys, and how do they help oceanographers learn more about our oceans?	Full article available here

Underwater Archaeology and the Search for Endurance (by Mensun Bound)	What is marine archaeology, and what should students expect from the underwater search for Endurance?	Full article available here
Deploying Ocean Monitoring Buoys	Insider's look at the day-to-day work of the South African Weather Service onboard the S.A. Agulhas II	Full article available here
Measuring Ice Thickness	Personal account of an afternoon spent supporting ice floe data collection in the Weddell Sea	Full article available here

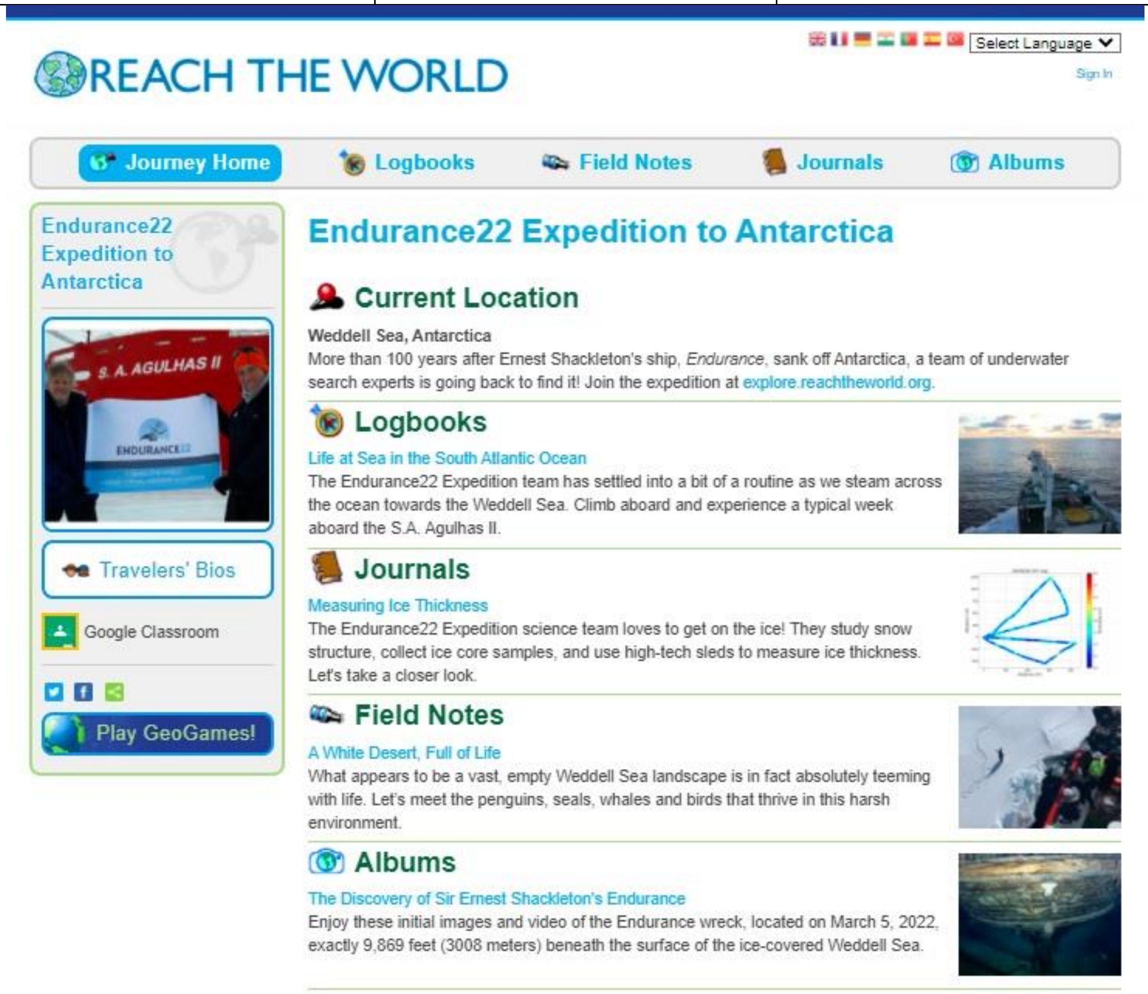

11. Concluding remarks

Although the primary aim of the Endurance22 expedition was to search for and survey the wreck of the Endurance, the ship operations in the remote western Weddell Sea provided the opportunity to undertake a high quality programme of associated sea ice research. The expedition also supported meteorological and oceanographic research, as well as ship engineering studies.

The expedition's international research programme was very successful producing many new observations from the western Weddell Sea, an area that has been little studied previously.

A unique dataset will be available after the expedition which will combine ice & snow properties and ship performance with optical and radar satellite measurements. This will enable the creation of new ice information products, an important topic and a common denominator for the research teams which joined the Endurance 22 expedition and beyond. The ultimate goal of those researchers and engineers is to create a "Google-maps" like representation for shipping in polar waters.

The expedition scientists will now analyse the samples of ice, and water, along with the remote sensing imagery, meteorological observations, and ship engineering data, in various laboratories around the world. We expect that the data analysis will result in a number of important scientific papers.

The data recorded by the AUV at the Endurance wreck site is a unique resource for deep-sea biologists and sedimentologists around the world. In-depth analysis of the high resolution footage will broaden the knowledge of the deep-sea lifeforms, sediments and ecosystems found in this remote place of our planet. Please contact the Falklands Maritime Heritage Trust if you are interested to work with those data. A separate report fully dedicated to the marine archaeology survey of the wreck of the *Endurance* will be published within the next few months.

12. Acknowledgements

We thank the Falklands Maritime Heritage Trust for funding and organising the Endurance22 expedition.

The Expedition Leader, Dr John Shears, provided outstanding support to the Science team, as did Captain Knowledge Bengu and the officers and crew of the S.A. Agulhas II. We would also like to thank Nico Vincent and Seb Bougant from Ocean Infinity for the excellent assistance provided to the Science team by the Subsea team

We are also very grateful for the help of the South African Antarctic Research Programme and Amsol.

13. References

Bekker, A. *et al.* (2014) 'Full-scale measurements on a polar supply and research vessel during maneuver tests in an ice field in the Baltic Sea', in *Proceedings of the International Conference on Offshore Mechanics and Arctic Engineering - OMAE*.

Bekker, A. *et al.* (2018) 'From data to insight for a polar supply and research vessel', *Ship Technology Research*, pp. 1–34. DNVGL (2015) 'DNVGL-CG-0129: Fatigue Assessment of Ship Structures', (October), pp. 1–129. Available at: https://rules.dnvgl.com/docs/pdf/DNVGL/CG/2015-10/DNVGL-CG-0129.pdf.

Haas, C., Nicolaus, M., Willmes, S., Worby, A., & Flinspach, D. (2008). Sea ice and snow thickness and physical properties of an ice floe in the western Weddell Sea and their changes during spring warming. *Deep Sea Research Part II: Topical Studies in Oceanography*, *55*(8-9), 963-974.

Haas, C., Gerland, S., Eicken, H., & Miller, H. (1997). Comparison of sea-ice thickness measurements under summer and winter conditions in the Arctic using a small electromagnetic induction device. *Geophysics*, *62*(3), 749-757.

Harms, S., Fahrbach, E., & Strass, V. H. (2001). Sea ice transports in the Weddell Sea. *Journal of Geophysical Research: Oceans*, *106*(C5), 9057-9073.

Kovacs, A., & Morey, R. M. (1991). Sounding sea ice thickness using a portable electromagnetic induction instrument. *Geophysics*, *56*(12), 1992-1998.

Nickerson, B. M. and Bekker, A. (2022) 'Inverse model for the estimation of ice-induced propeller moments using modal superposition', *Applied Mathematical Modelling*. Elsevier Inc., 102, pp. 640–660. doi: 10.1016/j.apm.2021.10.005.

Pferdekämper, K.-H. and Bekker, A. (2022) *Full-scale measurement and quantication of hull fatigue on a slamming-prone polar vessel*. Stellenbosch University.

Spreen, G., Kaleschke, L., & Heygster, G. (2008). Sea ice remote sensing using AMSR-E 89-GHz channels. *Journal of Geophysical Research: Oceans*, *113*(C2).

Worby, A. P., Griffin, P. W., Lytle, V. I., & Massom, R. A. (1999). On the use of electromagnetic induction sounding to determine winter and spring sea ice thickness in the Antarctic. *Cold Regions Science and Technology*, *29*(1), 49-58.

Appendix A - Data Summary

Active data link by April 14, 2022
https://www.dropbox.com/sh/ni40qf0ixd5wjhv/AACNM147h2e6HRV4y0fT8yuSa?dl=0
Password: Please contact rabenstein@driftnoise.com for data access.

Remote Sensing Data

- 6 km Sea-ice concentration, exported from IcySea
  - .\RS\Level3\SIC_6k
  - How to cite: Sea Ice Concentration from GCOM-W1 AMSR-2 swath data, processed by Drift+Noise GmbH
  - Format: geotiff
- 3 km Sea-ice concentration, exported from IcySea
  - .\RS\Level3\SIC_3k
  - How to cite: Sea Ice Concentration derived from GCOM-W1 AMSR-2 swath data, processed by Drift+Noise GmbH
  - Format: geotiff
- Sentinel-1 SAR images from IcySea - lowres
  - .\RS\SAR\Sentinel-1\IcySea\lowres(300m)\

    - Description: Exported Tiles from https://icysea.app in 300 m resolution
    - How to cite: Copernicus Sentinel data, processed by ESA, retrieved and enhanced by https://icysea.app
    - Format: geopng (png + pngw file), 50x50 km tiles in 300m resolution
- Sentinel-1 SAR images from IcySea -highres
    - .\RS\SAR\Sentinel-1\IcySea\highres(30m)\
    - Description: Exported Tiles from https://icysea.app in 30 m resolution
    - How to cite: Copernicus Sentinel data, processed by ESA, retrieved and enhanced by https://icysea.app
    - Format: geopng (png + pngw file), 50x50 km tiles in 30m resolution
- Sentinel-1 SAR images from FRAM-Sat
    - .\RS\SAR\Sentinel-1\FRAM-Sat\
    - Description: Exported imaged from the AWI Fram-Sat System, center directory is over the wreck site, the other folders relative to center
    - How to cite: Copernicus Sentinel data, processed by ESA, retrieved and enhanced by the AWI FRAM-Sat software
    - Geotiff in 40 m resolution
- Sentinel-3 ice classification
    - .\RS\Level3\Sent3_classified
    - How to cite: Provided by König und Partner Fernerkundung GbR (K&P) and based on Copernicus Sentinel-3
    - geotiff
- TerraSAR-X images
    - .\RS\SAR\TSX
    - Description: Processed 8-bit images. In case you need the raw data, to extract physical quantities please contact Thomas.Busche@dlr.de
    - How to cite: German Aerospace Center (DLR)
    - Format: geotiff
- ICEYE SAR images
    - .\RS\SAR\ICEYE
    - How to cite: 2022 © ICEYE Oy
    - 8-bit processed geotiff
- PlanetLabs optical satellite data
    - .\RS\Optical\PlanetLabs\
    - How to cite: Planet Labs PBC
    - Processed Geotiff
- MODIS optical satellite images
    - .\RS\Optical\MODIS\
    - Description: Daily subset of the two satellites with MODIS sensors Terra and Aqua
    - How to cite: Moderate Resolution Imaging Spectroradiometer (MODIS) images from the NASA Earth Observing System Data and Information System (EOSDIS)."
    - Geotiff
- Cryosat 2 Ice Thickness data
    - .\RS\Level3\Cryosat2_Ice_Thickness\

    - How to cite: Provided by ESA Sea Ice Climate Change Initiative (Sea_Ice_cci), Hendricks, S., Paul, S., Rinne, E., (2018) based on Cryosat 2 data
    - Format: geotiff and netcdf

Ice drift Forecast Data

- PRIIMA sea-ice drift forecast, hourly interval, 3 days forecast period (Mira)
    - .\Drift_Forecasts\PRIIMA\
    - How to cite: Ice drift forecasts provided by Drift+Noise GmbH, based on ICON
    - Format: shp files
- SIDFEX sea-ice drift forecasts, daily interval, updated every 6 hours, 7 days forecast period
    - .\Drift_Forecasts\SIDFEX\
    - How to cite:
    - Format: shp files

Cruise tracks

- ECDIS ship track
    - .\Position_Data\ECDIS_tracks
    - How to cite: Provided by S.A. Agulhas II
    - Format: Text files
- IceLaptop GPS tracks
    - .\Position_Data\NMEA_Files_GPS_Laptop\
    - How to cite: Recorded and processed by Drift Noise GmbH
    - Format: shp files
- Garmin inReach recordings
    - .\Position_Data\Garmin-in-reach\
    - How-to-cite: Data recorded by DriftNoise GmbH
    - Format: kml and gpx

In-situ Data from Ship

- Manual Ice Observations
    - .\Sea-ice-obs-ship\
    - Format: « Endurance_2022_Ice Observations Antarctica.xlsx »
- Ship EM Data
    - .\EM_ice_thickness\
    - Description: Processed ice thickness results as text files, histogram plots
    - How to cite: Endurance22 expedition, instrument provided by Alfred Wegener Institute, data processed by DriftNoise GmbH
    - Format: Text files, jpg plots
- Optical Camera Recordings
    - .\Sea-ice-obs-ship\Camera_CrowsNest\
    - More information see Camera_CrowsNest_ReadMe.rtf
    - Format: jpg files
- Infrared Camera Recordings
    - .\ir_camera\
    - Description: Raw ASC files

- How to cite: Data recorded by DLR with an IR camera system by University Bremen
- Contact: Dmitrii.Murashkin@dlr.de

In-situ data from ice floe

- GEM Ice thickness
    - Contact Jakob Belter <jakob.belter@awi.de>
- Ice Cores, snow data etc from AWI
    - Contact Stefanie Arndt <Stefanie.Arndt@awi.de>
- Ice core data from University Aalto
    - .\Sea-ice-obs-floes\
    - Format: IceCores_Aalto.xlsx
    - Contact: Jukka Tuhkuri jukka.tuhkuri@aalto.fi
- Snow buoy
    - .\Snow_buoy_2021S114\
    - Format : Excel file
    - More updated information : Meereisportal.de

S.A. Agulhas 2 characteristics

- Sound and Vibration Measurements
    - .\SUN_Ship_measurements\
    - Format: pdf plots and xlsx tables
    - More information: READ_ME.txt
    - Contact: Prof. Annie Bekker annieb@sun.ac.za
- Ice Loads
    - Contact: Prof. Jukka Tuhkuri jukka.tuhkuri@aalto.fi

Appendix B - Daily Ship EM ice thickness distributions

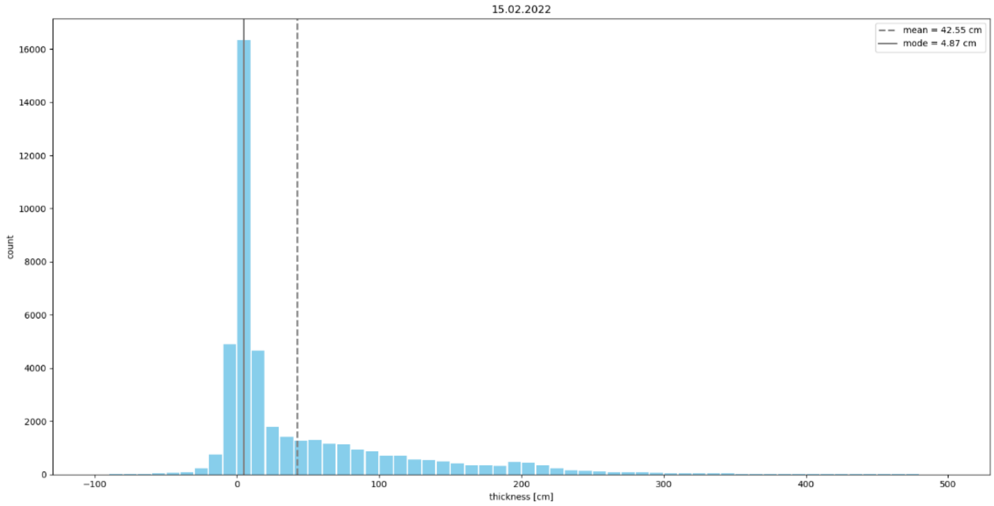

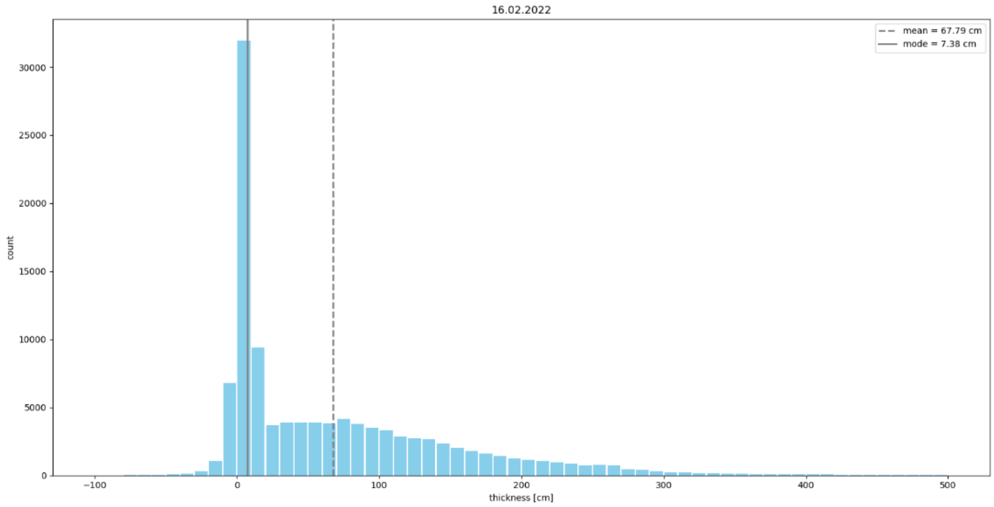

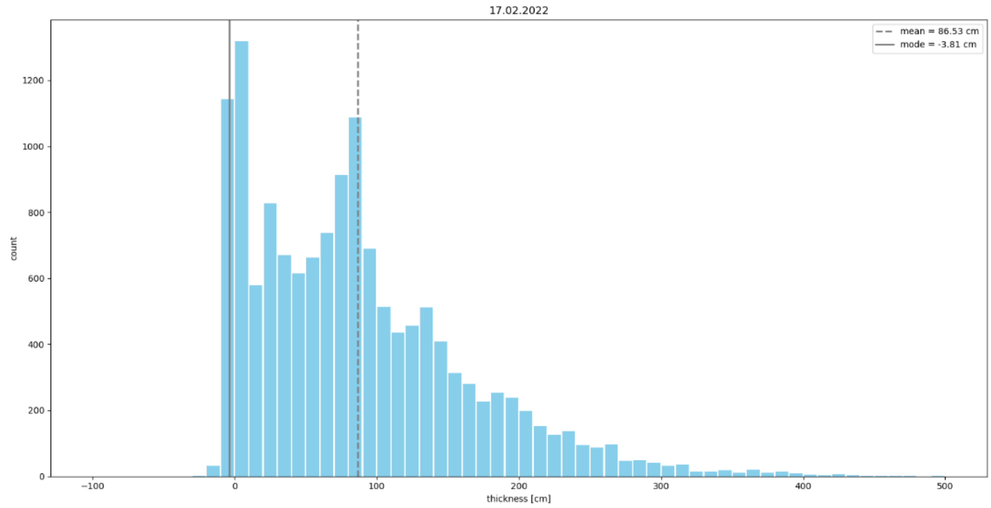
17.02.2022
mean = 86.53 cm
mode = -3.81 cm
count
thickness [cm]

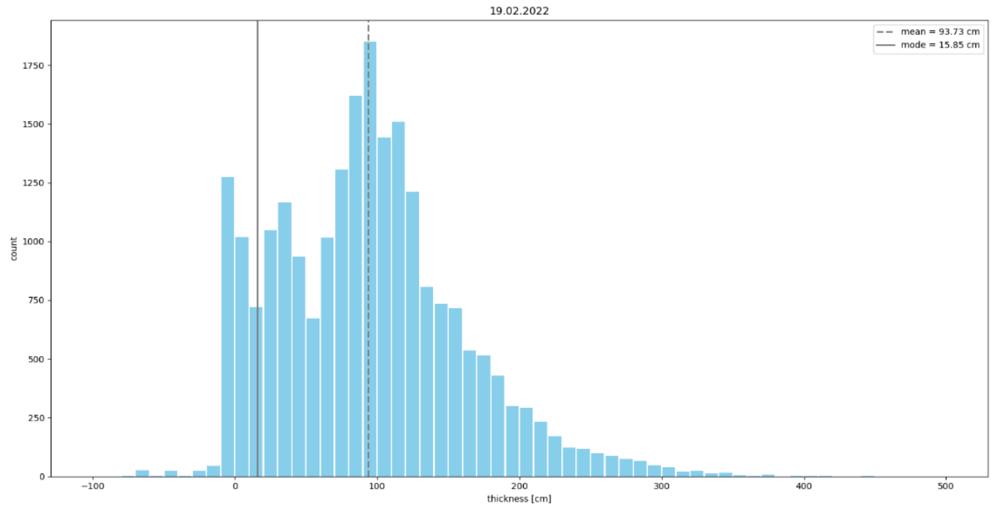
19.02.2022
mean = 93.73 cm
mode = 15.85 cm
count
thickness [cm]

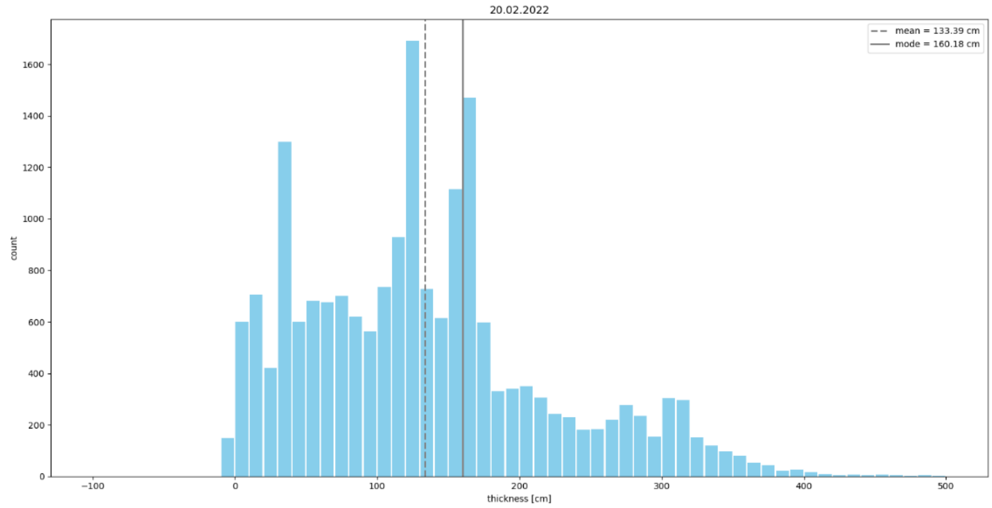
20.02.2022
mean = 133.39 cm
mode = 160.18 cm
count
thickness [cm]

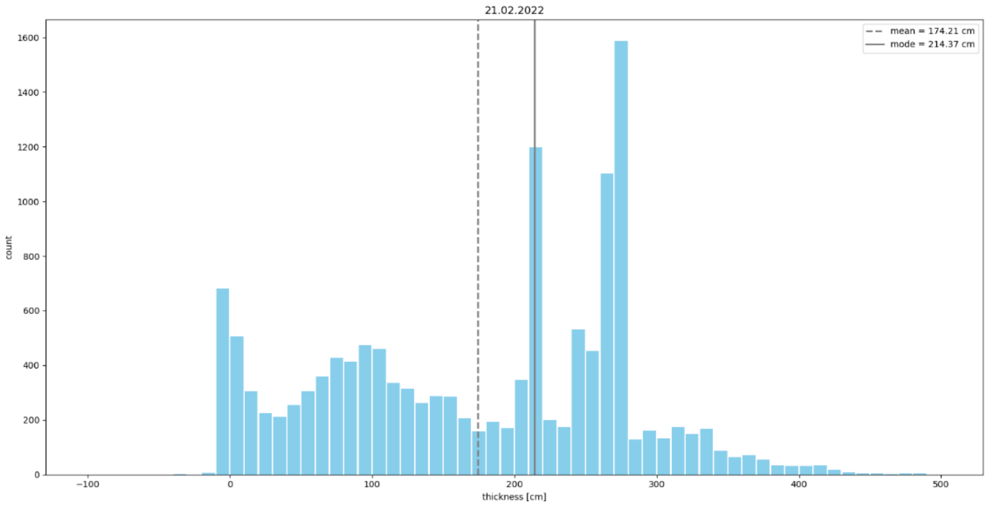
21.02.2022
mean = 174.21 cm
mode = 214.37 cm
count
thickness [cm]

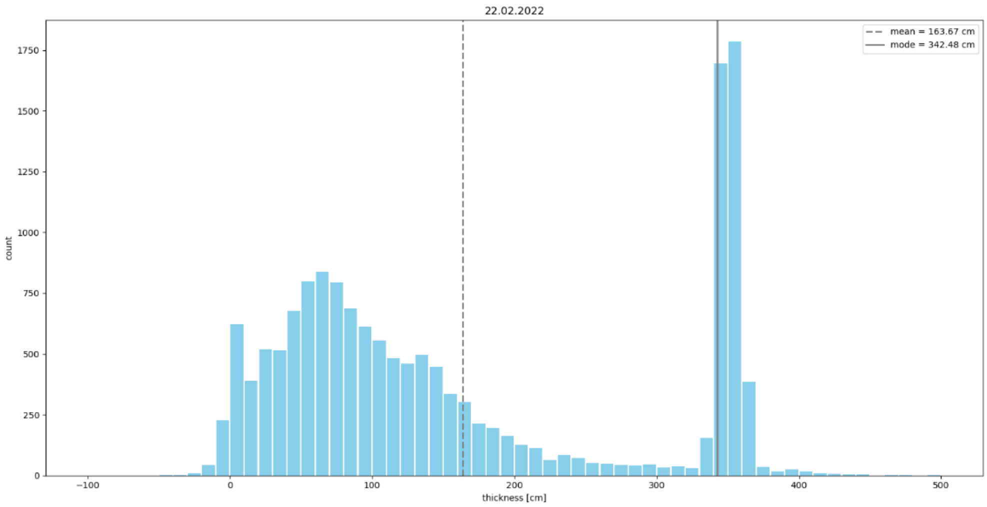
22.02.2022
mean = 163.67 cm
mode = 342.48 cm
count
thickness [cm]

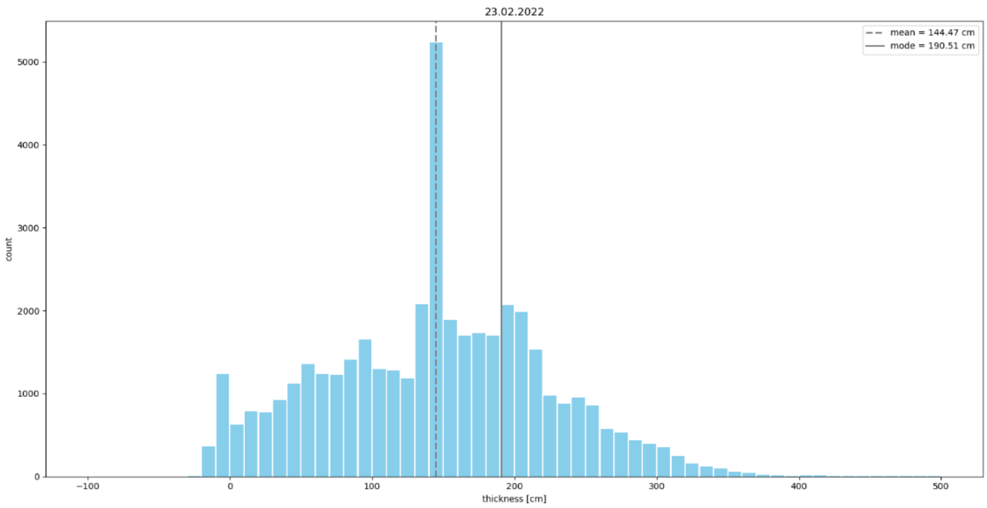
23.02.2022
mean = 144.47 cm
mode = 190.51 cm
count
thickness [cm]

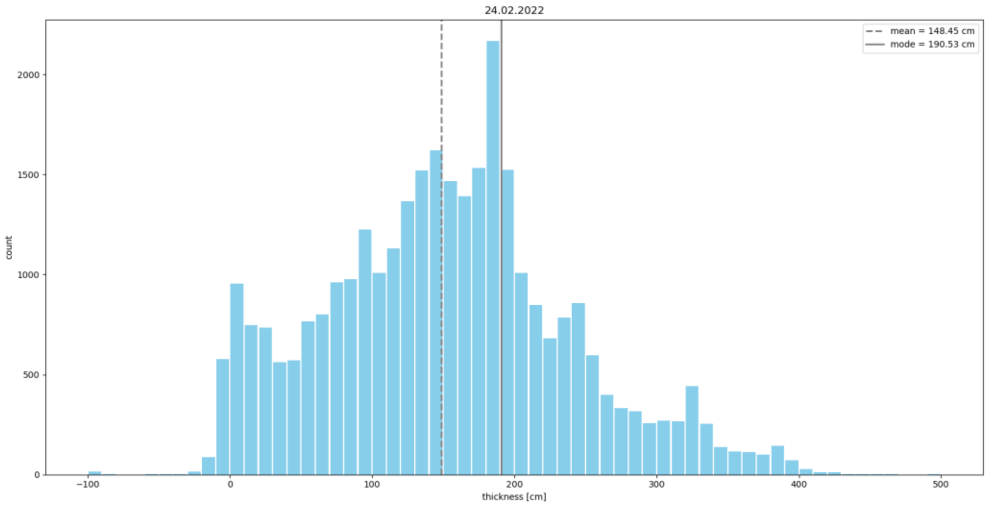
24.02.2022
mean = 148.45 cm
mode = 190.53 cm
count
thickness [cm]

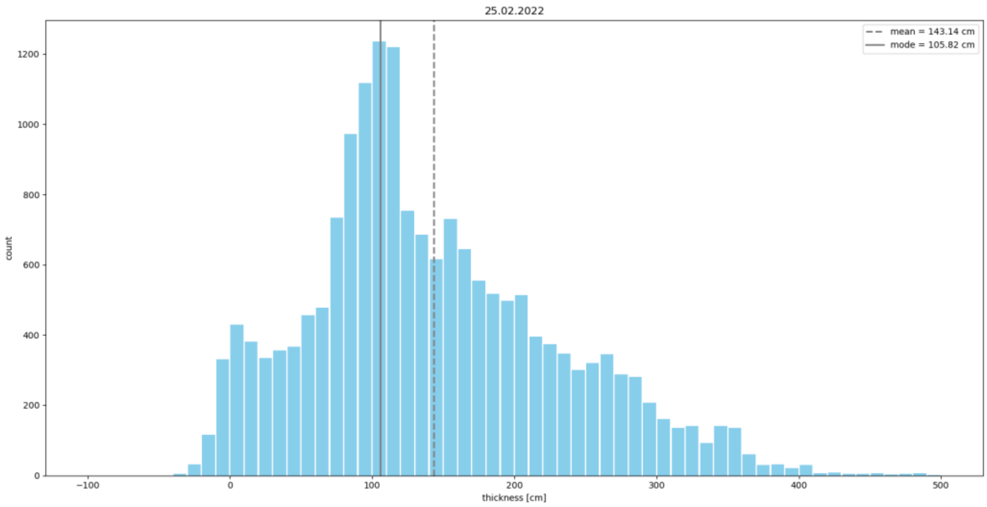
25.02.2022
mean = 143.14 cm
mode = 105.82 cm
count
thickness [cm]

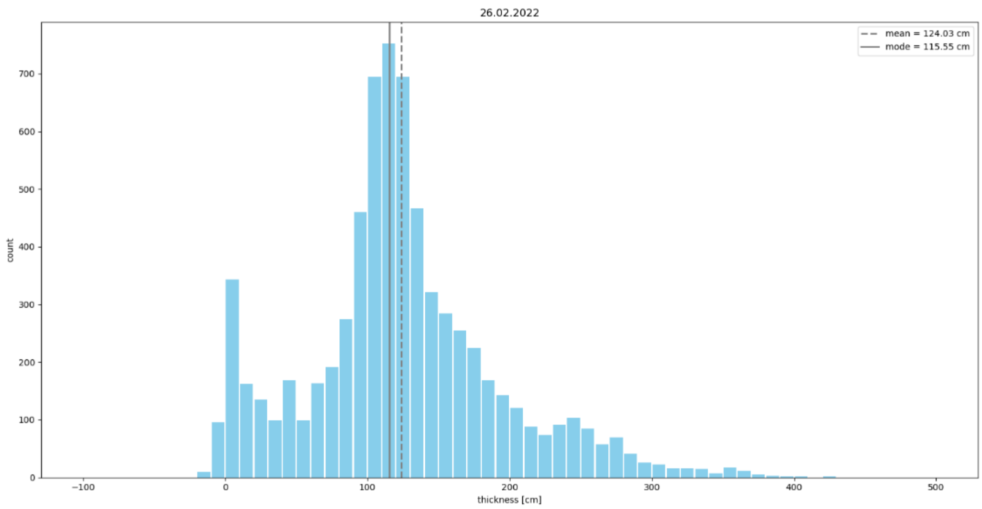
26.02.2022
mean = 124.03 cm
mode = 115.55 cm
count
thickness [cm]

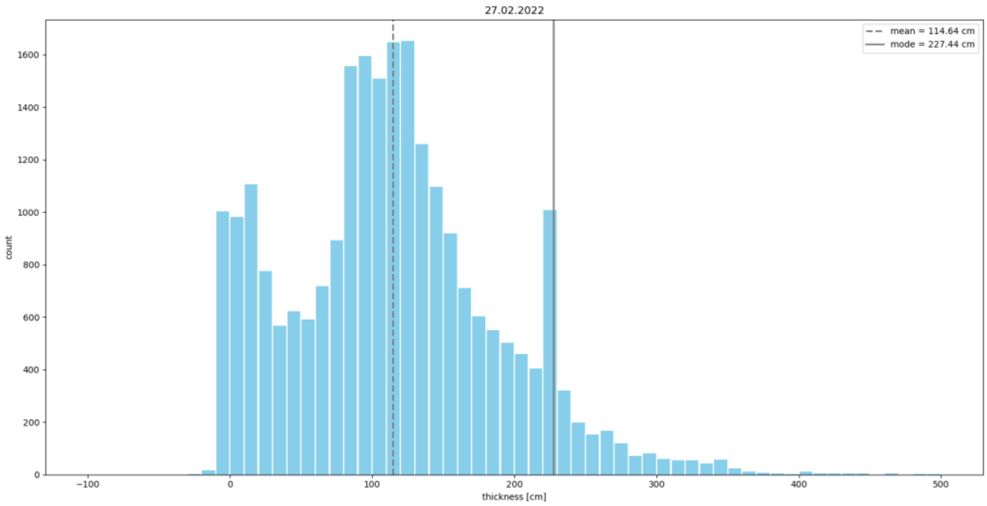
27.02.2022
mean = 114.64 cm
mode = 227.44 cm
count
thickness [cm]
−100
0
100
200
300
400
500
0
200
400
600
800
1000
1200
1400
1600

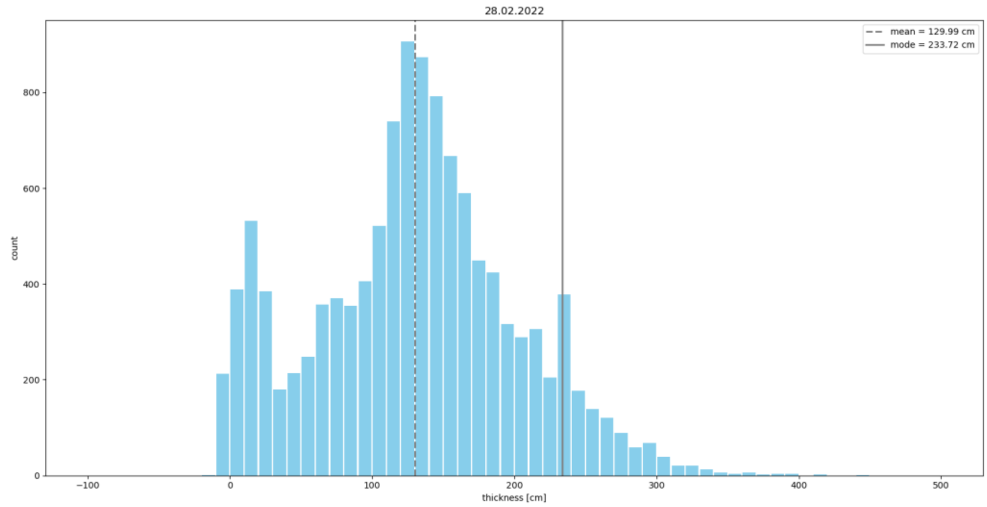
28.02.2022
mean = 129.99 cm
mode = 233.72 cm
count
thickness [cm]
−100
0
100
200
300
400
500
0
200
400
600
800

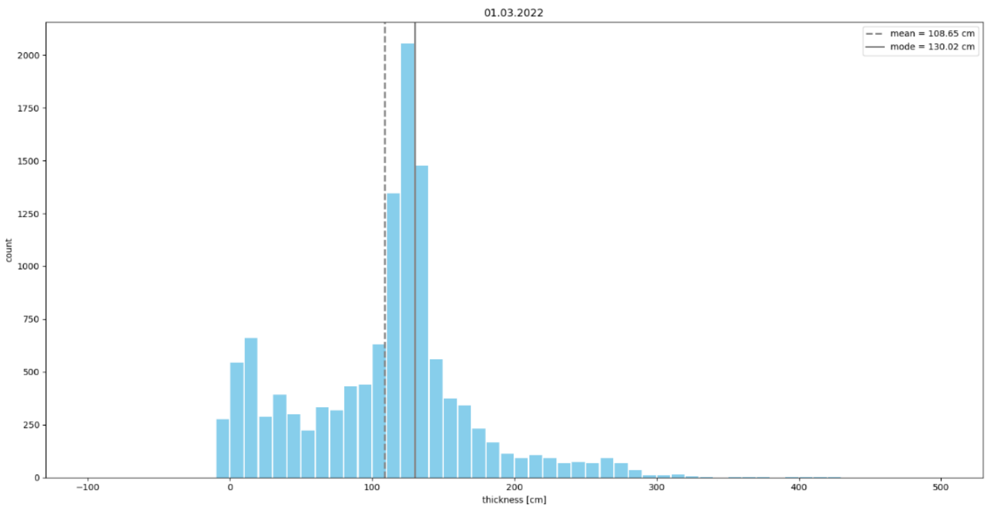
01.03.2022
mean = 108.65 cm
mode = 130.02 cm
count
thickness [cm]
−100
0
100
200
300
400
500
0
250
500
750
1000
1250
1500
1750
2000

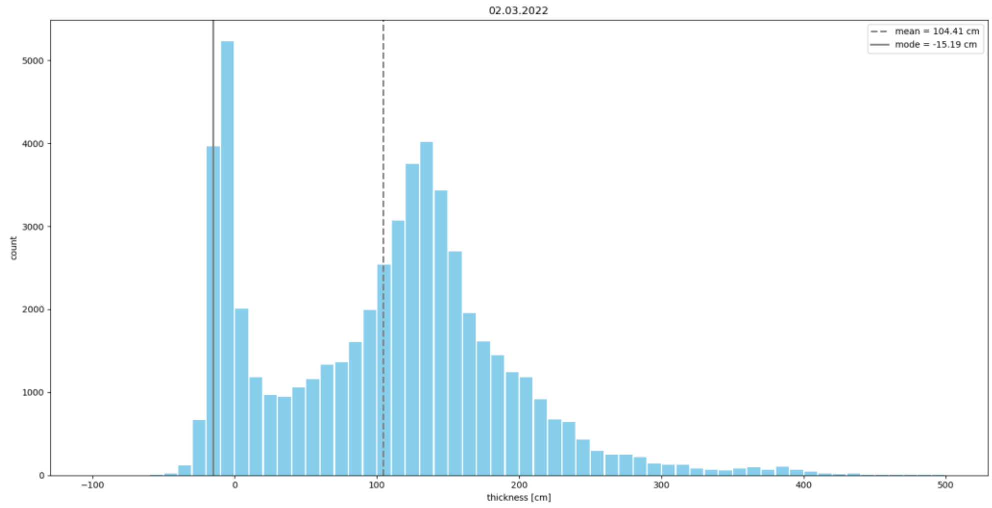
02.03.2022
mean = 104.41 cm
mode = -15.19 cm
count
thickness [cm]

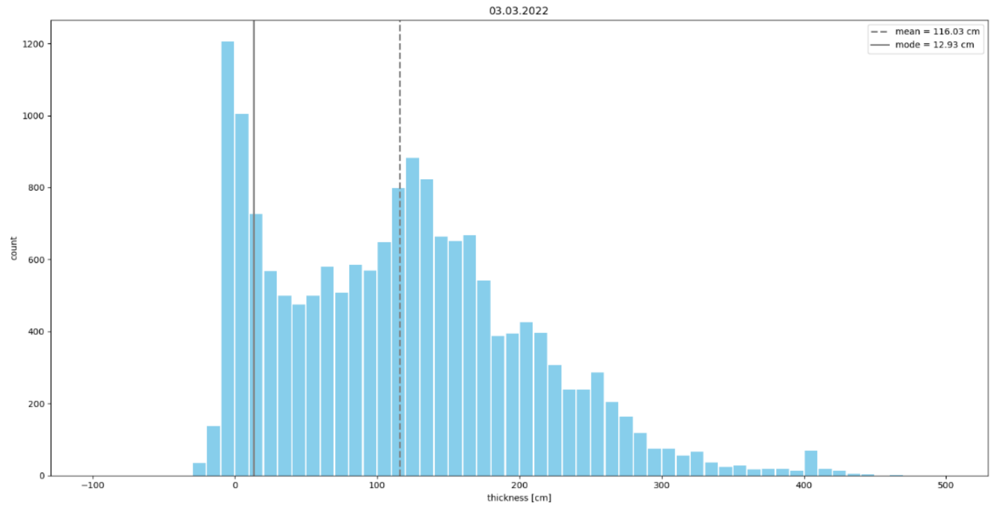
03.03.2022
mean = 116.03 cm
mode = 12.93 cm
count
thickness [cm]

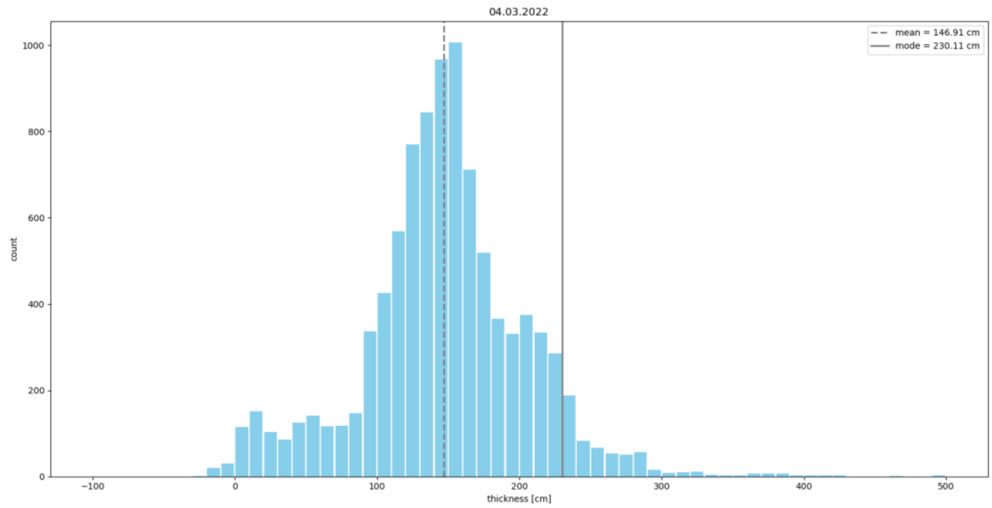
04.03.2022
mean = 146.91 cm
mode = 230.11 cm
count
thickness [cm]

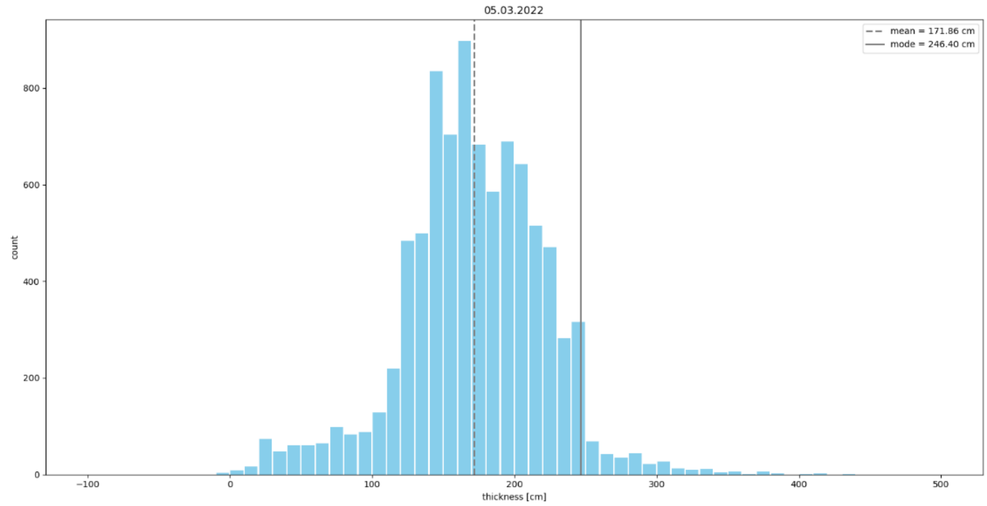
05.03.2022
mean = 171.86 cm
mode = 246.40 cm
count
thickness [cm]

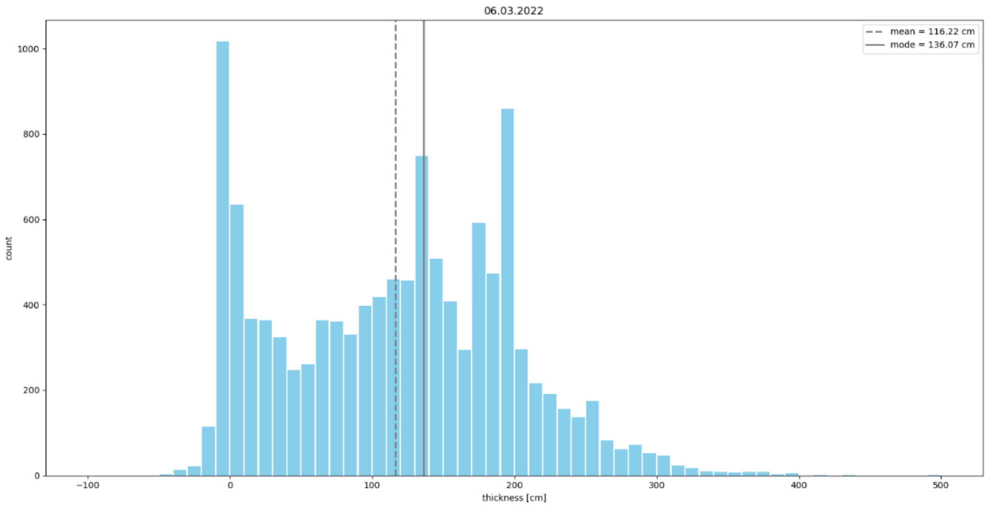
06.03.2022
mean = 116.22 cm
mode = 136.07 cm
count
thickness [cm]

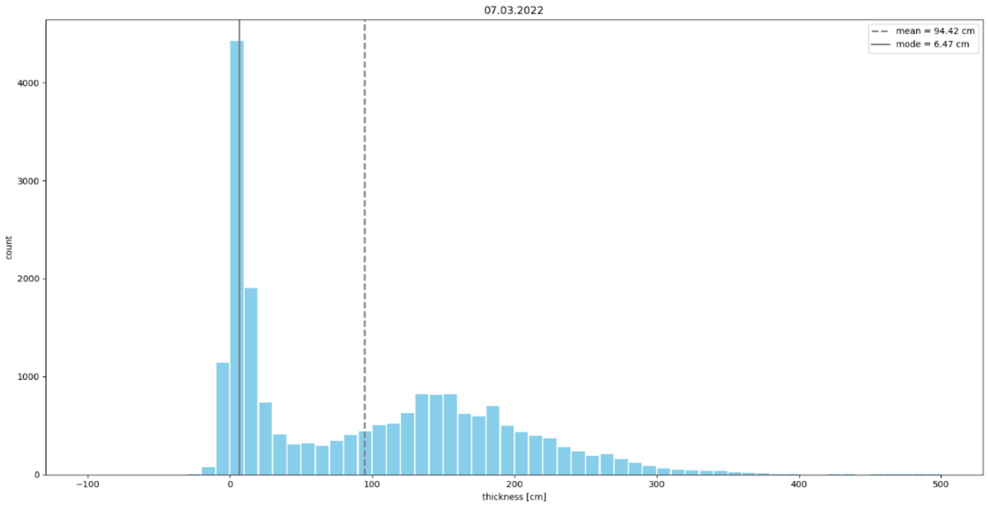
07.03.2022
mean = 94.42 cm
mode = 6.47 cm
count
thickness [cm]

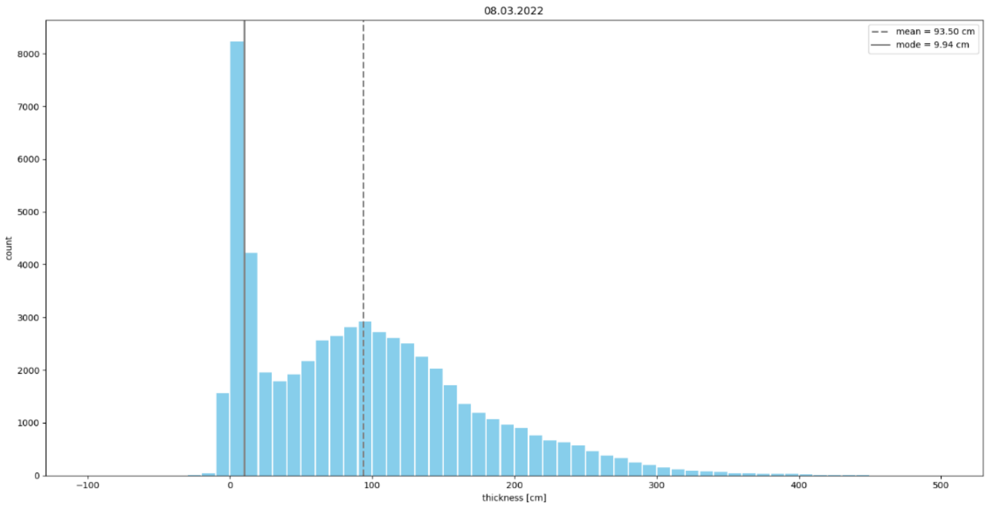
08.03.2022
mean = 93.50 cm
mode = 9.94 cm
count
thickness [cm]